UNIVERSIDAD DE JAÉN

ESCUELA POLITÉCNICA SUPERIOR
DEPARTAMENTO DE INGENIERÍA ELÉCTRICA

TESIS DOCTORAL

GASIFICATION APPLIED TO THE VALORIZATION OF OLIVE GROVE AND OLIVE MILL RESIDUES

PRESENTADA POR:
BÁRBARA DE MENA PARDO

DIRIGIDA POR:
DR. D. DAVID VERA CANDEAS
DR. D. FRANCISCO JURADO MELGUIZO

JAÉN, 7 DE ABRIL DE 2017

ISBN 978-84-9159-076-7

List of tables

List of figures

Chapter 1. Introduction. Objectives and structure of the thesis

Chapter 1. Introduction. Objectives and structure of the thesis

1.1. Introduction: Why valorise the residues of the olive sector?

The world energetic system is nowadays dominantly based on fossil fuels, which are finite in their availability and have dramatic effects to the planet's climate. The change to a more sustainable way of producing heat and power has led the development of numerous international compromises, starting with the United Nations Framework Convention on Climate Change (UNFCCC), an international environmental treaty negotiated at the Earth Summit in Rio de Janeiro from 3 to 14 June 1992, then entered into force on 21 March 1994. The UNFCCC objective is to "stabilize greenhouse gas concentrations in the atmosphere at a level that would prevent dangerous anthropogenic interference with the climate system" [1] The Kyoto protocol followed in December 1997, an international agreement linked to UNFCCC, which commits its Parties by setting internationally binding emission reduction targets. This launched the development of numerous national and European policies to mitigate climate change and global warming, reduce greenhouse gas and CO2 emmissions, as well as to include these concepts in different industrial sectors such as transport, manufacturing, and logically, heat and power production. The EU's Renewable Energy Directive sets a binding target of 20% final energy consumption from renewable sources by 2020. To achieve this, EU countries have committed to reaching their own national renewables targets ranging from 10% in Malta to 49% in Sweden. They are also each required to have at least 10% of their transport fuels come from renewable sources by 2020.

In parallel to these developments, the olive oil sector has consolidated itself as a very important agro-industrial sector in the European Union (EU): the EU is the largest producer, exporter and consumer of olive oil [2]. According to EUROSTAT, there are 1.9 million olive oil farms in the EU. Olive oil production is also linked to the production of large amounts of different waste streams, as it will be discussed in further chapters of the present thesis: depending on the production method used, pomace and wastewater are produced, which do not presently have a clearly beneficial disposal pathway. As it will be explained in

further chapters, millions of tons of these residues are produced only in Spain, which could instead of the present disposal solutions, be used for a more sustainable and economically beneficial agriculture.

In this framework, the olive oil sector could take a step forward adopting technologies that allow the valorization of the residues, such as the pomace and the wood and leaves result of pruning the trees. As it will be presented in this work, different initiatives have tried to find a solution for this issue, transforming the residues into resources, either as fuel or as a source of chemical compounds of economic interest.

Distributed Generation (DG) refers to the generation of electricity in a decentralized manner, i.e. geographically distributed over the area that is serviced and close to the consumer of energy (which often is the owner of the facility), [3,4]. This concept has gained great importance compared to traditional systems of electricity production in large hydro and thermal plants connected to the transmission grid for their flexibility and reduced infrastructure needed. Indeed, DG presents a very interesting option for standalone systems, such as those that could be used at olive mills vor the valorization of residues, and which ould provide heat and power required for the olive pressing.

The present thesis focuses on the energetic valorization of the wood, twigs and leaves from olive groves that are collected either at the grove or at the mill during the cleaning of the olives in Spain. About 5.3 million tons of these residues are produced yearly. Currently there is no direct use for these, apart from burning the pruning rests directly on the field, without an economic benefit, and often with transport costs associated to them.

An intelligent exploitation of these residues would represent a new source of income and employment for the olive mills, and would also contribute to the targets set by the Spanish Government and the European Commission to achieve a more sustainable society and agriculture.

1.2. Objectives of this thesis

The present thesis is set out to achieve the following objectives:

- To define the framework of the production of olive grove and olive mill wastes, focused on the production in Andalucía, Spain, as the largest producing region worldwide
- To study the potential of different valorization technologies for the specific case of these wastes
- Given the preliminary research related to the use of gasification for the olive oil sector, to study different plant configurations and gasifier types for the valorization of these residues
- To enable the widespread of distributed generation energy systems in the olive sector
- To contribute to the creation of a more sustainable agricultural sector in Europe, and to contribute to achieving the goals set for 2020 with regard to renewable energies and sustainability

In order to achieve these goals, the present thesis will develop the following tasks:

- Revision of the biomass streams produced at olive groves and mills, characterising their properties and amounts produced in Andalucía
- Identification of current research and uses of these waste streams, in order to ascertain that the energy valorization pathway is the most suitable
- Revision of different biomass valorization technologies, with special focus on gasification applied to small-scale, decentralized systems
- *Revision and evaluation of four different energy conversion systems*
- Development, modelling and simulation of four different biomass valorization systems, three of which include gasification
- Comparison of these four systems, and identification of the most suitable one, with special interest in finding a solution for high moisture and high ash content biomasses, such as the leaves and small branches collected at the mill and at the grove among the prunnings

1.3. Thesis structure

This thesis is divided in twelve chapters. The first one compiles the introduction, the objectives and the description of its structure. Chapter 2 describes the olive oil sector in Europe, and in Spain in depth. It depicts the olive oil production methods used nowadays and describes the olive oil by-products. Further focus is given in Chapter 2 to the definition of relevant phisico-chemical characteristics of biomass in general and of the olive oil by-products, as well as to theis quantification and valorization potential.

Biomass valorization technologies are thoroughly described in Chapter 3, from direct combustion to alcoholic fermentation. Special focus is given to gasification, due to the importance of this technology in the present thesis. Chapter 4 deals with the technologies applicable to the use of biomass, differentiating between internal and external combustion machines.

Chapter 5 compares two possible systems for the olive oil industry: an externally fired gas turbine and a gasifier-gas turbine system, both using leaves and twigs as fuel. The systems are feasible and can provide electricity on scale downto 30kWe and thermal energy (60 kWth). The systems have been modelled out using Cycle-Tempo® software.

Chapter 6 comprises the study of a downdraft gasifier and gas engine fueled with olive oil industry wastes (crushed olive stones, leaves and twigs), modelled for a medium-sized olive mill (10,000 tons olives/yr), developing a simulation model to predict steady- state performance of such a CHP plant based on a downdraft gasifier, a gas cooling and a cleaning stage and a gas engine connected to the grid. This power plant provides 70 kWe and 110 kWth as sanitary hot water needed in the olive oil extraction process.

Chapter 7 comprises the modelling and simulation study of an updraft gasifier and ORC system for high ash content biomass such as olive tree leaves and twigs, with the objective to give an alternative to this type of biomass, which presents several difficulties for its energetic valorization. This system is able to produce 93.8 kW of net electrical power and roughly 412 kW of thermal power for heating necessities of the mill, with a biomass

consumption of 240 kg/h. Chapter 8 compares the results obtained and analyses the suitability of each system for the use proposed, while chapter 9 deals with the conclusion and future works in this research line.

Finally, a curriculum vitae, list of contributions, as well as a list of references are compiled in chapters 10 to 12 respectively.

Chapter 2. The olive oil sector in Europe and in Spain

Chapter 2. The olive oil sector in Europe and in Spain

2.1. The olive oil sector in Europe and in Spain

The cultivation of olive trees and the production and use of olive oil has been a well-known and established practice in the Mediterranean region for more than 7000 years. Olives, and olive oil belong to the culture and tradition of European countries, and its use is deeply rooted in these cultures. The consumption of olive oil is extended to all the European Union (EU) Member States and beyond due to its high dietetic and nutritional value, and has become an important commodity for its producting countries, as export figures increase steadily year after year [5].

Olive trees (*Olea europaea* L.) are cultivated in the EU in Croatia, Cyprus, France, Greece, Italy, Portugal, Slovenia and Spain, although most of the area dedicated to this crop is concentrated in Spain (51% of the total area cultivated), Italy (23%) and Greece (19%)[6].

Spain is the first olive oil producer worldwide, followed by Italy and Greece, [7]. The number and size of the mills depends on the quantity of olives processed and the distribution of the olive oil market in each country, [7]. In Spain, with a total of 1,760 mills, the olive oil sector is mainly centralized in the South, being Andalusia the most representative region with 818 large and medium-size mills (**¡Error! No se encuentra el origen de la referencia.**). In contrast, Italy presents a more decentralized sector with a total of 4,597 small-size mills mostly located in Puglia (905) and Calabria (730). Finally, the Greek olive oil sector is characterized by a decentralized distribution with 2,325 small-size mills, mostly located in the Peloponnesus (834) and Crete (539).

Country	No. of mills	Average olive oil production* (miles of tons)	Most important regions (number of mills)
Spain	1,760	1,253.7	Andalusia (818) Castilla la Mancha (251) Catalonia (196)
Italy	4,597	475.0	Puglia (905) Calabria (730) Sicilia (580)
Greece	2,325	322.0	Peloponnesus (834) Crete (539) Central Greece (411)

Table 1 Main olive oil producers worldwide and number of mills by country.

* Average production from 2006 to 2012.

Fig. 1 Distribution map of *Olea europaea* L. Giovanni Caudullo - Guerrero Maldonado, N., López, M. J., Caudullo, G., de Rigo, D., 2016.

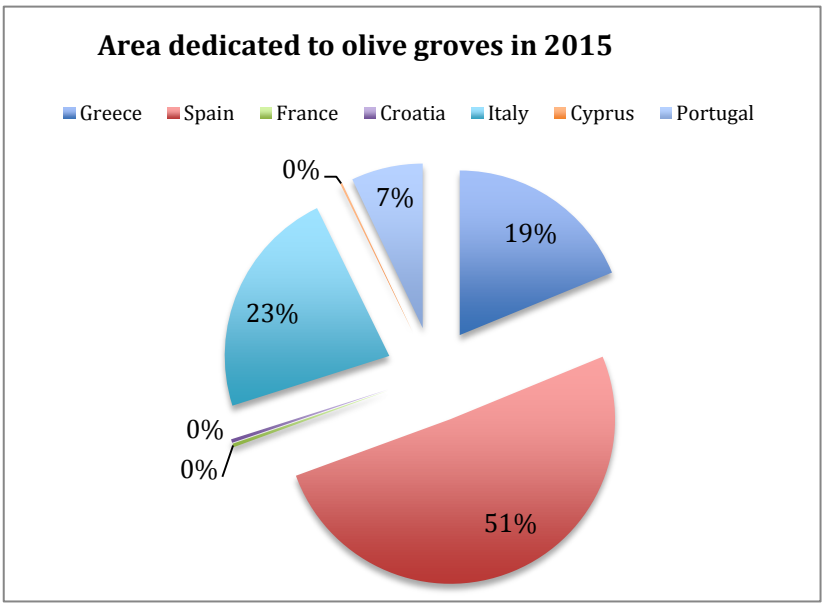

Fig. 2 Area dedicated to olive groves in 2015 [8]

In Spain, the largest producer worldwide, olive groves constitute the largest cultivated forest in Europe, with more than 180 million trees, which allows traveling for hundreds of kilometres without losing sight of this characteristical landscape, a total area of 2,503,675 ha. This surface produced 7,820,016 t of olives harvested in 2012, which resulted in 1,585,200 t of virgin olive oil [9] (1,781,500 in 2015 [10]). The olive industry is an important pillar of the economy in several regions of Spain, each year it generates around 16.650.000 days of paid work in harvesting and 15.350.000 days of paid work in other tasks (pruning, tending to the trees, etc) [11]. For this, it is a major source of employment, particularly in regions with high rates of unemployment where olive growing is the dominant monoculture. Besides having a positive impact on employment, the cultivation of olive trees generates additional benefits through the industries it supports: olive oil production, refining, packing and logistics.

After Spain, Italy follows in area planted and production (1,144,422 ha, 3,182,204 t olives collected and 543,000 t virgin olive oil produced), then Greece, (913,800 ha olive tree surface, 1,873,900 t olives harvested, and 331,200 t virgin olive oil produced) and Portugal (343,200 ha of olive groves, 443,800 t olived harvested, and 83,191 t virgin olive oil produced) [9]. Other producer countries comprise France, Slovenia, Croatia, Montenegro and Malta, with productions that only reach their domestic markets.

Olives are either pressed to extract their oil, or fermented and cured to be eaten as table olives. Table olives have a relative importance in worldwide markets, as only 8,2% of the total olives harvested are dedicated to this use. Alternatively, olive oil is without a doubt the main product obtained from olive groves, the average production worldwide for the period 2009 – 2015 being 2.911.200 tons [12].

2.2. Olive oil production methods

The basic steps in the production of olive oil are:

1. Cleaning the olives
2. Grinding the olives into a paste
3. Malaxing (or mixing) the paste
4. Separating the oil from the vegetable water and solids

How each of these steps are performed determines the overall productivity of the system and the by-products obtained. The processes used to produce olive oil are:

2.2.1. Olive presses

A very simple system, first the olives are ground into an olive paste using large millstones at an oil mill. After grinding, the olive paste is spread on fiber disks, which are stacked on top of each other, then placed into the press. Traditionally the disks were made of hemp or coconut fiber, but in modern times they are made of synthetic fibers which are easier to clean and maintain. These disks are then put on a hydraulic piston, forming a pile. Pressure is applied on the disks, thus compacting the solid phase of the olive paste and percolating the liquid phases (oil and vegetation water). The applied hydraulic pressure can go to 400 atm. To facilitate separation of the liquid phases, water is run down the sides of the disks to increase the speed of percolation. The liquids are then separated either by a standard process of decantation or by means of a faster vertical centrifuge.

Presses allow for the production of high-quality oils, but are much slower than all other methods.

2.2.2. Decanter centrifugation: three phases and two phases

The modern method of olive oil extraction uses an industrial decanter to separate all the phases by centrifugation. In this method the olives are crushed to a fine paste. This can be done by a hammer crusher, disc crusher, depitting machine or knife crusher. This paste is then malaxed in order to allow the small olive droplets to agglomerate. Afterwards the paste is pumped into an industrial decanter where the phases will be separated. Water is added to facilitate the extraction process with the paste.

The decanter is a large capacity horizontal centrifuge rotating approximately 3,000 rpm, the high centrifugal force created allows the phases to be readily separated according to their different densities (solids first, then vegetation water, then oil). Inside the decanter's rotating conical drum there is a coil that rotates more slowly, pushing the solid materials out of the system.

With the three-phases oil decanter, a portion of the oil polyphenols is washed out due to the higher quantity of added water (when compared to the traditional method), producing a larger quantity of vegetation water that needs to be processed, as well as a pomace as by-products.

The two-phases oil decanter was created as an attempt to solve the phenol washing problem. It uses less added water and therefore, reduces the phenol washing. The olive paste is separated into two phases: oil and wet pomace. This type of decanter, instead of having three exits (oil, water, and solids), has only two. The water is expelled by the decanter coil together with the pomace, resulting in a wetter pomace.

The main differences between these two extraction methods are due to water content. Two-phase pomace has moisture approximately 50-70% and contains a certain amount of sugars as a result of the presence of vegetation water, while pomace has a moisture content of between 25-30% in the press system, and 45-60% in 3-phase centrifugal systems.

Fig. 3 Residues generated in olive oil production and main characteristics of the production 2 and 3 phases systems.

2.3. Definition and characterization of the olive and olive oil industry residues and by- products

Andalucía keeps the surface used for olive cultivation practically constant, reaching 1,500,000 ha, which in an average campaign produce around 4,650,000 t of olives. From these, approximately 4,300,000 t/year are transformed into olive oil, an average of 900,000 t/year [13] . The production of olive oil generates a series of residues, or for the interest of the topic dealt with in this thesis, by-products, the disposal of which presents several hurdles as we will see in the following pages.

These "other products" are not necessarily to be seen as residues, but as an opportunity for further industrial uses, among which power generation is included:

Residue: something that remains after a part is taken, separated, or designated or after the completion of a process.

By-product: **1:** something produced in a usually industrial or biological process in addition to the principal products. **2:** a secondary and sometimes unexpected or unintended result [14]

Due to the fact that in the present thesis different solutions for the valorization of some of the "other products" obtained either in the cultivation of olive trees or in the pressing of olives into oil, we will refer to prunings, pomace or olive stones as by-products instead of residues.

The by-products result of the pressing of olives and the amounts produced by a two-phase olive mill are presented in Fig. 4 below:

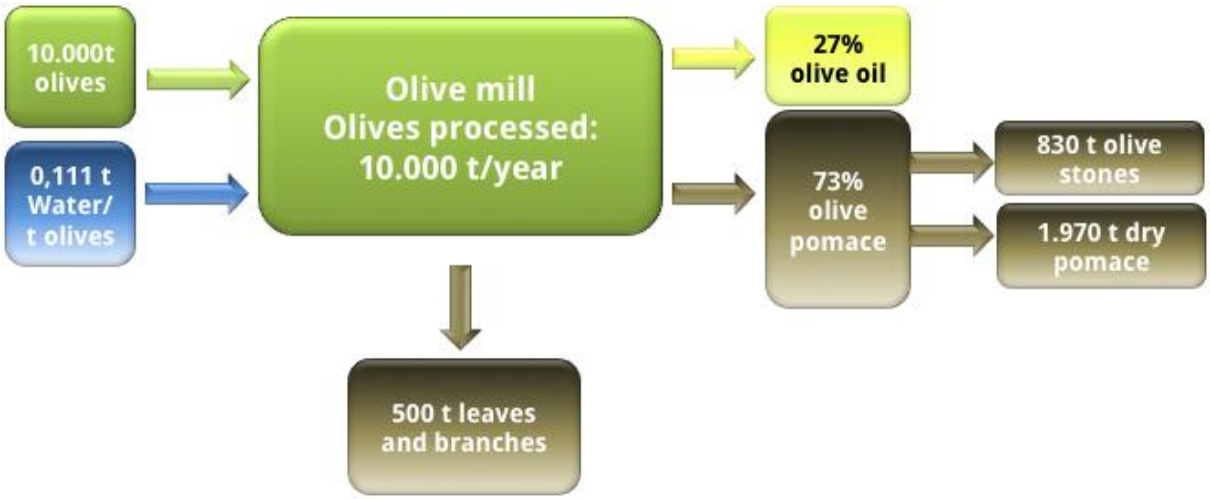

Fig. 4 Mass balance of an olive mill, taking as an example 10.000 tons of olives processed yearly.

2.3.1. Pomace

The process of extraction of olive oil consists in most of the olive mills in Andalucía of the crushing and posterior centrifugation of the olives, mostly on two-phases systems. Centrifugation separates the oil from the water, stones, pulp and skin of the fruits. This mix constitutes the pomace. One ton of olives yields approximately 0,27 ton of olive oil and

0,73 ton of pomace. Currently pomace is stored in large ponds at the the olive mill, often to be processed further, either to extract the last oil fraction present, or to dry it to a moisture content of about 40% and incorporate it into combustion plants.

2.3.2. Orujillo (exhausted pomace)

Once the pomace has been dried and its remaining oil has been extracted with hexanes, it becomes *exhausted pomace*. This by-product is suitable for combustion, with a moisture content of about 10% and a heating value of 4.200 kcal/kg in dry basis. On average, 840.000 ton of exhausted pomace are produced yearly. Its use is distributed between energy generation at the processing plant and export for co-firing. Some lighthouse projects, such as the combustion plant at Villanueva del Arzobispo operated by Energía La Loma, S.A., seek to valolrize these residues. Currently there are 63 pomace oil extraction plants in Spain, most of them located in Andalucía.

2.3.3. Olive stones

The stones are included in the pomace and later separated, either at the olive mill or at the extraction plant, crushed, with an average production of 360.000 t/year. They are an excellent fuel, due to their very appropriate characteristics: high density, average moisture of 15%, very uniform granulometry and a heating value of 4.500 kcal/kg on dry basis. This makes stones very appropriate for thermal uses both in the domestic and the industrial sectors. Additionally, they are very easy to handle, their very low particle emissions when used in combustion, as well as their odor neutrality. Their use in heating in residential areas has increased in the past decade, and the technologies used have experienced a great improvement in their performance as well as in their usability. The lower price of these stones against other fuels of similar characteristics, such as wood pellets, situate them as a preferred fuel.

Fig. 5 Olive stones collected at the olive oil mill after the extraction process

Fig. 6 Detail of olive stones

2.3.4. Leaves and twigs

Olive leaves are lignocellulosic residues usually found in two different points during the process of olive oil production. They are first found during the pruning of the trees, in which they constitute 25% of the whole pruning, but are usually burned or ground together with the remainder of the pruning by-products, such as larger branches. The second point is in

the olive mill. Leaves are separated from the fruits in the early steps of olive cleaning, and constitute 8% of the total weight that arrives at the mill [15].

Fig. 7 Olive leaves and twigs recovered from an olive mill after the cleaning stage

2.3.5. Prunings

Commonly, the olive trees producing olives for oil must be pruned every two years (trees for table olives are pruned yearly). One hectare of olive trees produces on average 3 tons of prunings, which consist in wood and leaves. Andalucía produces on average around 2.000.000 tons of these by-products every year.

Olive trees are pruned after fruit collection. Older branches are cut down, gathered into to the center of each row of trees, and further treated, within a short period, to avoid the risk of spreading vegetal diseases. Currently, two different applications for this pruned biomass are predominantly used: either it is ground and scatttered in the field as mulch [16], or by burned at the field, which is a source of environmental concerns, as well as a waste of a resource [15].

Fig. 8 Detail of olive tree prunings, chipped

2.4. Physico-chemical characteristics of biomass

The engineering properties of biomass highly affect the quality of feedstock for their use in either thermochemical applications. These properties include density, particle size, flowability, moisture content, heating value, ash content, and color, which are all important engineering properties for the design and operation of the downstream process. They also highly affect the design of handling and transportation systems, storage, and fuel conversion equipment. The most important properties for the technologies considered in the present thesis are described below:

2.4.1. Bulk density

It is a physical property defined as the total space occupied by a given amount or a group of particles . It can be determined by the following expression [17]:

$$\rho_{bulk} = \frac{total\ mass\ of\ the\ biomass\ particles}{aparent\ volume\ occupied\ by\ the\ biomass\ particles} \quad \text{Eq. 1}$$

2.4.2. Moisture content

Biomass moisture content is defined as the amount of water in the biomass expressed as a percentage of the material's weight. Moisture content has a significant effect on the engineering of the conversion process, either thermochemical or biochemical. Actually it has been estimated that an increase in the moisture content of biomass from 0% to 40% can decrease the heating value (in MJ/kg) by about 66% [18].

The moisture content can vary from less than 20% for many of the agricultural wastes, like husks and straws, and up to 60% for bagasse. Wood, which is an important source of large quantities of biomass, has a moisture content of about 40-50%.

2.4.3. Ignition temperature

Combustion of biomass is only possible if it reaches its ignition temperature. it is the lowest temperature at which a combustible substance when heated takes fire in air and continues to burn. It determines the highest temperature a fuel can be kept at in storage, as well as the lowest temperature that has to be achieved in every part of the combustion chamber. Ignition temperature usually decreases when the biomass' volatile content increases [19].

2.4.4. Heating value

The heating value of biomass is crucial to determine its energy that can be recovered during thermo-conversion. It is the energy contained in a fuel, determined by measuring the heat produced by the complete combustion of a specified quantity of it. This is expressed in kJ/kg.

The measure known as higher heating value (HHV) is determined by bringing all the products of combustion back to the original pre-combustion temperature, and in particular condensing any vapor produced.

The quantity known as lower heating value (LHV), or net calorific value, measures the heat release with water in the vapor phase [20]. It is determined by subtracting the heat of vaporization of the water vapor from the higher heating value. This treats any H_2O formed as a vapor. The energy required to vaporize the water therefore is not released as heat. LHV calculations assume that the water component of a combustion process is in vapor state at the end of combustion, as opposed to the HHV, which assumes that all of the water in a combustion process is in a liquid state after a combustion process. The LHV assumes that the latent heat of vaporization of water in the fuel and the reaction products is not recovered. It is useful in comparing fuels where condensation of the combustion products is impractical, or heat at a temperature below 150 °C cannot be put to use.

The calorific powers of biomass are determined in most cases by empirical correlations. For example, Channiwala and Parik [21] developed in 2002 a correlation for determining the HHV based on correlations existing 15 and 50 different fuels, including biomass liquid, gas and coal.

$$HHV\ (kJ/kg) = 349{,}1C + 1178{,}3H + 100{,}5S - 103{,}4O - 15{,}1\ N - 21{,}1Ash \qquad \text{Eq. 2}$$

Where *C, H, S, O, N and Ash* are the mass percentages of carbon, hydrogen, sulphur, oxygen, nitrogen and ashes, from the enemental analysis of the biomass in dry basis. This correlation is valid for the following ranges:

- 0 < C < 92%; 0,43 < H < 25%
- 0 < O < 50%; 0,43 < N < 5,6%
- 0 < ASH < 71%; 4745 < PCS < 55.345kJ/kg

The LHV of a solid fuel can be calculated using the HHV with the following relation [17]:

$$LHV(kJkg) = HHV - h_g\left(\frac{9H}{100} + \frac{M}{100}\right) \quad \text{Eq. 3}$$

Where H and M are the percentages of hydrogen and moisture, respectively. h_g represents the latent heat of the water vapor in the same units as the HHV (2.260 kJ/kg).

LHV is often used, mostly in European countries, to define efficiency in themal processes. In this way, performance expressed in terms of LHV will be higher than if the HHV is used (as it is common in the US and Canada).

2.4.5. Elemental analysis (ultimate analysis)

Elemental analysis, also known as ultimate analysis, is a process where a sample of some material is analyzed for its contents of inorganic elements, as well as moisture content. Elemental analysis can be qualitative (determining what elements are present), and it can be quantitative (determining how much of each are present). Usually the elemental analysis can be expressed with the following formula:

$$C + H + O + N + S + Ash + M = 100\% \quad \text{Eq. 4}$$

Where C, H, O, S and S represent weight percentages of carbon, hydrogen, oxygen, nitrogen and sulphur in the fuel. Moisture is represented by M, and therefore, the water content is not included in the amounts for H and O. ASH represent the ash content of the fuel.

The most common form of elemental analysis, CHN analysis, is accomplished by combustion analysis. In this technique, a sample is burned in an excess of oxygen and

various traps, collecting the combustion products: carbon dioxide, water, and nitric oxide. The masses of these combustion products can be used to calculate the composition of the unknown sample. Elemental analysis is usually costly. The following ASTM standards can be used for the elemental analysis of a fuel:

- Carbon, Hydrogen: E-777
- Nitrogen: E-778
- Sulphur: E-775
- Moisture: E-871
- Ash: D-1102

2.4.6. Proximate analysis

A more typical way of categorizing the organic composition of biomass is what is commonly called the proximate analysis: the breakdown of the fuel in moisture, volatiles, char or fixed carbon and ash. The standards used for ther analysis are [20]:

- Volatile matter: E-872
- Ash: D-1102
- Moisture: E-871
- Fixed carbon

The content of fixed carbon, "char", is calculated by subtracting from 100 the weight composition of the other compounds. Typically, controlled laboratory furnaces or specialized equipment such as thermogravimetric analyzers are used for the analysis.

Elemental (or ultimate) and proximate analyses, as well as LHV and HHV can be expressed on diferent bases:

• The "as received" composition (ar) includes the moisture content of the biomass, typically at the point of harvesting or delivery. It is the most valid composition to be used in terms of performing combustion calculations, estimating efficiencies, etc. On

the other hand, the exact as received composition is obviously affected by the moisture content and all the factors which affect it. Also, the moisture content is the most easily controlled quality parameter of the fuel, being subject to change through drying processes. As a result, the moisture of a sample may vary between the sampling point, the delivery point and the final analysis in the lab. Therefore, although extremely useful for actual applications, the *as received* composition is not typically a valid indication for comparisons between biomass types, [18].

• The "dry basis" composition (db) refers to the composition of the biomass excluding all water content. Obviously, this state can only be applicable for laboratory samples – all other types of drying in "real-life" applications always leave some of the moisture, however low, in the fuel. The dry basis is a good starting point for comparing the properties of different fuel types and is the typical format in which most laboratories report their results. Several types However, it does not take into account variations in the inorganic part of the biomass which may be due to the impact of the supply chain.

• The "dry, ash free" basis (commonly abbreviated as "daf") refers to the composition of biomass excluding all water and ash content. The dry, ash free basis is an even more ideal case than the dry basis, since actual separation of the ash from the organic part of biomass is impossible – in the laboratory and combustion applications, it is the organic part that is separated from the ash. However, this basis allows for the exclusion of all influences of the supply chain and for the direct comparison of the properties of different types of biomass fuels, [18].

Most biomass will have a higher volatile content than coals. Herbaceous biomass also tends to have slightly higher volatile content compared to woody biomass or certain agro-industrial residues; a general trend would be that the lower the lignin content, the higher the volatiles a biomass has. With waste biomass, depending on the fraction, the volatile content can be as high as 90 % of *daf*, with herbaceous it is usually in the range 70-85 and with woody biomass it is usually about 60-80 % of daf, [18].

2.4.7. Ash content

Ash is the general term used to describe the inorganic matter in a fuel. In biomass fuels, the ash content may originate from the biomass itself, e.g. materials that the plant absorbed from the water or the soil during its growth, or from the supply chain, e.g. soil collected along with biomass. In any case, after the collection of a sample the ash content is typically measured by combusting the biomass at a laboratory furnace under controlled conditions, taking into account the relevant standard EN 14775.

Following the preparation of a laboratory ash sample, European Standards exist for the determination of two main groupings of elements: minor elements and major elements. Minor elements include the following elements: As, Cd, Co, Cr, Cu, Hg, Mn, Mo, Ni, Pb, Sb, V and Zn, and should be measured according to EN 15297. Major elements should be measured according to EN 15290. They include the elements which are most abundant in the fuel ash: Al, Ca, Fe, Mg, P, K, Si, Na and Ti.

In terms of energy applications, a high ash content is not desirable, as it can produce severe problems in reactors and furnace systems [22]: Slagging and ash agglomeration due to fusion, and formation of clinkers. Ash from biomass is aggressive in nature and might corrode the gasifier, furnace and associated gas supply system.

2.5. Physico-chemical characteristics of the olive and olive oil industry residues and by- products

2.5.1. Orujo, olive pomace

Table 2 summarizes the results obtained in relevant literature for olive pomace. It is noteworthy that different studies use wet ([23,24]) or dried pomace ([25,26], which reflects in the values obtained.

	Miranda *et al.* (2012) [25]	E. Christoforou et al. (2016) [23]	P. Bartocci et al. (2015) [24]
Proximate analysis			
Moisture (%wb)	6.86	38.34	49.02
Ash (%db)	5.55	5.20	0.84
Fixed carbon (%db)	17.28	10.86	
Volatile matter (%db)	77.18	45.60	42.35
Ultimate analysis			
C (%db)	51.42	49.50	55.54 (*wb)
N (%db)	1.98	1.27	1.98 (*wb)
H (%db)	6.56	5.33	7.98 (*wb)
S (%db)	<0.1	0.09	
O(%db)	*n.d.*	43.81	34.5 (*wb)
LHV (MJ/kg) (db)	*n.d.*	19.23	*n.d.*
HHV (MJ/kg) (db)	22.03		5.7 (*wb)
Physical properties			
Bulk density (kg m-3)	780.00	920	*n.d.*

Table 2 Review of physico-chemical characteristics of olive pomace.

2.5.2. Orujillo, exhausted olive oil pomace

[a] *Calculated by difference*

	Project RESOLIVE [26] (dry pomace)	Capablo et al. (2016) [27]	Campoy et at. (2014) [28]	García- Ibáñez et al. (2004) [29]
Proximate analysis				
Moisture (%wb)	5.92	8.19	8.7	8.9
Ash (%db)	5.01	10.38	14.2	8.5
Fixed carbon (%db)	17.93	16.93	20.8	17.1
Volatile matter (%db)	71.13	64.50	65.1	74.4
LHV (MJ/kg) (db)	21.5	*n.d.*	17.3	18.5
HHV (MJ/kg) (db)	21.47	*n.d.*	18.3	19.5

Ultimate analysis				
C (%db)	51.31	41.51	53.3	52.7
N (%db)	1.99	1.56	2.1	1.6
H (%db)	6.4	5.17	6.1	7.2
S (%db)	0.26	0.33	0.17	0.07
O(%db)	34.71	*n.d.*	38.3	38.1 [a]
Physical properties				
Bulk density (kg/m^3)	*n.d.*	*n.d.*	*n.d.*	659

Table 3 Review of physico-chemical characteristics of exhausted olive pomace.

2.5.3. Olive stones

[a] *Calculated by difference*

	Zabaniotou et al. (2000) [30]	Skoulou et al. (2008) [31]	Pattara et al. (2010) [32]	Present work
Proximate analysis				
Moisture (%wb)	21.50	4.59	8.8	10.20
Ash (%db)	3.90	3.46	2.3	2.06
Fixed carbon (%db)	*n.d.*	16.39	16.2	21.58
Volatile matter (%db)	*n.d.*	75.56	72.7	76.36
LHV (MJ/kg) (db)	20.5	*n.d.*	*n.d.*	17.2
HHV (MJ/kg) (db)	*n.d.*	20.39	19.4	*n.d.*
Ultimate analysis				
C (%db)	44.30	48.61	46.5	50.08
N (%db)	0.00	n.d.	0.4	0.64
H (%db)	5.85	6.41	6.4	5.90
S (%db)	n.d.	<0.05	0	0.02
O(%db)	49.85	46.31 [a]	*n.d.*	41.03
Physical properties				
Bulk density (kg/m^3)	*n.d.*	*n.d.*	*n.d.*	709

Table 4 Review of physico-chemical characteristics of olive stones.

2.5.4. Leaves and twigs

[a] *Calculated by difference*

	García-Maraver et al. (2014) [33]	D. Vera et al. (2011) [34]	Present work
Proximate analysis			
Moisture (%wb)	11.02	4.76	8.5
Ash (%db)	14.17	4.2	8.6
Fixed carbon (%db)	11.07	16.31	19.88
Volatile matter (%db)	63.74	74.73	71.41
LHV (MJ/kg) (db)	18.01	16.3	13.0
HHV (MJ/kg) (db)	19.64	17.6	*n.d.*
Ultimate analysis			
C (%db)	45.71	47.1	45.08
N (%db)	1.56	0.55	0.52
H (%db)	6.66	6.18	5.89
S (%db)	0.11	0.1	0.09
O(%db)	*n.d.*	41.66	39.7 [a]
Physical properties			
Bulk density (kg/m^{-3})	*n.d.*	*n.d.*	108

Table 5 Review of physico-chemical characteristics of olive tree leaves and twigs.

2.5.1. Prunings

	Ramos Casado et al. (2016) [35]	Skoulou et al. (2008) [31]	Vera et al. (2014) [9]	Buratti et. Al (2016) [36]
Proximate analysis				
Moisture (%wb)	7.2	4.84	10.00 [a]	*n.d.*
Ash (%db)	4.9	0.62	3.50	1.7
Fixed carbon (%db)	13.7	8.47	17.13	18.4
Volatile matter (%db)	81.4	78.31	78.46	79.9
LHV (MJ/kg) (db)	16.19	*n.d.*	16.3	*n.d.*
HHV (MJ/kg) (db)	17.62	20.39	17.6	19.2
Ultimate analysis				
N (%db)	0.64	n.d.	0.55	0.4
H (%db)	6.2	6.41	6.18	8.3
S (%db)	0.07	<0.05	0.10	*n.d.*
O(%db)	41.06	*n.d.*	42.57 [b]	44.4 [b]
Physical properties				
Bulk density (kg/m^3)	*n.d.*	*n.d.*	184	*n.d.*

[a] *After solar drying*

[b] *By difference*

2.6. Availability of the residues in Andalucía (Spain) and their valorization potential

2.6.1. Orujo, olive pomace

According to [37], the amount of pomace produced in 2008 was 4.920.000 ton, between 600 and 650 kg of pomace produced per ton of olives. As an example, the production of 2008 once dried would produce 1.328.400 tons of fuel, representing around 524 kTPE (tons

petroleum equivalent). This would account for 5% of Spain's total coal demand. Furthermore, using these residues would represent avoiding the emission of almost 2 million CO_2 tons yearly.

The high moisture content of 2-phases olive pomace (i.e. 38,34% as described by [38], or 49,02% in [24], even though at the mill it is usually higher, between 60 – 70% entails the first problem for its valorization, as it will require a drying step for any thermochemical process or transport. On the upside, olive pomace is exclusively produced at the oil mill and kept in basins, and therefore the structures necessary for its storage are already in place at the mills.

The main valorization route that the olive pomace follow currently is the second extraction of oil with solvents.

Direct soil application as a soil amendment could be a use, considering its high potassium content [39]. However, it causes serious imbalances in the nutrient cycles in soil, and is not adequate, as for example, olive mill watewater (from 3-phases processes) is used in Italy.
Anaerobic digestion is possible, although in unstable systems. The anaerobic digestion of different by-products from olive oil production were tested, alone and mixed with other co-substrates and pre-treatments. The best results were obtained for olive pomace mixed with hen litter, a production of methane 262 Nml/goTS [40]. Positive results are also reported by Orive et al. (2016) [41], although the effect of inhibitions due to the high amount of polyphenols present is also reported. Borja et al. studied as well the digestibility of plive pomace at mesophilic temperature, [42], observing higher methane production rateswhen higher OLR were applied. Despite the good results obtained in numerous research papers, the valorisation of olive pomace through anaerobic digestion at large scale plants continues to be a challenge. Fermentation to obtain ethanol has not been thoroughly researched and will require further efforts in the future. Abu Tayeh et al. (2014) [43] isolated two strains of yeasts present in olive mill wastes, *Issatchenkia orientalis*, and *Pichia galeiformis/manshurica*. All strains were able to utilize xylose and produce xylitol but not ethanol. *I. orientalis* showed best efficiency in producing of ethanol when supplemented with glucose. Using SSF process following pretreatment of olive pomace, the average

ethanol yield was low as 3 g/100 g dry OMSW. The results of this study render fermentation as not ecomically viable.

Regarding thermochemical conversion technologies, the main focus of the present thesis, several technologies have been studied. Slow pyrolysis of olive pomace was studied by Özveren and Özdogan, (2013) [44] using thermogravimetric analysis coupled with mass spectrometry. Zabaniotou et al. (2015) [45] proposed to use the residues from the olive grove (prunings) and from the olive oil extraction (pomace) are used as feedstock to supply a pyrolysis plant. However, this authors stress the need of a drying stage as a weakness for the success oftheir model. Good results have been obtained from the investigation of the combustion behavior of pomace and their co-combustion with other fuels such as coal. The results of solid fraction combustion indicated good combustion behavior of olive kernels and the residual olive pomace, with suitable efficiency and a reduced presence of unburnts [46].

2.6.2. Orujillo, exhausted olive oil pomace

Exhausted olive oil pomace is primarily used at the extraction plant („orujera"), as this requires a drying step to bring the moisture of the pomace to approximately 8%. The hot drying gases required for this step come from the combustion of residual exhausted pomace, obtained after the extraction process. On average, 27% of each ton of olives harvested will end up as exhausted olive oil pomace. In an average campaign Spain produces about 840,000 t/year of this by-product. The consumption in power plants located in Andalucía in 2010 increased from previous years to 510,000 t, and the consumption at extraction plants reached 125,000 t, which usually fluctuate depending on the campaign. An average availability of 200,000 – 300,000 t/year can be estimated for other thermal uses and export [13].

Apart from this use, gasification has been the most studied application for exhausted pomace. García-Ibáñez et al. (2004) [29] researched the gasification of leached orujillo in a a 300 kWth atmospheric circulating fluidised-bed (CFB) gasification facility. This study found

exhausted pomace to be well suited for air gasification in a fluidised bed. Vera et al. (2011) [47] modeled a CHP system consisting of a downdraft gasifier and EFGT fuelled by olive wastes (leaves and prunings, pits/stones and exhausted pomace). The system would provide electricity on a scale down to 70 kW and thermal energy as sanitary hot water (about 160 kW). The result is a plant able to achieve an electric efficiency around 20% and overall efficiency around 65%. In this paper the electric efficiency attained with exhausted pomace is slightly lower than the one obtained with olive stones (19.1% against 19.6%), due to the fact that the gasification process with exhausted pomace yields a product gas with lower calorific value (4.35 MJ kg−1). On the other hand, thermal energy increases with exhausted pomace (about 170 kW_{th}) and the η CHP is slightly higher (65%). In general, orujillo has a high heating value but contains large amounts of alkali metals (primarily potassium), which can cause serious deposit formation and agglomeration in high-temperature processes like fluidised- bed gasification or combustion [48].

2.6.3. Olive stones

As lignocellulosic material, hemicellulose, cellulose and lignin are the main components of olive stones as well as protein, fat, phenols, free sugars and oils, these are a good fuel. On average, the olive oil industry generates 360,000 t of crushed olive stones every year [13]. Olive stones have a widespread commercial use nowadays as a preferred fuel for many domestic heating systems in Southern Spain. A 25kW boiler capable of using wood pellets and olive stones costs around 3,500 € [49]. The prices range from 0.21 €/kg (including transport, [50]) to 0.17 €/kg [51], against wood pellets (0.23 €/kg [50] – 0.25 €/kg, transport not included [51]). Although prices fluctuate depending on the season and availability of raw materials, the price of olive stones remains usually at a lower level than that of wood pellets at comparable LHV: 17.2 MJ/kg for olive stones according to [52] against 18.2 MJ/kg as characterized by [28].

As with pomace and exhausted pomace, the valorization directly at the olive mill has special relevance, as it eliminates the need to transport the fuel from source to sink. Olive stones are also a by-product of the table olive industry. 36% of all table olive industries perform

de-stoning of the olives. These stones are usually sold to olive oil mills for their further valorization [53].

Pyrolysis has been thoroughly studied, including the research of the effect of different parameters (i.e. temperature, heating rate, particle size, gas flow rate, etc.). Zabaniotou et al. (2000) [30] studied the effects of temperature on the yields and composition of the main pyrolysis products with promising results. Bartocci et al. (2015) has also studied the suitability of olive stones for pyrolysis. In this study, the high content of volatiles present in the base material allowed to obtain a gas yield of more than 40% by weight and the significant presence of methane, carbon monoxide and hydrogen gave to the produced pyrogas an interesting low calorific value equal to 16 MJ/kg [24]. Gasification has been also studied for olive stones, in Vera et al. (2011) [47] and de Caprariis et al. (2015) [54]. In general olive stones are, with prunings, the most interesting residues for energetic valorization, and the ones that have already a stablished market value.

2.6.4. Leaves and twigs

Callejo López et al. (2010) [53] calculated the available amount of leaves and small twigs collected at the mill for the campaign of 2007/2008 in 9.934 t. According to the data in this study, 35% of the leaves are composted with other agricultural residues or spread on soil. 31% is used as fodder, although as described in other works, as in Abbeddou et al. (2011) [55], their high lignin and total phenol content limited their digestibility in sheep. Callejo López et al. (2010) also point out to energetic valorization, 10% ot the total in biomass power plants and 2% for heat generation at the olive mills. 5% is burned without any energetic valorization, and 16% has no further valorization. Despite these values, the work carried out for the present thesis indicates a lower overall use of olive leaves. The use described as „spreading on soil" at the harvest or after pruning could very possibly account for a neglect in collecting the residues.

It is estimated that 5-10% in weight of the whole received at the mill are leaves and small twigs [56] [57]. The Outlook of biomass in Andalucía, prepared yearly by the Agencia

Andaluza de la Energía (Andalusian Energy Agency) presents an estimation of 8% in weight of the total olives processed are leaves and twigs, collected at the olive mills, which would entail that the total available amount of olive leaves in Andalucía would be around 345.108 t yearly.

Additionally, Velázquez Martí et al (2011) in their study about the quantification of olive tree biomass points out that leaves are 48% of the weight of all material pruned [58].
Most of the current research concerning olive leaves is focused to the extraction of valuable compounds such as phenolic compounds (oleuropein and hydroxytyrosol), as well as flavonoids with antioxidant capacity, and sugars (mannitol, oligosaccharides, etc). The concentration of these compounds in the leaves, depends on several factors including olive variety and cultivation conditions. Guinda et al. (2015) [59] reported that up to 14% of oleuropein (dry basis) was present in olive leaves, while hydroxytyrosol accounted for up to 0.94–1.12% dry weight, and therefore, there has been extensive research in extraction methods and their optimization.

Energetic valorization of olive leaves has been also studied for different technologies: García Maraver et al. (2015) [33] studied the quality of pellets produced from residual biomass from olive trees, including leaves. Their results conclude that pellets made from olive leaves exceeded the values for ash, nitrogen and sulfur that the guidelines have established for non-industrial pellets. The system modeled by Vera et al. (2011) [47], a CHP system composed of of a downdraft gasifier and EFGT fuelled by olive wastes, including leaves, obtained satisfactory results.

2.6.5. Prunings

Velázquez Martí et al. (2011) [58] carried out a study quantifying the biomass obtained from pruning olive trees. They found that the residual biomass from olive pruning reaches an average of 1.31 t/ha in trees which are pruned every year, and 3.02 t/ha in those which follow a biennial pruning pattern. The Agencia Andaluza de la Energía (Andalusian Energy

Agency) published a more conservative estimation of 2 -2.5 t/ha, without differentiating between annual and biannual pruning schemes.

The amount of biomass produced depends on the growth experienced, climatic conditions and the variety of the tree. For anual pruning, the *picual* and *manzanilla* varieties showed the highest yields (11,851 kg/tree and 11,479 kg/tree, respectively) and the *frantoio* and *grossal*, the lowest (2,431 kg/tree and 1,335 kg/tree respectively). It is important to remark that the variety *Picual* is the predominant in Jaén, the centre of olive oil production in Spain.

On energetic terms, García Maraver et al. (2012) [60] have quantified the biomass potential of olive tree residues in 803 ktoe/year, a 24% of the total biomass potential of the region.

The traditional use of olive tree pruning has been using the wood for domestic heating. Nowadays, with the dynamization of the sector experienced with the development of pellet heating systems and the valorization of agricultural residues, the use of prunings is becoming again more popular, even though currently only 20% of the total produced is valorized [13]. There is as well a great difference between different geographical areas, and there are districts where the valorization rate is negligible. There is interest in developing adequate machinery to facilitate harvesting this biomass, as described in Spinelly and Pichi (2010) [61]. Other common uses of prunings are as mulch [16], or it is directly piled up in the field and burned.

Other energetic valorization pathways have been extensively researched, due to the low moisture content and amount of available systemss for the valorization of wood. The potential of olive prunings for energy purposes have been studied by López et al. (2010) [62], García Maraver et al. (2012) [60] and Rosúa and Pasadas (2012) [63]. Prunings are often mentioned as an ingredient of mixtures for pellets, together with pomace. This allows the pellets produced to comply with the standard requirements in terms of mechanical durability and nitrogen and copper content [64]. Amirante et al (2016) studied the performance of pre-dried olive tree pruning residues directly used as solid fuel in a tri-generative power plant of about 280 kWe. This study considers of a biomass combustor, a co-generative ORC system and an absorption chiller, which ensures chilled water in the

summer. Lanfranchi et al (2016) have described large economic and environmental benefits from the valorization of different by-product os the olive oil process, including pruning, for the Valdemone DOP [65]. With regard to gasification, detailed studies of the potential of olive prunings can be found in Vera et al. (2011) [47] and Vera et al (2014) [9].

Chapter 3. Biomass valorization technologies

Chapter 3. Biomass valorization technologies

The EU's Renewable energy directive sets a binding target of 20% final energy consumption from renewable sources by 2020. To achieve this, EU countries have committed to reaching their own national renewables targets ranging from 10% in Malta to 49% in Sweden. They are also each required to have at least 10% of their transport fuels come from renewable sources by 2020.

All EU countries have adopted national renewable energy action plans showing what actions they intend to take to meet their renewables targets. These plans include sectorial targets for electricity, heating and cooling, and transport; planned policy measures; the different mix of renewables technologies they expect to employ; and the planned use of cooperation mechanisms.

After a rapid expansion in the past decade, renewables contributed 27.5 % of total gross electricity generation in 2014, compared with 14.4 % in 2004 [66]. Hydropower remained the largest source, but was declining in relative weight as wind, solar and biogas were developing rapidly.
Moreover, renewable energy provided 17.7 % of Europe's energy for heating and cooling in 2014, up from 10.2 % in 2004 [66]. Solid biofuels delivered the largest share of the total renewable share, followed by minor contributions from biogas, solar thermal, and ambient heat captured by heat pumps [66].

In this line, there have been legislative efforts to tackle the need to understand certain streams as feedstocks, and not only residues: the Biomass: Directive 2009/28/EC of the European Parliament and of the Council of 23 April 2009 on the promotion of the use of energy from renewable sources defines biomass as: 'biomass' means the biodegradable fraction of products, waste and residues from biological origin from agriculture (including vegetal and animal substances), forestry and related industries including fisheries and aquaculture, as well as the biodegradable fraction of industrial and municipal waste;

This has allowed the further technial development of the renewable energy sector and, the main focus of the present thesis, of the biomass sector in particular.

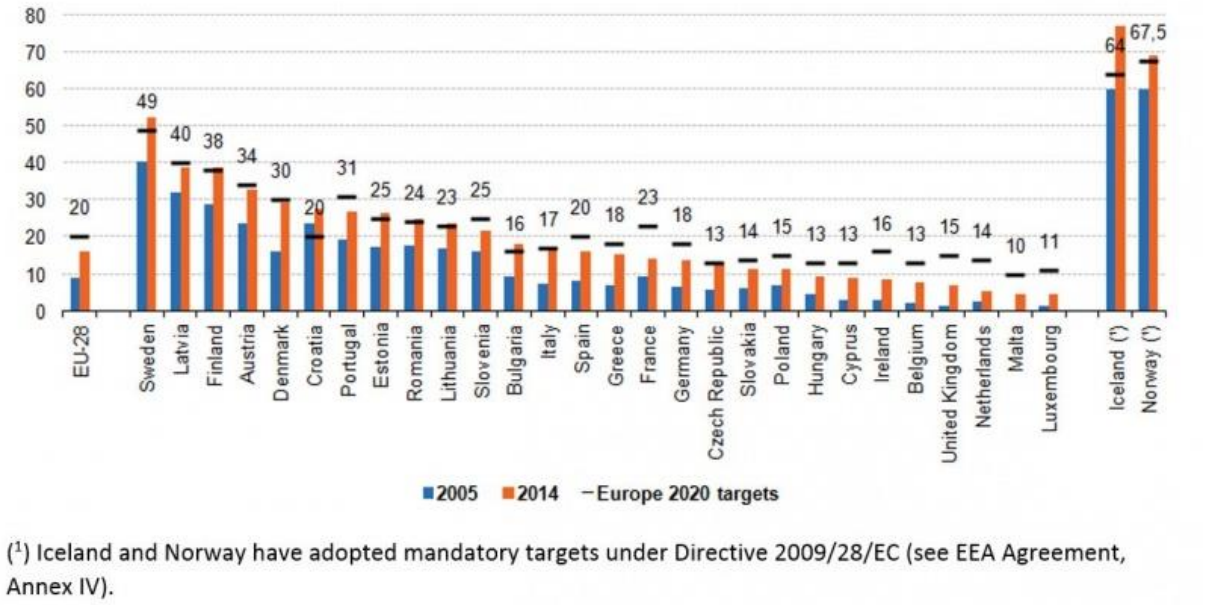

Fig. 9 Share of renewable energy in GFEC, by country, 2005 and 2014. [66]

The technologies used for this kind of renewable energy sources are experiencing a period of great development. Research is focused on increasing the energetic performance of the systems (boilers, reactors, motors, power plants, etc), minimizing the negative environmental impacts of the valorized residues and from the technologies, to increase the market competitiveness of the products and to allow new uses of high interest through preliminary treatments, such as biofuels. Therefore, energy can be obtained from biomass through the processes that will be described in the next sections:

3.1. Direct combustion

Direct combustion of biomass or incineration has been the method most used by man to generate heat. It is an exothermic oxidation reaction with air at temperatures close to 1000 ° C, and provided that the moisture content is less than 40% [67]. The LHV of residual biomass can range from 7,000 to 20.000 kJ / kg. The chemical reaction that represents the direct combustion of any biomass with air as oxidizing agent can be expressed generally as:

$$CH_aO_bN_cS_dCl_eAsh_f + n_1H_2O + n_2(O_2 + 3,76N_2) \rightarrow$$
$$n_3CO_2 + n_4H_2O + n_5O_2 + n_6N_2 + n_7CO + n_8CH_4 + n_9NO + n_{10}NO_2 + n_{11}SO_2 +$$
$$n_{12}HCl + n_{13}Ash + n_{15}C + Thermal\_Energy$$

Eq. 5

a, b, c... represent the number of atoms which conform the biomass' chemical formula (which can be obtained through its elemental or ultimate analysis). n_1, n_2,...n_{15} are the kmols/s of moisture content of biomass (n_1), air (n_2) and combustion products (n_3, n_4,..., n_{15}), respectively. The biomass ash content (*Ash*) depends of its nature. However, ash is usually made of the alkali elements, such as K, Ca, Mg, Na, Fe, Si and Al among others.

3.2. Pyrolysis

Pyrolysis is a thermochemical process which consists in heating the biomass in a rector at temperatures between 380-530°C in the absence of oxygen [67,68] thus, the constituents are transformed into a solid fraction consisting of carbon (coke), a liquid fraction (tars, aldehydes acids, ketones, water, alcohols and phenolic compounds) and another gas (primarily CO, CO_2, CH_4, H_2, C_2H_6, C_2H_4, C_6H_6, C_2H_2, H_2O). The pyrolysis products are dependent on temperature, heat ratio, particle size and biomass residence time in the reactor [67,69]. The products obtained in the pyrolysis of biomass and its possible applications are represented in the following block diagram:

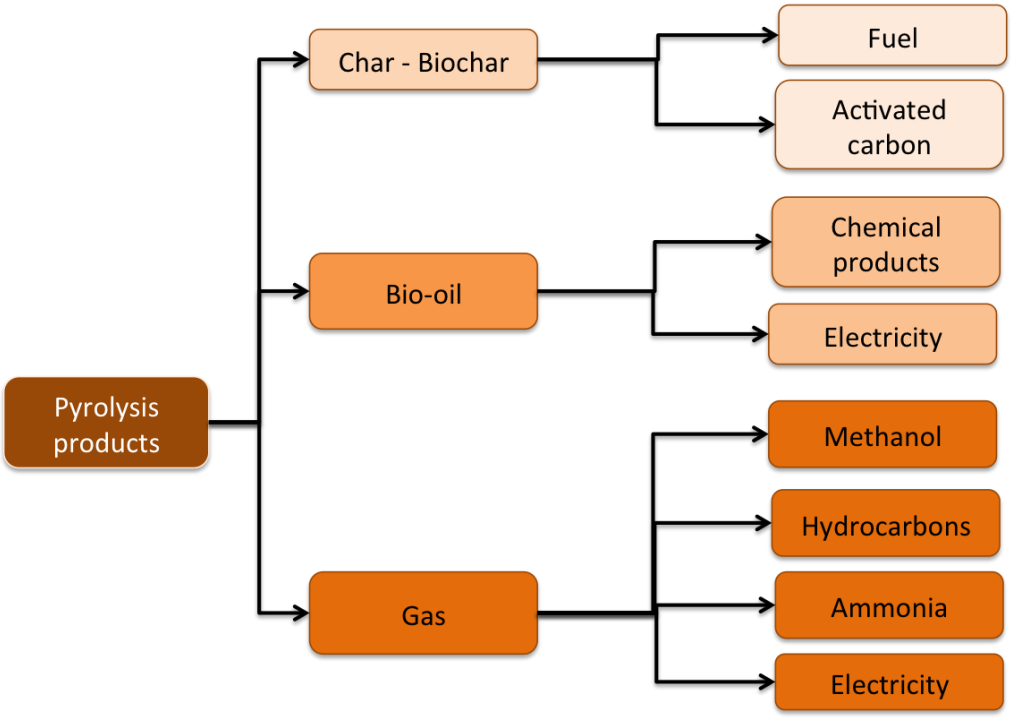

Fig. 10 Products of pyrolysis of biomass.

Table 6 compares the heating value (LHV) of gas from pyrolysis with other types of fuel, [19].

Fuel	Petroleum coke	Bituminous coal	Wood	Bio-oil	Pyrolysis gas
LHV(MJ/kg)	29-30	25-27	16-20	13-18	11-20

Table 6 LHV of different kids of fuel [19]

3.3. Gasification

Gasification is a complex thermochemical process consisting of a set of chemical reactions that occur within a bed (stationary or mobile as will be discussed), and which results in an incomplete combustion of the biomass, [70]. The lean gas[1] obtained contains CO, H_2, N_2,

[1] Lean gas, syngas or fuel gas refers to the gaseous product of low calorific obtained by the gasification of

and CH_4 among others, has a heating value of 4-10MJ / m3 which depends mainly on the type of gasification, biomass and / or gasifícation agent, [68,70]. Gasification is an intermediate step between pyrolysis and combustion. It is a two-step, endothermic process. During the first step the volatile components of the fuel are vaporized at temperatures below 600°C by a set of complex reactions. No oxygen is needed in this phase of the process.

Hydrocarbon gases, hydrogen, carbon monoxide, carbon dioxide, tar and water vapour are included in the volatile vapours. Char (fixed carbon) and ash are the by-products of the process which are not vaporized. In the second step, char is gasified through the reactions with oxygen, steam and hydrogen. Some of the unburned char is combusted to release the heat needed for the endothermic gasification reactions.

Main gasification products are gas, char, and tars. Gasification products, their composition and amount are strongly influenced by gasification agent, temperature, pressure, heating rate and fuel characteristics (composition, water content, granulometry). Gaseous products formed during the gasification may be further used for heating or electricity production. The main gas components are CO, CO_2, H_2O, H_2, CH_4 and other hydrocarbons.

3.3.1. Gasifier types

Gasification can be classified according to the following criteria:

biomass.

a) Considering the gasifying agent:

- Air
- Oxygen
- Water vapor
- Carbon dioxide

b) Form of heat supply

- Direct
- Indirect

c) Type of reactor

- Moving bed or fixed bed gasifiers
- Fluidized bed gasifiers
- Entrained flow gasifiers

The stages of the gasification process, chemical reactions and temperature are intimately linked to the type of reactor used. Mainly, the gasifiers are classified according to the mode of contact between the gas-solid medium (bed) and the gasifying agent. In this way, we can classify the gasifiers into three main types: fixed or mobile bed, fluid and entrained. According to Fig. 11, each of them can be subdivided into other types of specific gasifiers. Table 8 shows a comparison of the most important operating parameters of eacht type of gasifier, [17], [71] .

Reaction type	Reaction	
Char reduction reactions		
R1 (Bouduard)	$C + CO_2 \longleftrightarrow 2CO$	**(ΔH=+172 kJ/kmol)**
R2 (water-gas or steam)	$C + H_2O \longleftrightarrow CO + H_2$	**(ΔH=+131 kJ/kmol)**
R3 (hydrogasification)	$C + H_2 \longleftrightarrow CH_4$	**(ΔH=-74.8 kJ/kmol)**
R4	$C + 0.5\ O_2 \rightarrow CO$	**(ΔH=-111 kJ/kmol)**
Oxidation reactions		
R5	$C + O_2 \rightarrow CO_2$	**(ΔH=-111 kJ/kmol)**
R6	$CO + 0.5\ O_2 \rightarrow CO_2$	**(ΔH=-284 kJ/kmol)**
R7	$CH_4 + 2O_2 \longleftrightarrow CO_2 + 2H_2O$	**(ΔH=-803 kJ/kmol)**
R8	$H_2 + 0.5O_2 \rightarrow H_2O$	**(ΔH=-242 kJ/kmol)**
Shift reaction		
R9	$CO + H_2O \longleftrightarrow CO_2 + H_2$	**(ΔH=-41.2 kJ/kmol)**

Metanization reactions		
R10	$2CO + H_2 \rightarrow CH_4 + CO_2$	**(ΔH=-247 kJ/kmol)**
R11	$CO + 3H_2 \longleftrightarrow CH_4 + CO_2$	**(ΔH=-206 kJ/kmol)**
R12	$CO_2 + 4H_2 \rightarrow CH_4 + 2H_2O$	**(ΔH=-165 kJ/kmol)**
Methane reforming reactions		
R13	$CH_4 + H_2O \longleftrightarrow CO + 3H_2$	**(ΔH=+206 kJ/kmol)**
R14	$CH_4 + 0.5O_2 \rightarrow CO + 2H_2$	**(ΔH=-36 kJ/kmol)**
Other reduction reactions		
R15	$C + 2H_2O \rightarrow CO_2 + 2H_2$	**(ΔH=+78.7 kJ/kmol)**
R16	$CO + 3H_2O \longleftrightarrow CH_4 + H_2O$	**(ΔH=-88 kJ/kmol)**
R17	$CO_2 + H_2 \rightarrow CO + H_2O$	**(ΔH=+41.2 kJ/kmol)**

Table 7 Reactions during the reduction and combustion stages in the gasification process (reaction heat is 25°C)

Each type of gasifier is used in a given thermal power range output. For low thermal power plants (10kWt - 10MWt), fixed bed reactors are more suitable for intermediate powers (5MWt - 100MWt) than fluid bed gasifiers , Whereas for large installation powers (greater than 50MWt) the entrained type are more appropriate, [17]. Fig. 11 also shows the power application range of some of these reactors.

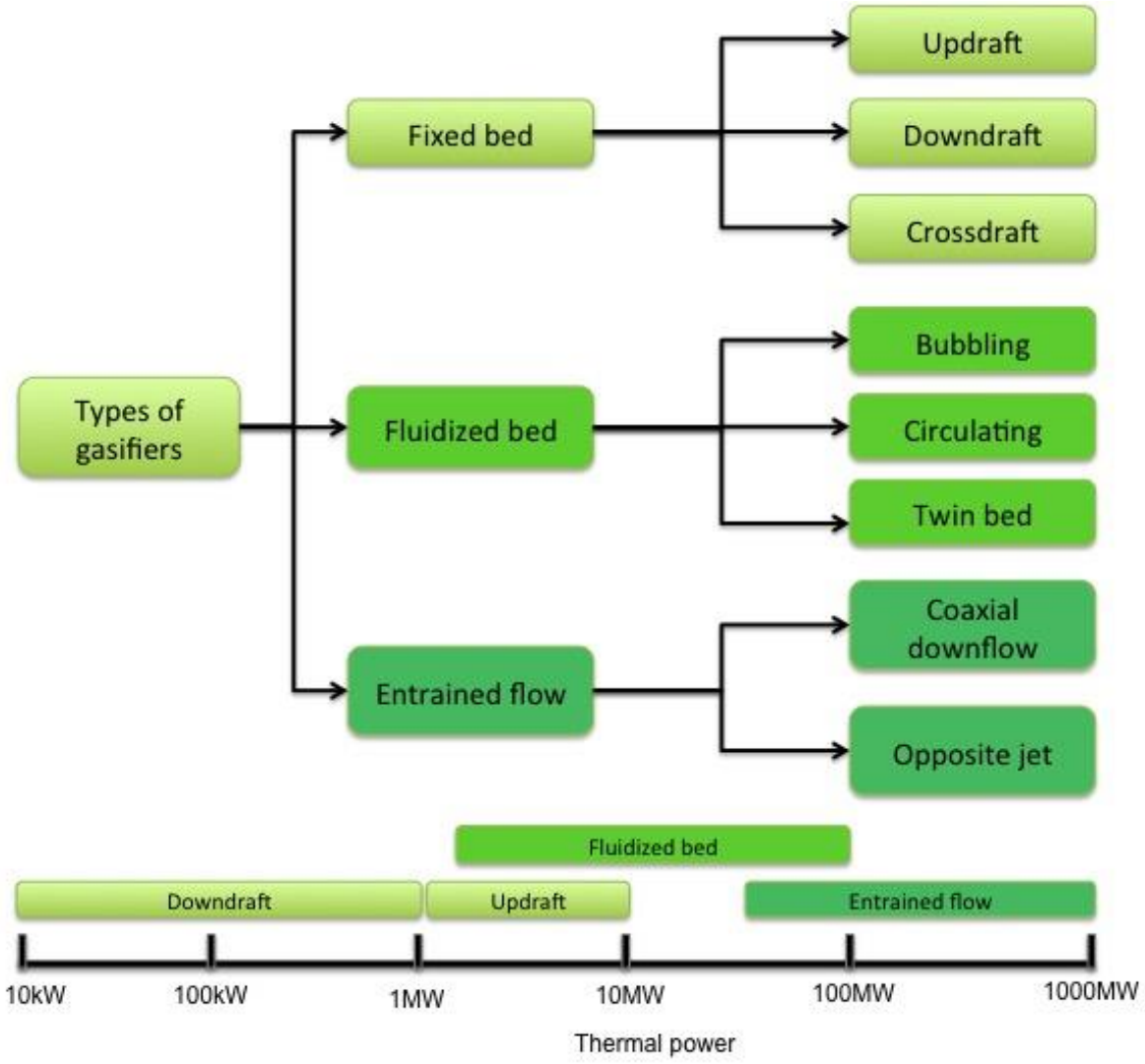

Fig. 11 Types of gasifiers and their power application ranges

Parameter	Fixed bed	Fluidized bed	Entrained bed
Biomass particle size	<51 mm	< 6 mm	<0.15 mm
Tolerance to small particles	Limited	Good	Excellent
Tolerance to coarse particles	Very good	Good	Bad
Exit temperature (°C)	450 - 650	800 – 1,000	>1,260
Raw material	Lignite and biomass	Lignite and excellent for biomass	Coal of high energetic value
Oxidant requirements	Low	Moderate	High
Steam requirements	Low-Moderate	Moderate	Low
Reaction temperature (°C)	1,000 – 1,100	800 – 1,000	1,800 – 2,000
Status of the ashes	Dry	Dry	Wet
Gasification performance	75 - 85	80 - 85	80 - 85
Power ranges (MW)	0.01 - 10	1 - 100	50 – 1,000
Residence times	Medium - Low	High	Very low
Main inconvenients	Use of small particles. Tar (updraft)	C conversion	Producer gas cooling

Table 8 Comparison of the most important operating parameters of eacht type of gasifier

- **Fixed bed gasifiers**

In fixed bed gasifiers, the fuel is introduced through the top of the reactor. The height at which the gasifying agent is injected is different. It also receives the name of „moving bed

gasifier" since the fuel (biomass) moves from top to bottom along the entire section of the reactor. Because of their simple construction, these types of reactors are designed for small-scale thermal powers (see Fig. 11). For this reason, there are at large a large number of gasification plants in operation based on fixed-bed reactors [72], [71], [73], [74]. In these gasifiers the fuel distribution, temperature and composition of the product gas is not uniform throughout the entire gasifier section.

We can distinguish three types of fixed bed gasifiers (Fig. 11) updraft, downdraft and crossdraft. In Table 9 the characteristics of each of them for wood as input fuel are summarized, [17], [70], [71].

Parameter (wood)	Updraft	Downdraft	Crossdraft
Max. admissible moisture (%)	60	25	10-20
Max. ash content (%)	25	6	0,5 – 1,0
Max. fusion temp. (°C)	> 1,000	>1,250	-
Average particle size (mm)	5 - 100	20 - 100	5 -20
Application range (MW_t)	2 -30	0.1 - 2	-
Gas exit temperature (°C)	300 - 400	700 - 800	1,250
Tars (g/Nm^3)	30 - 150	0.01 - 3	0.01 – 0.1
LHV producer gas (MJ/Nm^3)	5 -6	4- 5	4 – 4,5
Gasification performance (%)	85 -90	80 - 85	75 - 90

Table 9 Charactersitics of different types of fixed bed gasifiers

- **Updraft gasifiers**

The first gasifiers to be designed were the updraft reactors. In them, the agent or gasifying medium (air, oxygen and / or water vapor) moves up (ascending), while the fuel bed moves downwards, i.e. the gas produced and the solids that are formed flow countercurrent. As we can see in Fig. 12 the producer gas exits the gasifier at the top and air enters the bottom. The air (gasifying agent) encounters solid particles (ash and char) that descend from the top

of the reactor, where the oxygen comes into contact with the char, producing exothermic combustion reactions R4 and R5 (Table 7).

The reaction R5 consumes rapidly the available oxygen giving way (when the environment is poor in oxygen) to the reaction R4, releasing energy of moderate form (111 kJ / kmol). The hot gas formed by CO, CO_2 and water vapor (which comes from the raw material or gasifying agent) moves towards the top of the reactor, entering the reduction zone. Here, the char produced from the top is gasified according to the reactions R1 and R2 (and to a lesser extent R3 and R15). The energy (heat) required for the formation of these endothermic reactions comes from the reactions R4 and R5 formed above, the temperature of the gases formed falls.

Pyrolysis occurs above the gasification zone. The residual heat of the hot gases produced in the previous stage is responsible for decomposing the incoming biomass into low molecular weight gases, condensates (tars) and char. As the char and other solid particles descend, the gases originating in this zone are joined to the ascending ones formed in the earlier stages of reduction and combustion. After the pyrolysis, the incoming raw material is dried in the upper zone in contact with the ascending hot product gas. The resultant product gas is therefore a mixture formed by the products of the pyrolysis and those coming from the reduction zone.

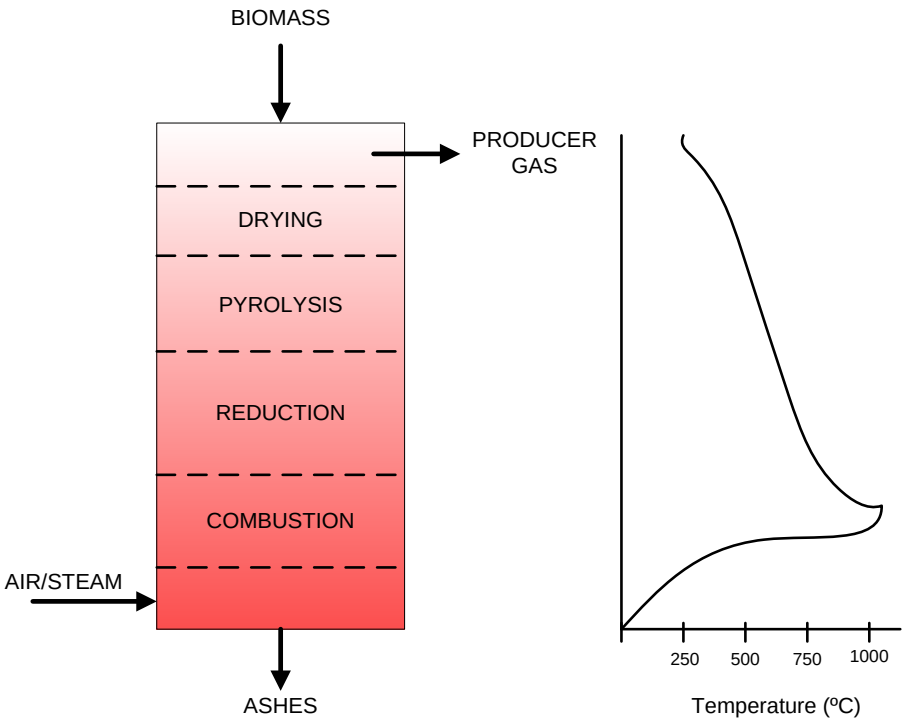

Fig. 12 Gasification stages and temperatures in an updraft gasifier

Updraft gasifiers are most suitable for biomass with high ash content (up to 25%) and humidity (up to 60%); However, they are not indicated for fuels with high volatile content. In these gasifiers the gasification performance achieved is very high (90%), [71]. In addition, they are the most suitable for direct applications of combustion of the product gas, where cooling or cleaning of the product gas is required. The product gas exits the reactor at a temperature of 400-500 ° C.

- **Downdraft gasifiers**

In the downdraft gasifiers the regions where the gasification stages occur differ from the updraft reactor. Here the gasifying agent enters a certain height of the reactor and the product gas exits the reactor from the bottom, i.e. it moves downwards along with the solid particles. As we can see in Fig. 13, the first stages of the gasification process are the drying and pyrolysis of the biomass. Pyrolysis products (low molecular weight gases, tars and char) also receive a small amount of oxygen (air) from the lower stage, causing a partial burn of these products (this process is called flamed, or flaming pyrolisis), [17]. The products

originated up to this point (together with ashes) pass to an area rich in oxygen, producing the combustion stage. Here, the char reacts rapidly releasing CO_2, CO and sufficient energy for subsequent reduction reactions. The temperature reached in this stage exceeds 1200 ° C, [17], [70]. This facilitates the thermal cracking[2] of the tars formed in the pyrolysis step.

Finally, the high temperature gases from the combustion (CO_2 and CO), together with the remaining unreacted char and water vapor (from the biomass and / or the gasifying agent) go to the last stage of reduction. In this zone the temperature decreases as a result of the endothermic reactions that generate CO and H_2. However, the outlet temperature of the product gas remains above 700 ° C, [17], [71].

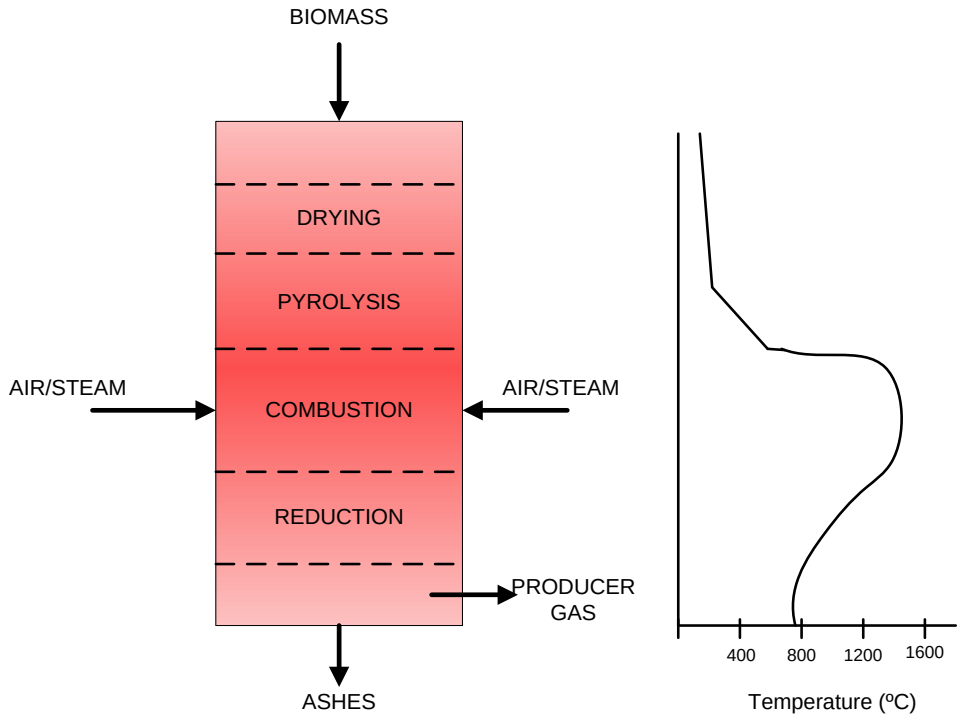

Fig. 13 Gasification stages and temperatures in a downdraft gasifier

[2] Thermal cracking is the decomposition of large molecules that form a compound in gases lightweight low molecular weight (CO_2, CO, H_2, CH_4, ..., coke), and requires very high temperatures (> 1000 ° C)

Depending on the construction and design of a downdraft gasifier, we can distinguish two types: strangled or non-strangled (or open center), [17]. Its difference lies mainly in that the central zone (where the combustion stage occurs) where there is a strangulation of the reactor section. A reduction in the reactor section (at the height where the combustion stage occurs) forces all the products from the pyrolysis to pass through that zone, facilitating the thermal cracking of most of the tar. In Table 8 we can see the main characteristics of the downdraft reactors as well as the purpose and restrictions of use.

- **Crossdraft gasifiers**

In this type of gasifiers, the fuel is also introduced through the top of the reactor, while the gasifying agent (air) is injected at a high speed through the lateral zone (see Fig. 14). The producer gas is released from the side opposite the air injector. These types of reactors are designed for the gasification of coal with low ash content, [17]. The excess air near the injector facilitates combustion of part of the char, creating an area at very high temperature (> 1500°C), [71].

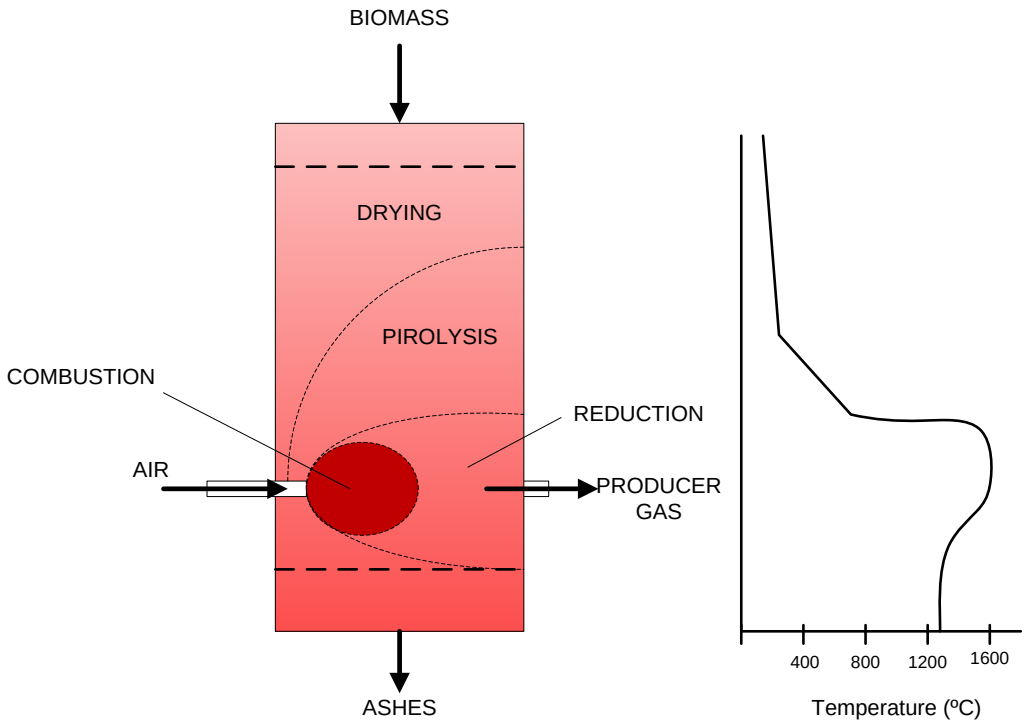

Fig. 14 Gasification stages and temperatures in a crossdraft gasifier.

The non-oxidized char is converted to CO in the next reduction step. The heat released by the rapid combustion of the char goes to the pyrolysis zone, thus contributing to the decomposition of the incoming biomass. This type of gasifiers are used for small scale units. In addition, due to the low production of tar (0.01 -0.1 g / Nm^3) and rapid response to load changes, its application is very attractive in ICE small scale, [17]. Other characteristic features of this type of fixed bed reactor can be seen in Table 8.

- **Fluidized bed gasifiers**

A fluidized-bed gasifier is shown in Fig. 15. The bed supports the solid fuel while the gasifying agent moves upwardly during the complete gasification process. The result is the formation of whirls that favor the gas-fuel mixture. In a first phase, the fuel particles rapidly reach the temperature required for drying and pyrolysis, producing gas, tar and char. The oxygen (air) inlet at the bottom of the reactor is rapidly associated with the solid carbon particles suspended in the bed, the combustion reactions (R4, R5 and R8, Table 7). The heat released by these reactions is transferred rapidly through the entire fluid bed, the reactor reaches a uniform temperature. As the gas rises, the endothermic reduction reactions (gasification) are formed. In this type of gasifiers, the product gas is displaced from the bottom of the reactor to its top outlet (resembling a flow-piston system). In order to avoid the melting and subsequent agglomeration of ash in the reactor walls, these gasifiers operate in the temperature range between 800-1,000° C and at a pressure of up to 10 bar, [17].

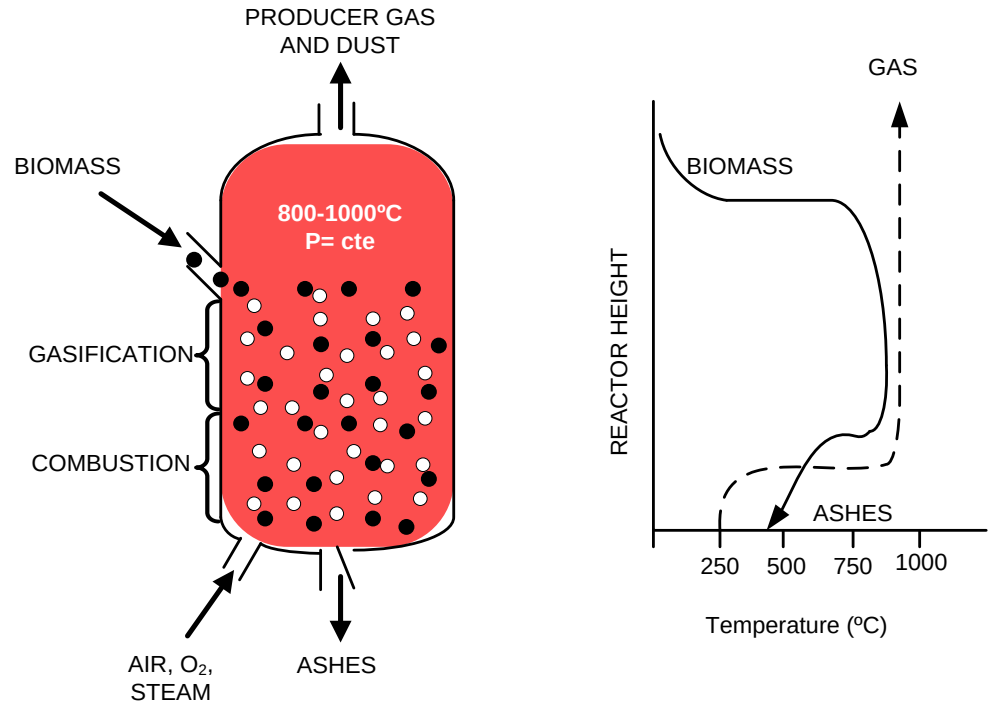

Fig. 15 Bubbling fluidized bed gasifier and temperatures profile.

Fluid bed gasifiers have the drawback of not achieving complete conversion of the char particles, since many of them become part of the fluid bed and usually leave the reactor together with the product gas. For this reason, to improve the conversion efficiency of the carbon contained in the biomass, the small char particles (not gasified) leaving the reactor are separated in a cyclone and returned by the bottom [71]. Another important drawback is the poor response to charge change, ie, the biomass needs high residence times in the reactor.

The advantage of these reactors lies in the properties of the fluid bed: Temperature, pressure and uniform product gas composition. They have a high flexibility in the type of biomass that can be used, although this must be previously ground to obtain a good fluidization in the bed, [75]. In addition, the production of tars is not very high (1-50 g / Nm^3). There are two main types of fluid bed reactors: bubbling fluidized bed and circulating (cilculating fluidized bed). The main difference between both lies in the hydrodynamics of the bed, that is, the fluidization rate is much higher in the circulating fluid bed gasifiers (3.5-5.5 m / s) than in the bubbling bed (0, 5-1.0 m / s), [17],[71].

- **Entrained flow gasifiers**

These gasifiers operate at high gasification temperatures (> 1400 ° C) and pressure (20-70 bar), [17], [71]. Preferably, they are used in high-power gasification plants (> 50MW_t) where the fuel is usually coal, petroleum coke or refinery waste. Its use is ideal with most of the existing coals, except those with low energy properties such as lignite, [76].

The fuel (normally sprayed) is introduced into the reactor next to the gasifying medium, producing the combustion reactions (R5 first and R4). When working at high pressures (about 70 bars), the fuel and gasifying agent are usually mixed with water, facilitating the feed system. In this case, a kind of mud is formed whose main drawback lies in the size of the reactor, i.e. large volumes are needed to evaporate the high amounts of water mixed with the fuel, [17]. Combustion reactions consume all the oxygen introduced, giving rise to the reduction reactions of char in an atmosphere rich in CO_2 and H_2O (mainly R1, R2 and R15).

Entrained flow gasifiers are characterized by a low production of tars, a very short residence time (on the order of seconds), high temperatures and working pressures, high conversion performance of coal particles and very suitable for the generation of synthetic gas (high content in CO and H_2 and low in CH_4), [17]. Depending on the fuel and oxidizing agent inlet zone, these gasifiers can be classified into downstream reactors (the input occurs from the top), or from opposite flows (lateral input), [70].

3.4. Anaerobic digestion

Anaerobic digestion is the biochemical conversion of organic material into combustible gas, which is composed mainly of methane and carbon dioxide, called biogas. By bacterial action, biomass is converted to biogas in an anaerobic environment (absence of oxygen). This process applies to all biodegradable biomass, both primary and secondary. Systems of this kind of are mainly classified into suspended and fixed biomass systems. The biogas can

be used as fuel in microturbines, combustion engines and fuel cells in order to generate heat and power, (Combined Heat and Power, CHP), [67,77].

3.5. Alcoholic fermentation

It is the production of liquid fuels from vegetables. This chemical process transforms the carbohydrates vegetal biomass (with large sugar content) in alcohol (ethanol) by the action of microorganisms such as yeasts that produce enzymes which catalyze the reaction, [67].

Chapter 4. Technologies applicable to the use of biomass

Chapter 4. Technologies applicable to the use of biomass

Distributed Generation (DG) refers to the generation of electricity in a decentralized manner, i.e. geographically distributed over the area that is serviced and close to the consumer of energy (which often is the owner of the facility), [3,4]. This concept has gained great importance compared to traditional systems of electricity production in large hydro and thermal plants connected to the transmission grid.

In the present thesis the definition of distributed generation definition proposed by Ackermann et al. [78] is used, in which GD is considered as a source of power generation connected directly to the power grid or the low-voltage grid. The definition of GD is therefore in terms of the location and connection to the generator system. Although this definition does not impose any restriction on either the technology used or the production capacity of the plants, in general, we can say that these plants are smaller than the core of traditional generation, while the maximum capacity of the generators included in GD has been increasing in recent years (up to 10 MW, 50 or even 100 MW).

Distributed systems encompass the so-called alternative energies (for they constitute an alternative to conventional) or renewable (for use inexhaustible fuel), within which it is included therefore biomass. Among GD technologies for the processing of biomass into electricity and / or heat we highlight the following:

4.1. Internal combustion machines

4.1.1. Steam turbines

Steam turbines are turbomachines for the production of electricity through a fluid at high pressure and temperature (usually water vapor). Thermal plants based on steam turbines develop the The most common type of biomass-fueled power plant today uses the conventional Rankine cycle [20]described in Figure 2.5, [79]. A steam power plant consists

essentially of: turbine (coupled to an electrical generator), pump (normally coupled to an electric motor), condenser (connected to a cooling tower) and a steam generator (boiler large). The installation is completed by a system of storage, transportation and fuel supply, and other auxiliary systems.

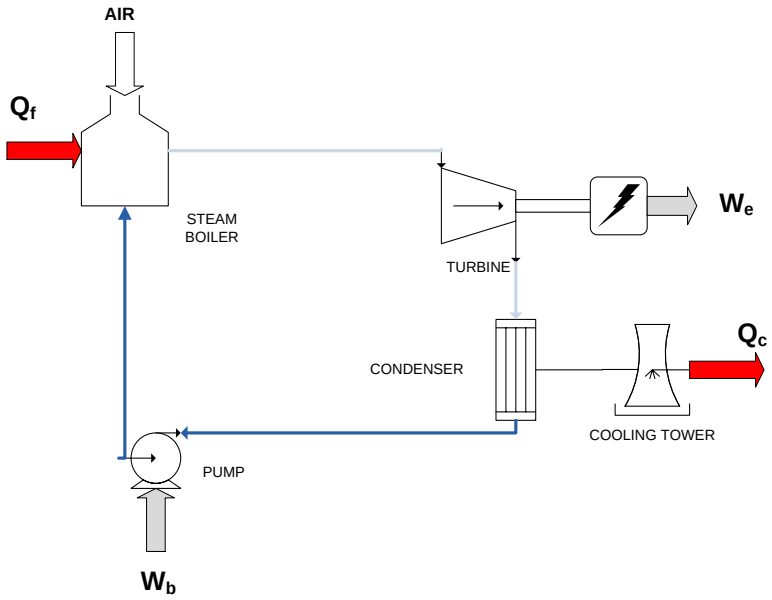

Fig. 16 Simplified diagram of a steam plant (Rankine cycle).

The thermal energy required (Q_f) for obtaining the water vapor at certain thermodynamic conditions is obtained in the combustion chamber. The fuel is burned by the action of an oxidizing agent (usually air in excess) obtaining the necessary heat energy (Equation 6, [79]). To date, traditional high power steam power plants (> 100 MW) use fossil fuels like coal, natural gas, gasoline, etc. to achieve the steam thermodynamic characteristics required.

$$Q_f\,(kJ) = \eta_{cc} m_f PCI_f \qquad \text{Eq. 6}$$

Where η_{cc} expresses the combustion efficiency (currently very efficient boilers where this performance can reach values of 95-98% are designed), m_f the flow of fuel injected into the combustion chamber (kg), and PCI_f represents the lower heating value the fuel used (kJ/ kg).

Currently, development and commitment worldwide to DG systems make steam turbines remain relegated to the background, as for power generation to small-medium scale (5 kW-50MW, [78]) this technology is less cost effective and efficient than other technologies such as microturbines and gas internal combustion engines [75,80]. Besides, these latest

technologies allow the development of production systems which use electricity and heat simultaneously (Combined Heat and Power, CHP). However, biomass is currently taking a very important role as a partial substitute for coal in traditional steam power plants, are so-called co-combustion or cofiring plants, [81]. Currently, developed countries such as Norway, Finland, Germany and Denmark are betting heavily on the replacement of much of the coal consumed (arriving at some plants to 40-50%) by wood pellets. The central co-combustion of biomass and coal offers a number of very attractive advantages, [81,82].

- Significant reduction in emissions of gaseous pollutants (SOx, NOx), particulate matter and CO_2: In addition to providing an opportunity to combat climate change help meet the Kyoto protocol [83], this type of plant offers economic advantages as cost reduction in CO_2 emission. For example, in 2011 Spain spent about 770M € in the purchase of CO_2 emission rights and has become the second country after Japan, that purchased the most more CO_2 emission rights [84]. Currently the price of a tonne of CO_2 emitted is 5.90 € [85].
- There are incentives from governments to generation companies and projects that promote the reduction of greenhouse gases. The co-combustion plants are thus incentivized in this regard.
- In terms of large-scale generation, the energy efficiency of co-combustion plants is significantly higher than plant using the same technology centers using only biomass.
- The investment required for the adaptation of old coal plants to plants co-firing with biomass is relatively low compared to biomass plants of the same power. According Splitehoff [81], capital investment in a biomass combustion plant cost is around € 2,500-3,000/kW_e of installed capacity, while adapting to a central co-combustion (coal-biomass) requires a capital investment of 300 €/kW_e (associated to the % substitution of biomass).

4.1.2. Organic Rankine cycle (ORC)

The Organic Rankine Cycle (ORC) is operationally similar to a typical Rankine cycle but uses an organic fluid as working medium instead of water. Basically, the ORC is composed of the following components: a pump, evaporator, turbine and condenser (Fig. 4a). The pump supplies the organic fluid to the evaporator at the working pressure (1-2 process), here the fluid is heated and vaporized (2′-3). The steam enters into the turbine where it is expanded close to the condensation pressure (3-4) and, finally, it is condensed to saturated liquid (4-5). In order to improve the thermal efficiency, an internal heat exchanger is used to recover the thermal energy at the turbine outlet (point 4) and preheat the compressed organic fluid before the evaporator (2-2′ process). Fig. 4b shows the T-s diagram for a typical organic fluid with superheated conditions at the turbine inlet.

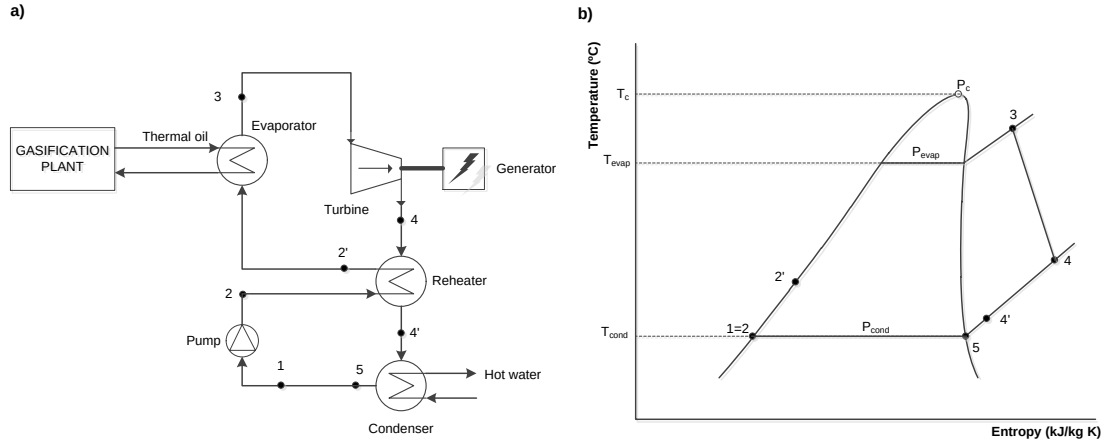

Fig. 17 a) ORC plant layout; b) typical T-s diagram with internal heat exchanger and superheated conditions.

The ORC thermal efficiency with an internal heat exchanger is defined as follows:

$$\eta_{ORC} = \frac{P_t - P_p}{Q_{in}} \quad \text{Eq. 7}$$

$$P_t = \dot{m}_{org}\,(h_3 - h_4)\,\eta_{e-m} \quad \text{Eq. 8}$$

$$P_p = \dot{m}_{org} (h_2 - h_1) \eta_{e-m}$$ Eq. 9

$$Q_{in} = \dot{m}_{org} (h_3 - h_{2'})$$ Eq. 10

Where the subscript t means turbine, p: pump, org: organic, e-m: electro-mechanical.
In ORC applications, the proper choice of the organic fluid is crucial in order to guarantee reliable operations and maximize the system efficiency. The fluid selection depends strongly on both the heat source temperature and the configuration of the ORC; also, the environmental aspects are very important here. There are some recommended fluids which have been recently used in most of the studies and/or the commercial ORC plants for high temperature sources as biomass combustion (>900°C). Some of them are, toulene (T_c= 318.6°C), ethylbenzene (T_c= 344°C), decane (T_c= 344.55°C) and cyclohexane (T_c= 280.5°C), [86].

ORC is commonly applied for low-temperature sources as the exhaust gases of IC engines (< 350°C), hot water (<140°C) and low-temperature geothermal, [86–88]. In this case, most of the documented research studies include a screening of suitable working fluids based on different criteria such as their environmental impact and thermo-physical properties, [87]. On the other hand, high temperature waste heat (specifically from biomass) coupled with ORC is not very common and must be investigated in depth. Zhang *et al.*, [89], carried out a comparative study based on various CHP systems which regard ORC as a bottoming cycle to recover the engine's high temperature exhaust heat, also R123, R245fa and R600a for ORC system are considered to analyze the influence of working fluids. Algieri and Morrone, [90], presented a comparative study of several ORC working fluids used for biomass applications (>900°C), the critical conditions for pressure and temperature were assessed in depth for cyclohexane, decane and toluene; moreover, the authors studied the impact of a real application case in the Sibari district (Southern Italy). Drescher and Brüggemann, [91], carried out a simulation approach to choose the best working fluid applied for biomass CHP plants, reaching the best performance results for the family of alkylbenzenes.

Only a few authors have focused on the combination of biomass gasification with ORC technology for small-scale generation. Under this scope, Arena *et al.*, [92], reported a techno-economic evaluation of a CHP plant which includes a bubbling fluidized bed reactor, a MILD combustor, a 400kWe ORC generator and an air pollution control system feeding the gasifier with solid recovered fuel. In the same way, Rentizelas *et al.*, [93], carried out a techno-economic comparative study of two CHP systems: biomass combustion with ORC and biomass gasification with an IC engine. Finally, the investigation of the theoretical performance of a distributed generation plant made up of a gasifier, internal combustion engine and ORC machine as a bottoming unit was studied by Kalina in [94]. The aim of this study was to maximize de electricity production from biomass in the case where there is no heat required.

Currently EFGTs and Stirling engines are not technologies developed at industrial scale and most of the works presented in the literature focus on small CHP prototypes supported by specific R&D programs or funding by their local Governments, [95–98]. In contrast, ORC systems are a growing technology, and more than one hundred ORC plants are now operating to generate electricity and heat commercially, [99]. Also, ORC systems have been applied to diverse fields including industrial waste heat, solar thermal power, geothermal heat, biomass combustion heat, and engine exhaust gases among others, [100]. ORC manufacturers such as ORMAT, Turboden, BNI, Adoratec, UTC, and Electratherm have been present on the market since the beginning of the 1980s. For example, in Europe, more than 120 ORC plants are in commercial operation, with sizes ranging from 0.2 to 2.5MW using biomass combustion heat, [100].

ORC technology is commonly applied for low-temperature sources as the exhaust gases of IC engines (< 350°C), hot water (<140°C) and low-temperature geothermal, [86–88]. In this case, most of the documented research studies include a screening of suitable working fluids based on different criteria such as their environmental impact and thermo-physical properties, [87]. On the other hand, high temperature waste heat (specifically from biomass) coupled with ORC is not very common and must be investigated in depth. Zhang *et al.*, [89], carried out a comparative study based on various CHP systems which regard ORC as a bottoming cycle to recover the engine's high temperature exhaust heat, also R123, R245fa

and R600a for ORC system are considered to analyze the influence of working fluids. Algieri and Morrone, [90], presented a comparative study of several ORC working fluids used for biomass applications (>900°C), the critical conditions for pressure and temperature were assessed in depth for cyclohexane, decane and toluene; moreover, the authors studied the impact of a real application case in the Sibari district (Southern Italy). Drescher and Brüggemann, [91], carried out a simulation approach to choose the best working fluid applied for biomass CHP plants, reaching the best performance results for the family of alkylbenzenes.

Only a few authors have focused on the combination of biomass gasification with ORC technology for small-scale generation. Under this scope, Arena *et al.*, [92], reported a techno-economic evaluation of a CHP plant which includes a bubbling fluidized bed reactor, a MILD combustor, a 400 kWe ORC generator and an air pollution control system feeding the gasifier with solid recovered fuel. In the same way, Rentizelas *et al.*, [93], carried out a techno-economic comparative study of two CHP systems: biomass combustion with ORC and biomass gasification with an IC engine. Finally, the investigation of the theoretical performance of a distributed generation plant made up of a gasifier, internal combustion engine and ORC machine as a bottoming unit was studied by Kalina in [94]. The aim of this study was to maximize de electricity production from biomass in the case where there is no heat required.

4.1.3. Internal Combustion Engines

A combustion engine is a type of machine that obtains mechanical energy directly from chemical energy of a fuel that burns inside (or outside) of a combustion chamber, the main part of the engine. Depending on the location of the combustion chamber they can be classified into two types: internal combustion engines (Otto and Diesel) and external combustion (Stirling), which will be discussed in 4.2.

The internal combustion engine (ICE) is the most widely used technology for use as power supply in case of emergency, and although the power range that this technology can be

used is very wide, it is more common use as equipment for generation below 1MW. There are two types of internal combustion engines: diesel engines (using mainly diesel fuel, but which can work from other products derived from biomass such as biodiesel) and gas engines or spark ignition (fueled with natural gas, biogas or gasified biomass). Generally, the efficiency of diesel engines is greater than the gas engines (which develop an Otto cycle). Most internal combustion engines used for power generation (also called stationary engines) are four-stroke engines [101].

Currently, there are numerous applications where biomass by ICEs can be utilized in electrical systems, thermal generation and transportation:

- The lean gas or synthesis gas from gasification of biomass can be used in gas engines for use in systems DG, [72,102]. Fig. 18 shows a gasification plant installed in Ubeda (Spain) result of the European-Funded Project RESOLIVE [26]. This plant has an ICE which is fed with synthesis gas from the gasification of residues from the olive industry (unsing olive stones and olive prunings). The plant is capable of generating 70kW$_e$ and 150kW$_t$.

Fig. 18 Gasification plant (left) with a gas motor Cummins ® G855G (right), operated with syngas from the gasification of biomass.

- There are also numerous applications where the biogas from the anaerobic digestion of waste from farms, landfills and sewage treatment plants is burned at an ICE for the generation of in-situ electrical and thermal energy, [103]. In Figure 2.7 we can see

a biogas plant from the anaerobic digestion of manure in Styria, Austria. This plant has an ICE which is capable of generating 500kW$_e$ and around 600kW$_t$, [104].

Fig. 19 Biogas plant using anaerobic digestion of manure (left) with a Jenbacher® gas motor (right).

- Nowadays, biodiesel from rapeseed and palm oil are used in ICEs. These biofuels reduce polluting emissions maintaining efficiency of a conventional diesel engine.
- In some countries the bio-alcohol or ethanol, derived from the alcoholic fermentation of biomass has been used for some years as a partial or total substitute for gasoline in an ICE Otto cycle, known generically as gasohol. Otto engines require minor modifications to use ethanol instead of gasoline or ethanol / gasoline blends. The bio-alcohol can even be mixed with diesel for diesel cycle engines.

The cost of generation units based on ICEs is the lowest among the DG technologies, but the costs of operation and maintenance are among the highest. Among the main disadvantages of using ICEs are:

- The maintenance cost, highest among GD technologies due to the large number of moving parts.
- NOx emissions are highest among GD technology, although it is true that the use of natural gas, biogas or gasified biomass as fuel reduces these emissions.
- The noise produced is low frequency and therefore, more difficult to control than other technologies; However there are mechanisms to achieve the attenuation of this noise.

Some of the features that make this technology attractive are:

- The initial investment required is the lowest of DG technologies.
- The efficiency obtained is good (from 28% to 42% of PCI).
- Cogeneration is possible recovering heat in the exhaust gases (the temperature of the gases resulting in combustion can be more than 400 ° C).
- Modularity is excellent and it allows serving with this technology loads ranging from kW to MW.

4.1.4. Gas turbines

A gas turbine (GT) is a type of heat engine that extracts energy from a flow of gases from the ignition of compressed air and a liquid or gaseous fuel (typically natural gas). Gas turbines usually operate on the principle of the Brayton cycle, [80,101]. According to the scheme of Fig. 20, fresh air at ambient conditions is introduced into the compressor where its temperature and pressure rise. The high pressure air continues towards the combustion chamber where it is mixed with fuel and combusted at constant pressure. Later, the high temperature gases which are entering the turbine, where they expand to atmospheric pressure, producing mechanical work. Engines in gas turbines, the temperature of the exhaust gases exiting turbine usually quite higher than the temperature of the air leaving the compressor. Therefore, the high pressure air leaving the compressor can be heated by transferring heat from hot exhaust gases in a counterflow heat exchanger, which is also known as a regenerator or recuperator. If the exhaust gases leaving the turbine are exhausted out (not recirculated), the cycle is classified as an open cycle.

Traditional gas turbines are characterized by generating electrical power on a large scale (in the order of hundreds of MW) it is also very common their use in combined cycle (gas turbines and steam). In this thesis, GD applicable to technologies will be studied, which can be used with biomass fuel, more specifically waste from the olive industry. Within the broad field of development of gas turbines, we will focus on gas microturbines (MTs) and externally-fired gas turbines (EFGT).

4.1.5. Microturbines

MTs are a type of turbines that have passed the stage of experimental prototype to become an alternative for the generation of electrical energy on a small scale. Current technology trends for small MTs in the range of 30-200 kW can allow building a large number of them in series and not on demand as in the higher power. The designs combine the reliability of gas turbines in the aviation industry with the low cost of automotive turbines.

Basically, a MT comprises of a simple stage radial compressor and turbine and a recuperator which allows using the heat of exhaust gas in the turbine outlet (see Fig. 20). Part of the great success of microturbines is due to advances in the field of electronics, which have allowed MTs operate unattended and to can be connected to the commercial power network. Power electronics is used to convert the unregulated supply power to a useful form, preventing the alternator having to be synchronized with the grid. In addition, the DSP (Digital Signal Processing) technology allows controlling efficiently not only the power electronics but the system as a whole. The design and manufacture of the recuperator is complex because these elements have to be able to work under high pressure and subjected to considerable temperature gradients.

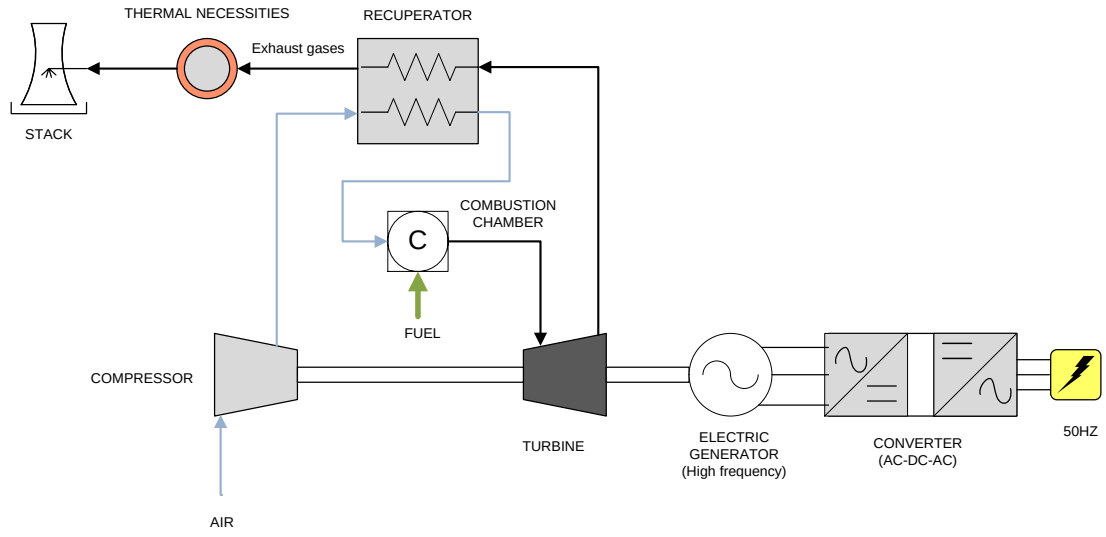

Fig. 20 General scheme of a gas microturbine for distributed generation.

The main features of this technology include the following [80,105]:

- The most distinctive feature of microturbine technology over other technologies based on gas turbines is the high speed rotation of the turbine. The turbine rotates up to 120,000 rpm and generator to 40,000 rpm.
- The MTs can use low combustion temperatures which allows for low NOx emissions. They also have a small weight and reduced dimensions which facilitate their installation.
- Low levels of noise emissions (70 dB at 1 meter away).
- The investment cost is not too high and the maintenance cost is lower than other technologies because they require very few moving parts (sometimes only the axis). fixed costs of € 800-1300 / kWe are estimated [80,106].
- The generating units available, allow to achieve power range 25-200 kW and can be easily combined to generate greater power.
- The efficiencies achieved in DG systems using microturbines typically vary from 25% to 40%. In cogeneration systems efficiencies above 50% are possible, and even reaching efficiencies of 60-70% in hybrid systems (e.g. fuel cell), [107,108].
- Fuel flexibility: they can use natural gas, diesel, ethanol and biogas.

MTs represent a relatively new technology and in development. It is the topic of numerous research, especially in the use of renewable energies such as biomass,[109–111]. Currently, there are different microturbines manufacturers such as Capstone®, Honeywell®, Elliot®, Turbec®, etc. For example, Turbec® markets their model T100 microturbine consisting of a single microturbine shaft with operating pressure to 3.5 bar, an air mass flow of 0,75kg / s, at a turbine inlet temperature of 950°C and generates 100kWe, [112].

This model achieves an electrical efficiency of 30% using natural gas at ISO conditions. The T100 model includes a system of waste heat recovery from the exhaust gases to produce domestic hot water (DHW).

4.2. External combustion machines

4.2.1. Externally-fired gas turbines

As in Stirling engines, externally-fired gas turbines (EFGT) are characterized in that the ignition of the fuel is located on the outside of the gas turbine, i.e., it is done in an external combustion chamber at constant pressure. The operating principle of a EFGT is described in Fig. 21 [112]. The solid fuel (biomass) fed to an external combustion chamber with hot air from the turbine outlet. Combustion gases arising are introduced to a heat exchanger high efficiency and raising the temperature of the air from the compressor to the inlet temperature of the turbine. The cooled flue gases can be used for waste heat recovery system (for example, ACS systems). The control valve fulfils the task of introducing the amount of combustion air required required by the external combustion chamber.

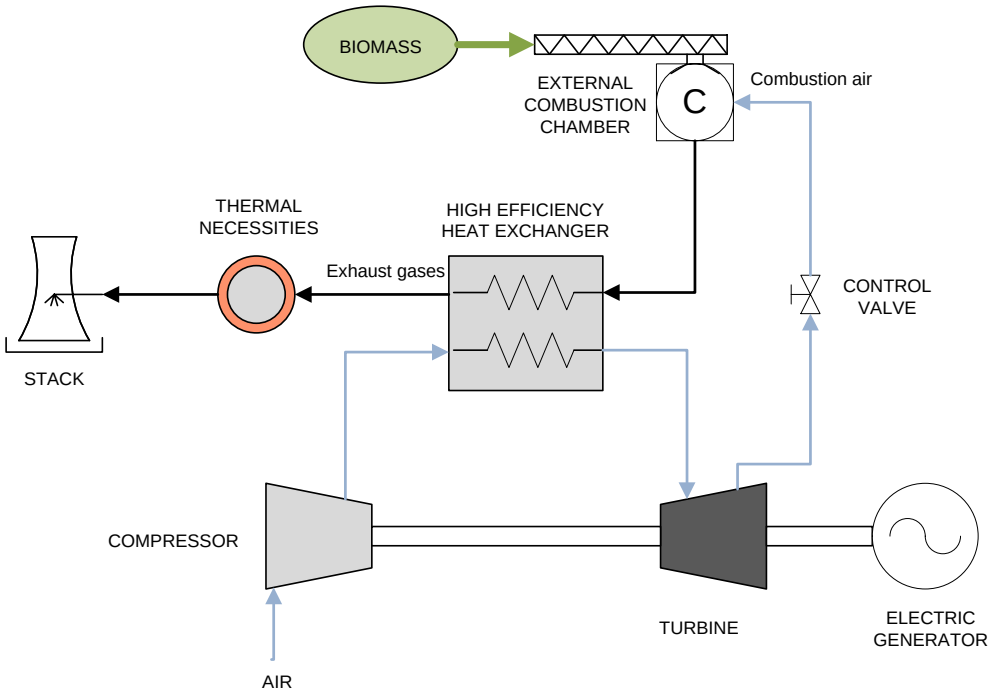

Fig. 21 Basic scheme of an externally fired gas turbine fueled with solid biomass.

Today, this type of technology is experiencing strong growth and development, as it offers a number of advantages to take into account with respect to conventional MTs (internal combustion), [112–114]:

- Allows the direct use of solid biomass as fuel without being transformed into biogas or syngas. Conventional MTs require liquid or gaseous fuel introduced into the system at the pressure governing the combustion chamber. This causes an additional power consumption for the compression of said fuel. With EFGT this does not entail a critical problem because the available external combustion chamber can use all types of fuels (including solid such as biomass).
- The use of gaseous fuels of low or medium energy density (syngas or biogas) requires the modification of the injectors of the combustion chamber of existing MTs, as they are designed initially for natural gas. This entails spending on research and development for current major manufacturers and thus represents an obstacle in its development applied to the use of biomass. Currently, Capstone® sells some microturbine models (internal combustion) operating with biogas from anaerobic digestion, called CR (Capstone Renewable), manufactured in modules from 30kW to 1MW of electrical power, [115]. Conversely, there is no manufacturer who produces MTs using with the syngas from biomass gasification.
- In EFGT the fluid flowing through the expansion turbine is simply air (at high pressure and temperature), this causes the blades are not being subject to the possible effects of corrosion and wear as in the case of conventional MTs. In the case of MTs using biogas, a very important aspect is the content of H2S, because if the cleaning phase of biogas is not optimal, the turbine blades may be exposed to corrosion, therefore decreasing their useful life.

The main drawback of this type of technology is the high efficiency heat exchanger. The maximum allowable working temperature for this system is at around 100-150°C above the air inlet temperature to the turbine, [34,112]. In addition, the low heat transfer coefficients of air and flue gas entails manufacturing heat exchangers of a considerable size (necessary to increase the exchange surface), which make this tehnology more expensive. In the long run, EFGT could experience a leap in their development, especially with the development of ceramic materials, capable of withstanding operating temperatures 1200-1300°C.

4.2.2. Stirling engines

In an external combustion engine, fuel ignition it is located on the outside (outside the cylinders) and is carried out at constant pressure [101]. When the working fluid of these engines is air, H_2 or He, it performs the cycle known as Stirling (in honor of its discoverer Robert Stirling (1816)). Heat transmission from the external combustion chamber is transferred to the working fluid through a regenerator (high efficiency heat exchanger). This type of engine has superior performance to internal combustion engine (Otto or diesel), [101].

Nowadays due to their low noise emmissions, Stirling engines are mainly used in submarines and yachts as auxiliary power generators. However, there is a broad field of research associated with the use of these motors and their application in solar concentrators [116] and in systems of electric and thermal generation (CHP) biomass [117,118]. Fig. 22 shows the layout of a power plant and 200 kW_t 75kW_e using a Stirling engine 8-cylinder and is fueled with wood chips. The plant was built in 2005 in Austria and has an electrical efficiency of 27% and an overall efficiency (CHP) of more than 85% [119].

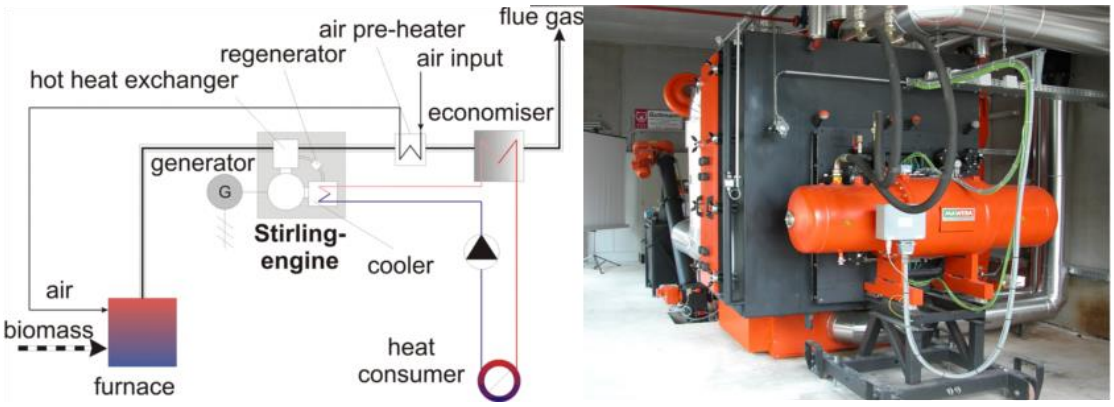

Fig. 22 Scheme of a power plant based on a Stirling engine and fueled with biomass (Upper Austria, Austria).

The most important advantages of the Stirling engine are as follows:

- The working fluid in the Stirling engine (air, He or H2) are never released to the outside, so there are no intake valves or exhaust, or gases under high pressure or

explosions inside the cylinders as in the ICE . This is the reason that Stirling engines are so quiet.

- Application in small-scale systems (DG) and in cogeneration plants (CHP). In addition, Stirling engines have higher yields to achieving high cogeneration yields MCI [101].
- The Stirling cycle uses an external heat source, which can vary from fossil fuels to solar energy and biomass. Combustion does not occur inside the cylinders.

Among the main and most important disadvantages of this technology we include its high investment cost (€ / kW_e). Stirling engines are under extensive research, so it is still early for their commercialization and large-scale application. Currently, the only power plants based on Stirling engines are based on pilot plant results of research projects funded by different means, [119].

4.3. Fuel cells

Fuel cells (FCs) are based on the use of electrochemical conversion devices similar to energy batteries, but which differ from these in that are designed to allow continuous replenishment of the reactants consumed. A single device (sometimes called cell or fuel cell) allows a voltage of approximately 1.2 V. To obtain higher voltages, several cells are connected in series forming a fuel cell stack, typically more than 45 cells are used to form the stack. In addition, part of the heat produced can be used, which makes this an interesting technology for cogeneration applications (CHP).
The basic unit consists of three main elements [75]:

- The anode to which fuel is supplied.
- The cathode where the oxidant element is supplied (usually air).
- The electrolyte that allows the ion flux (but not of electrons and reactants) from anode to cathode.

The net chemical reaction is identical to the one that would de obtained if the fuel would burn, but due to the spatial separation between the reactants, the electrochemical cell conducts electron current that flows spontaneously from the reducing element (fuel) to the oxidant (oxygen) for its use in an external circuit. That is, in a fuel cell an electrochemical direct fuel conversion occurs avoiding intermediate transformations that occur in common conversion devices (chemical → mechanical → electrical), this is the main reason for the high efficiency of this type of device.

Any substance susceptible to chemical oxidation and continuous supply can be used as fuel. Probably the most interesting fuel cell system is based on the oxidation of hydrogen to form water vapor as the sole product. The hydrogen used as fuel has a high reactivity in the presence of suitable catalysts, and can achieve a high energy density. However, hydrogen does not occur in nature freely and energy is needed to extract it from water (electrolysis), from hydrocarbons or from biomass. Some methods for obtaining hydrogen include reforming [3] the methane, the partial oxidation of fossil fuels, water electrolysis, decomposition of methanol or ethanol, and from biomass by thermochemical processes such as gasification, alcoholic fermentation or anaerobic digestion.

Table 10 shows a summary of the above technologies, [80,120], [121–125].We have studied all the technologies applicable to DG that can be used as biomass fuel or derived from it (biogas, syngas). As it can be gleaned from the table, ICEs offer some of the best possibilities in the use of biomass for electricity and heat generation. Although its performance is not the highest and operating costs and maintenance are the highest, it offers many advantages over other technologies lesser degree of R&D. ORC shows also promising properties at a higher investment cost, despite a lag in its development, which is the problem shared by other technologies.

[3] Catalytic reforming is a process by which hydrogen (H_2) is obtained from gaseous hydrocarbons, whose main component is methane (CH_4). The reformed consists basically in separating carbon from hydrogen.

Tech. Family	Technology	Distr. Generation	CHP	Use of biomass	Development	Typical power range (MW)	Investment cost (€/kW)	Electric efficiency	CHP efficiency
Rankine	Steam					> 1	6.00-1.000	22-37	-
	ORC					0,1-2	1.500-2.000	18-24	65-75
Combustion engines	ICE					0,05-20	300-600	25-45	50-55
	Stirling					0,05-0,1	1.000-1.500	29-40	65-75
Gas turbines	Microturbines					0,025-0,3	600-900	28-33	50-58
	EFGT					0,01-0,2	2.000-4.000	20-30	50-60

Table 10 Summary of technologies reviewed for distributed generation (DG). Costs, efficiencies and ranges

From all the by-products of the olive oil industry, olive tree leaves and prunings have the most straightforward path to valorisation. In the present thesis the performances of four different technologies are studied and compared: an externally fired gas turbine and gasifier-gas turbine system, a downdraft gasifier and a gas engine, and an updraft gasifier and ORC system.

Chapter 5. Comparison between externally fired gas turbine and gasifier-gas turbine system for the olive oil industry

Chapter 5: Comparison between externally fired gas turbine and gasifier-gas turbine system for the olive oil industry

The performace of two CHP systems is evaluated: a fixed bed biomass gasifier with a conventional gas turbine (FBG-GT) and a biomass combustor with an externally fired gas turbine (EFGT). Both systems are capable of producing 30kW$_e$ and domestic hot water (DHW). The following pages will explain the system and work performed.

5.1. Gasifier and conventional gas turbine

The gasifier modeled is a FBG (fixed bed type), downdraft, stratified and with an open top. These gasifiers can handle biomass with moisture contents lower than 20% and they operate at atmospheric pressure wit ha reaction temperature around 800-900 °C ([126], [127]). The proposed system consists of a fixed bed reactor (downdraft), gas cooling and cleaning section where ash, dust, tar and inorganic impurities are removed from the product gas, and a microturbine using the clean gas (Fig. 23).

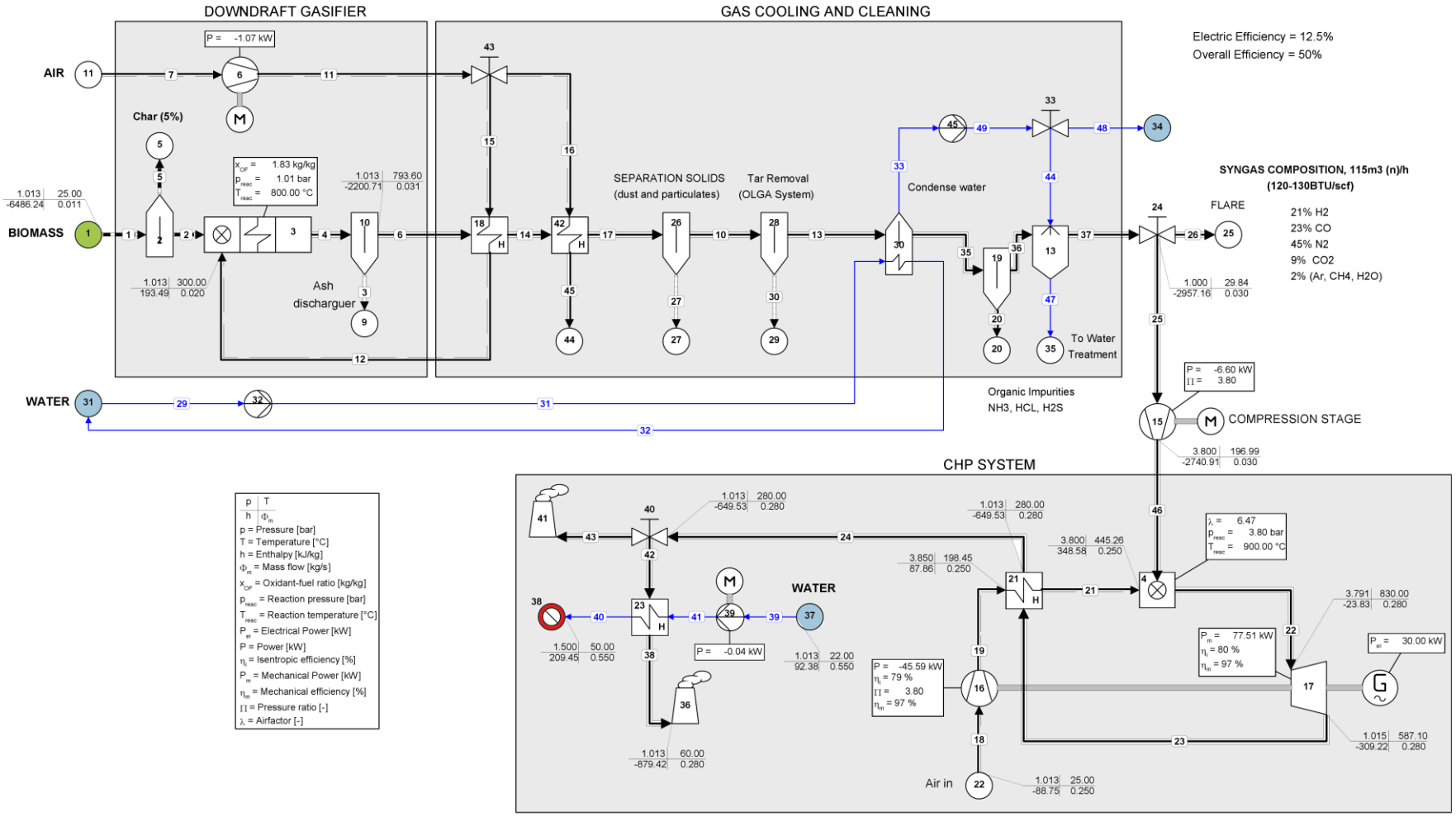

Fig. 23 Cycle-Tempo® gasifier-gas turbine system (FBG-GT).

The gas cleaning takes place at temperatures above tar dew point [128]. Previously, the clean gas must be compressed at combustion chamber pressure (internally fired gas turbine) in order to produce electrical power (30 kW_e). Turbine exhaust is used to produce sanitary hot water (SHW) at 45 °C (about 60kW_{th}). The model and simulation of the biomass power plant have been performed with Cycle-Tempo® software. This program employs a Gibbs free energy minimization based routine. The procedure is use for equilibrium calculations in the gasifier model and combustor model. Details of these models are available in the Cycle-Tempo® manual [129] and in other similar works such as Aravind et al. [130], Toonssen et al. [131], Carlos R. Altafini et al. [132] and Colonna and Gabrielli [133]. The assumptions used in the simulations are:

- The CHP system is operating in steady state.
- Environment and reference state at T0 ¼ 298 K and P0 ¼ 1.013 bar.
- It is assumed that residence time is sufficient to achieve the gasifier equilibrium mode.
- Ashes are mainly composed of SiO_2, Al_2O_3 and Fe_2O_3.
- The product gas is at the gasifier temperature (800 °C).
- It is assumed a 5% of unconverted carbon (char) [132,134].
- According to De Souza-Santos [135], it is assumed external gasifier losses around 2% of the thermal fuel input.

This CHP system comprises the following subsystems:

5.1.1. Gasifier subsystem (blocks: 2, 3, 10 and 18)

The air blown fixed bed type (down-draft) gasifier is operating at atmospheric pressure and 800 °C temperature. The gasifier reaction temperature is adjusted by specifying the air (oxidant)/ biomass ratio, x_{OF}. It should be noted that the preheating of gasifier inlet air up-to 275-300 °C (using waste heat of gas cooling subsystem) increases gasification efficiency around 3-4%. Gasification efficiency is calculated according to eq. 11, [123,136].

$$\eta_{gasif} = \frac{m_{p.gas} LHV_{p.gas}}{m_{biomass} LHV_{biomass}} \quad \text{Eq. 11}$$

5.1.2. Gas cleaning and cooling

Purification of product gas is very important for all applications, except for direct combustion after the gasifier. In general, in the gas cleaning-cooling subsystem can be identified the following gas treatment steps (Fig. 23).

1. Product gas cooler: gasifier exit temperature (800-850 °C) is cooled up to 400-450°C through several heat exchangers (blocks 18 and 42). Noticed that this stage shall exchange heat between two gases, which are very hot. This requires a lot of surface and costly materials.
2. Particle and dust removal: cyclone and filter (block 26).
3. Organic impurities (block: 12, 14 and 28). Tar removal is most important and, in this paper, it is proposed an OLGAtar removal system [128]. OLGA operates above the water dew point, but decreases the tar dew point to a level under the lowest process temperature; thereby, tar and water are not mixed.
4. Water steam removal of product gas by water condenser (70-90 °C to 35°C, block 30).
5. Removal of inorganic impurities (NH_3, HCl, H_2S, etc.) by scrubber technology (blocks 13 and 19).

5.1.3. CHP subsystem: microturbine

The Brayton cycle has been also modeled with the aid of Cycle-Tempo® software [137]. The basic structure of a real microturbine consisting of an air compressor, recuperator, combustion chamber and expansion turbine (in Fig. 23, blocks no. 16, 21, 4 and 17 respectively). A fuel booster compressor (block 15 in Fig. 23) brings the clean product gas at the combustor operating pressure. An ambient air stream is used for combusting the product gas fuel and in the first step it is compressed to a pressure of 3.8 bar [138]. The high pressure air proceeds into the combustion chamber, where the fuel is combusted at constant pressure. The resulting high-temperature gases then enter to the turbine, where they expand to the atmospheric pressure while producing power (30 kW_e). Values for important parameters used in the system calculations are given in Table 11 [115,130,138]. In

this thesis, turbine exhaust heat has been used to obtain a water flow of 35 l/min at 45 °C (about 60kW$_{th}$ of DHW.

Table 11 summarizes the values of important parameters used in the system calculations.

Performance characteristics	Value
Nominal electrical power (kW)	30
Isentropic efficiency for gas turbine (%)	80
Isentropic efficiency for gas turbine compressor (%)	78
Mechanical efficiency for gas turbine (%)	97
Mechanical efficiency for gas turbine compressor (%)	97
Isentropic efficiency for other compressors, blowers and pump (%)	76
Mechanical efficiency for other compressors, blowers and pump (%)	95
Turbine exhaust temperature (°C)	275-285
Turbine inlet temperature (°C)	830
Generator efficiency (%)	90
ac/dc/ac conversion efficiency (%)	97

Table 11 Microturbine system: typical performace parameters

5.2. Gasifier and externally fired gas turbine (EFGT) power plant

The externally fired gas turbine (EFGT) is different from the directly fired gas turbine in that the combustion process takes place outside the working fluid circuit. This has the following implications:

- The combustion process takes place at atmospheric pressure.

- A high temperature (and efficiency) heat exchanger (HTHE) is required to transfer heat to the gas turbine working fluid.
- Clean air is expanded through the turbine.
- The EFGT may be realized either with solid, liquid or gaseous biofuels.
- The cycle can employ dirty and low cost fuels.

The use of product gas in conventional gas turbine can involve several problems [113,139]:

- Gas turbines are sensitive machines that require extremely clean gas to avoid damage in the turbine blades (erosion, incrustation and corrosion) and blockage of filters and fuel injectors. This requires installation of expensive gas clean up system, consisting of scrubbers, ceramic filters, cyclones etc., at the gasifier outlet (Fig. 23).
- In the FBG-GT described in Fig. 23, the producer gas must be compressed to the operational conditions of the internal combustion chamber. Thus, the system requires installation of a gas compressor and an additional electric consumption. This decreases the electric and overall efficiency of the gasification plant.
- The low calorific value of the gas produced necessitates a high fuel flow. It calls for a design modification in the combustor and the turbine inlet guide vanes.

Most of the components of the EFGT are standard parts. The only new items are the HTHE and the combustor for alternative fuels. The biomass is directly burned in a furnace at atmospheric pressure (preac) and reaction temperature of 950°C (Treac). The thermal energy of combustion gases are transmitted to the turbine through HTHE. The size of the heat exchanger and the material cost are two important considerations that decide the economy of the plant. The present HTHE is composed of nickel based super alloys and it allows the turbine inlet temperature to reach 830 °C [114,139]. In this work, the modeling and simulation of the EFGT plant has been carried out using Cycle-Tempo® software [137]. Next, the operating parameters like biomass consumption, turbine inlet temperature, air factor (l), pressure ratio (P), HTHE efficiency will be analyzed.

5.2.1. Plant description

Fig. 24 displays the Cycle-Tempo® scheme of the CHP system (about 30k W_e and 60 kW_{th}) based on EFGT system. The biomass feeds the external furnace (block 8) together with the hot air from the turbine exhaust (pipe 10), the combustion process is carried out at atmospheric pressure and 950°C. The air amount must be sufficient for the complete combustion process of the biomass, this amount is controlled by air ratio, through by-pass valve (block 9). The high temperature gases produced by the biomass combustor are cooled in the high temperature heat exchanger (HTHE, blocks 4 and 5) by heating the compressed air up to required turbine inlet temperature (about 825-830 °C). The exhaust waste heat is recovered in a low temperature heat exchanger for hot water production (blocks 12 and 13).

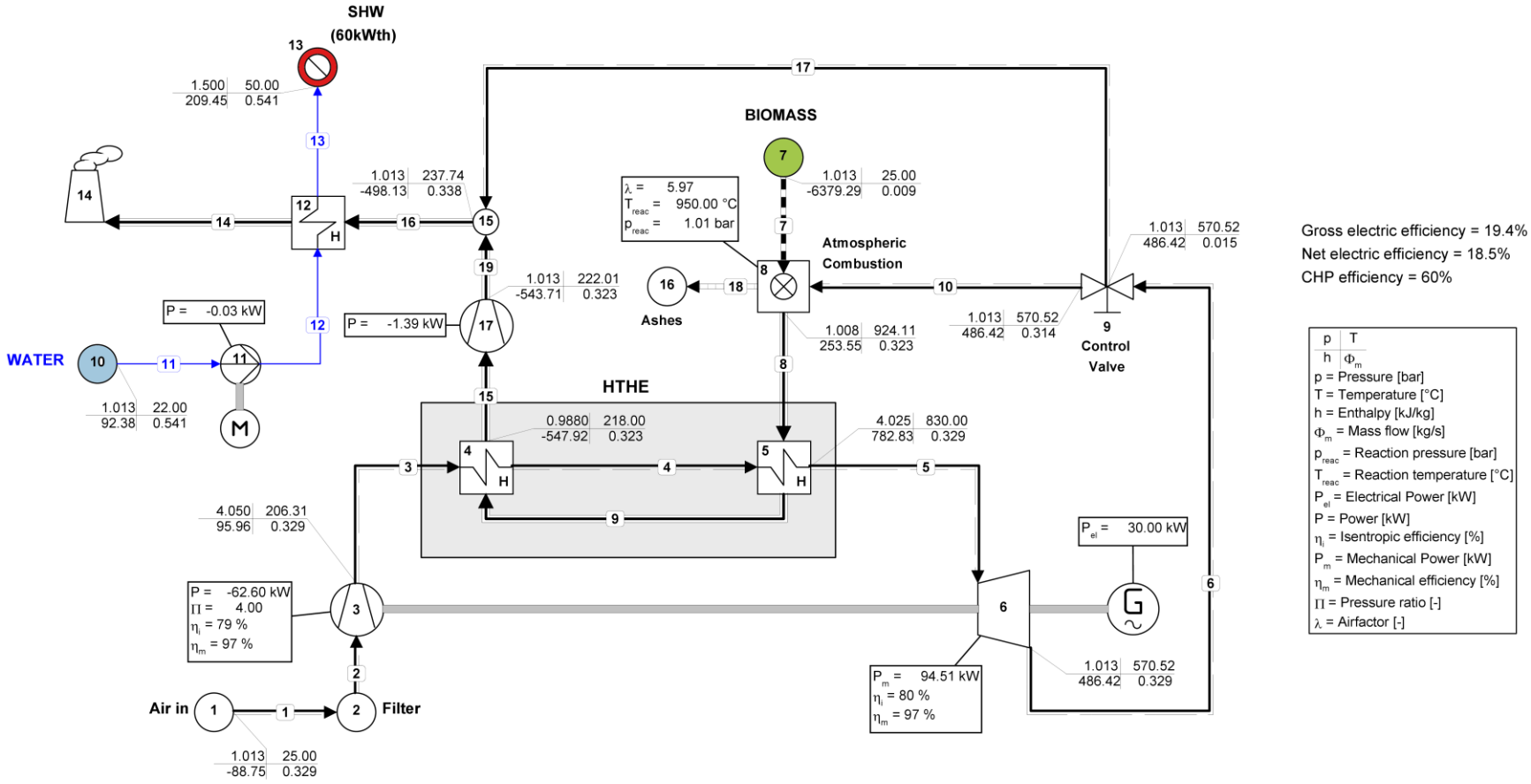

Fig. 24 Cycle-Tempo® EFGT Plant.

The assumptions considered in this simulation are as follows:

- The CHP system operates in steady state.
- Environment and reference state at T_0 =298 K and P_0 = 1.013 bar.
- The residence time is sufficient to achieve the combustion equilibrium mode.
- A pressure drop of 0.5% of the inlet pressure takes place across the combustion chamber [139]. 4% of heat losses (radiation, convection and conduction) have been assumed.
- A pressure drop in HTHE cold side is 3% of the inlet pressure, while in the hot side the pressure drop is 2%.
- The typical performance parameters for the turbine and compressor are the same of the microturbine utilized in gasification system (Table 3).
- 15% of heat losses have been assumed for HTHE.
- The turbine inlet temperature is set at 830 °C. Therefore, hot side temperature difference, ΔT_{hs} (between the inlet flue gas and and the outlet air) is about 95 °C.

Outlet temperature of the combustion gases is fixed to 920- 925 °C, this temperature is also controlled by air ratio through by-pass valve (block 9). The waste air (pipe 17) is mixed with the combustion gases (pipe 15) for hotwater production (about 60kW_{th}) in order to improve the overall efficiency of this CHP system. The HTHE is the most critical and expensive component of the overall EFGT systems [112]. In fact, the maximum operating temperature of the HTHE is 100-150 °C higher than the turbine inlet temperature. Moreover, the low heat transfer coefficients of air and combustion gas lead to very large heat exchanger surfaces. Therefore, the development of the HTHE involves noticeable problems, as the availability of suitable materials for high temperature opera- tion, the long-term reliability of welding and sealing devices, as well as the reduction of construction costs. On short term, metallic heat exchangers are a good option in small-scale systems (30-500 kW), reaching temperatures between 850 and 900 °C. However, the best option in the long run will consist of ceramic heat exchangers. With these systems it will be possible to achieve temperatures above 1100 °C (increasing consistently the plant efficiency) [140].

5.3. Results obtained

5.3.1. Gasification system (FBG-GT)

According to the assumptions cited in section 5.1 for the FBG-GT system (Fig. 23), the results of the simulations carried out with the Cycle-Tempo® software are presented in the following section. Pressure ratio (U) is defined as the compressor operating pressure (block 16) between atmospheric pressure (1.013 bar). In Fig. 25, it is observed that, for a particular turbine inlet temperature, the net electric efficiency (helN) of FBG-GT system first improves with the increase in pressure ratio up to achieve a maximumvalue. Then, the electric efficiency decreases with further increase of U. On the other hand, higher turbine inlet temperature ensures higher electric efficiency at all U.

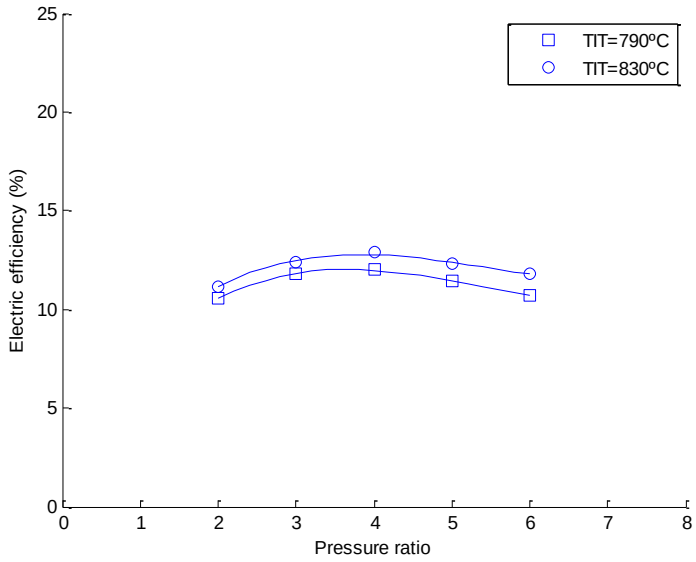

Fig. 25 Effect of Π and turbine inlet temperature.

As a result, the efficiency peaks of 11.9% and 12.3% are obtained for turbine inlet temperatures of 790°C and 830 °C, respectively. However, when the turbine inlet temperature rises above 900 °C turbine maintenance requires expensive and complex

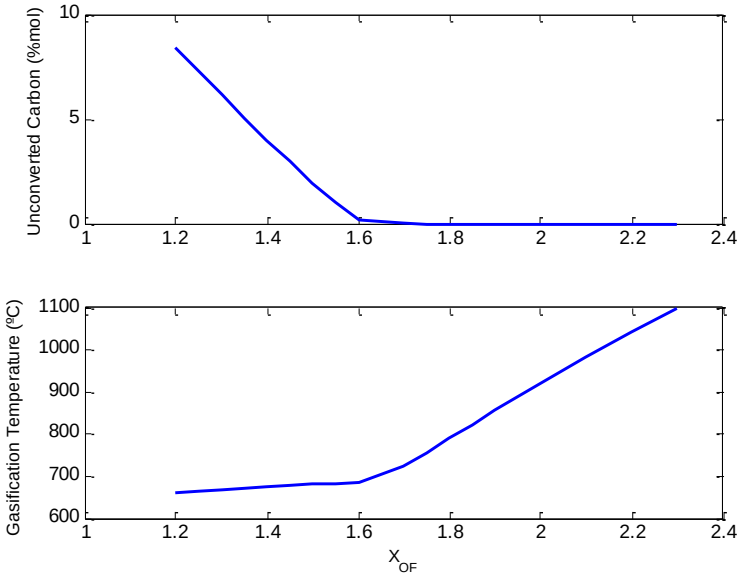

Fig. 26 Unconverted carbon and temperature in gasification zone.

cooling systems, this increases the capital cost of the plant [138]. The optimum conditions are reached for pressure ratios around 3.8-4. Fig. 26 shows the unburned carbon fraction and temperature in the gasification zone. According to [141], the reaction temperature must be above 700 °C to achieve the complete carbon conversion in gasification process. Moreover, regulation of the bed temperature to 700-900 °C gives a product gas with a low tar content, typically <1-3 g/Nm_3 [142]. As mentioned before, the gasifier operates at atmospheric pressure, biomass feed flow is 0.011 kg/s (around 40 kg/h) and the inlet air temperature is 300 °C. As shown in Fig. 26, x_{OF} must be fixed to 1.8-1.84 to avoid unconverted carbon creation. In this case, the reaction temperature rises to 800 °C.

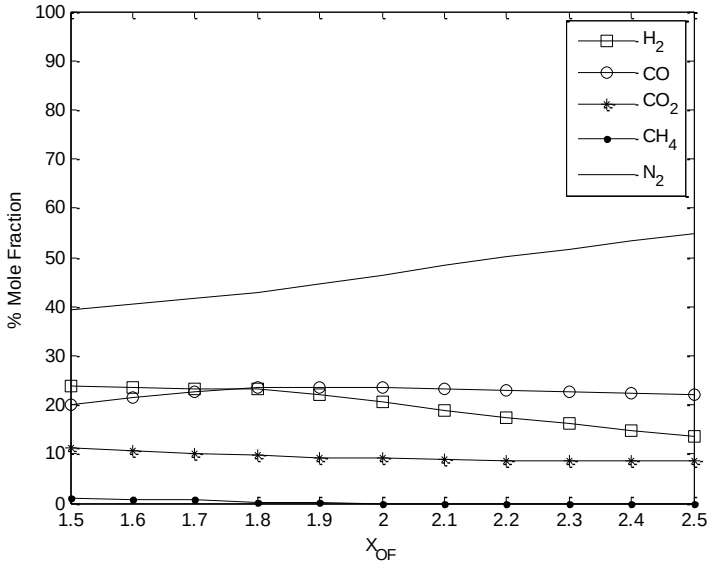

Fig. 27 Product gas composition on dry basis.

The effect of the gasification temperature in fuel gas composition is depicted in Fig. 29.

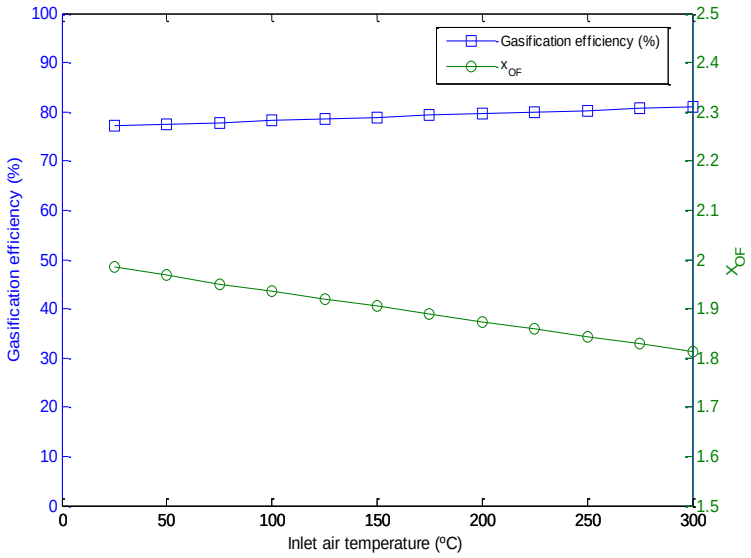

Fig. 28 Effect of preheating gasifier inlet air

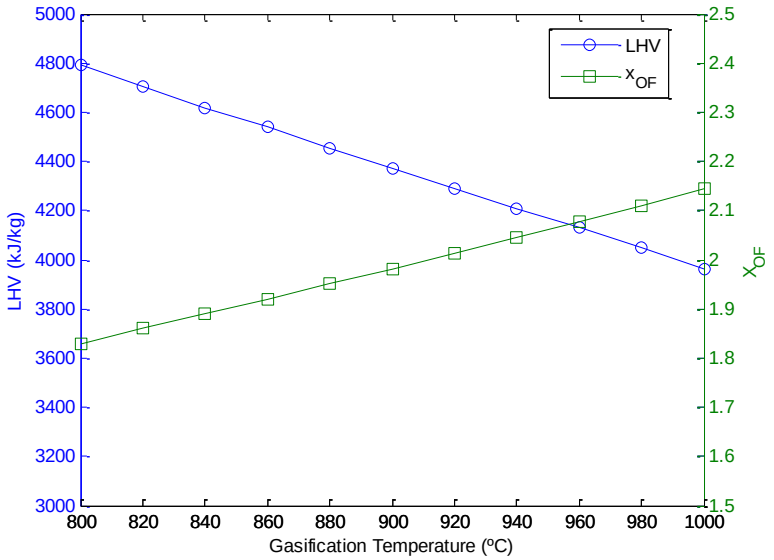

Fig. 29 Effect of gasification temperature increase

As a consequence of the results shown in Fig. 26 and Fig. 27, it shows a reduction in the percentages of H_2, CO and CO_2. Moreover, x_{OF} increase brings a larger presence of N_2 in the fuel gas composition. The reduction of CO and H_2 content with gasification temperature explains the decrease in the product gas LHV. Finally, Fig. 30 depicts the exergy distribution in the gasification plant.

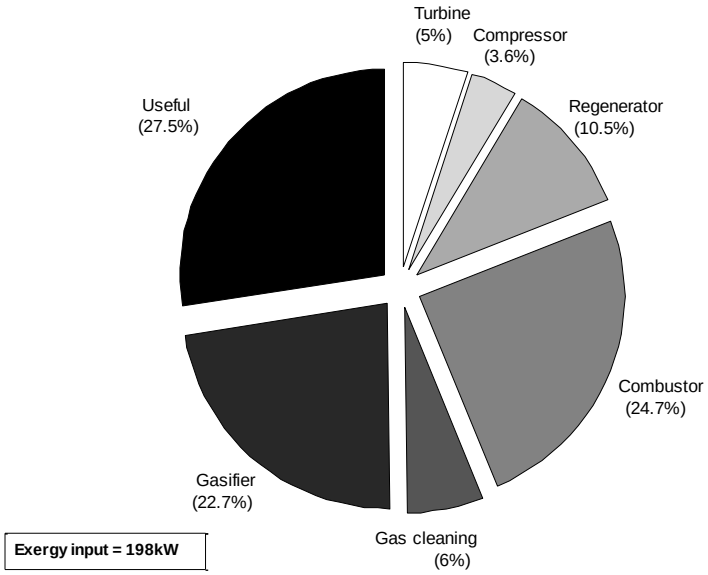

Fig. 30 Exergy balance of the gasification plant.

The biomass chemical exergy (198 kW) is converted into 30 kW_e and the residual exergy (23.8 kW) is used to produce thermal energy, both streams represent the useful exergy of the gasification plant (27.5%). The other parts of the diagram give an overview of the exergy losses in the system, these losses are due to irreversibilities produced in each of the gasification plant components (gasifier, combustor, gas cleaning and cooling, turbine, compressor and regenerator). It is observed that the major exergy destruction takes place in the combustor (24.7% of exergy input) and gasifier (22.7%). The lower exergy efficiency in these systems (76.4% and 77.3% respectively) is attributed to the irreversibility pertaining to the chemical reactions occurring there. According to [130], gasification is a process with significant exergy destruction as hot gaseous fuel is generated from cold solid fuel and a part of the solid carbon remains unconverted. On the other hand, the exergy destruction in the gas cooling and cleaning system, turbine, compressor and regenerator are much lower. In this thesis, exergy losses are calculated as the difference between inlet and outlet exergy flows, i. e. exergy loss in gasifier subsystem is defined as the difference in total exergy value of the hot product gas (pipe 14 in Fig. 23) and the exergy supplied for the biomass (pipe 1) and hot air (pipe 12).

5.3.2. EFGT plant

The Cycle-Tempo model described in Fig. 24 has been used to evaluate the performance parameters of an EFGT system at different operating conditions. This system fueled by biomass (olive tree leaves and prunings, generates 30kW$_e$ and thermal energy (about 60kW$_{th}$) for distributed power generation. The simulation has been evaluated with reference to parameters depicted in Table 11. Simple operation and low cost are two important factors in the system profitability. In this effort, net electric efficiency (helN), overall effi- ciency (hCHP), pressure ratio (P), turbine inlet temperature, hot side temperature difference in the HTHE (ΔT_{hs}) and exergy analysis have been assessed. It is found that the efficiency reaches a maximum value at an optimum P of the cycle. Fig. 31 shows the variability in the electrical efficiency with respect to P at three different turbine inlet temperatures (830 °C, 900 °C and 970 °C).

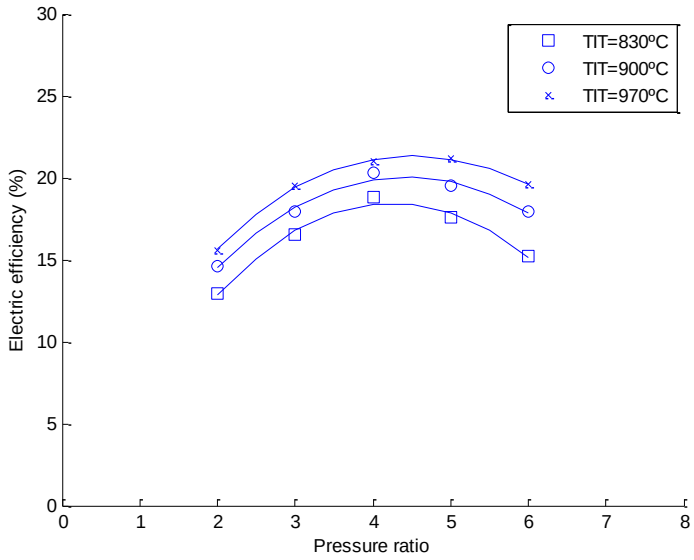

Fig. 31 Effect of pressure ratio and turbine inlet temperature.

It can be seen as the EFGT efficiency increases with the pressure ratio up to optimum value (about 4.0-4.5 bar) from which, the efficiency decreases with further increase in the U. Moreover, it is observed the system efficiency increases with the turbine inlet temperature (e.g. in optimum conditions, the electrical efficiency for 830 °C turbine inlet temperature is about 18.9% and for 970 °C this efficiency reaches 21.2%). However, the turbine inlet

temperature rise (above 900 °C) requires expensive turbine and HTHE materials and complex cooling systems for the turbine blades, thereby increasing the plant capital cost as well as the maintenance complexity [138,140]. In the Cycle-Tempo® simulation have been set the following operational parameters: turbine inlet temperature (830 °C), PelG (30 kW_e) and ΔT_{hs} (about 100 °C).

The HTHE is one of the most critical components in the EFGT cycle. The HTHE material cost and system size require to be optimized. However, the design of the heat exchanger also influences the energy efficiency of the power plant, by influencing the exhaust gas loss from the system. Fig. 32 shows the performance influence of this key equipment.

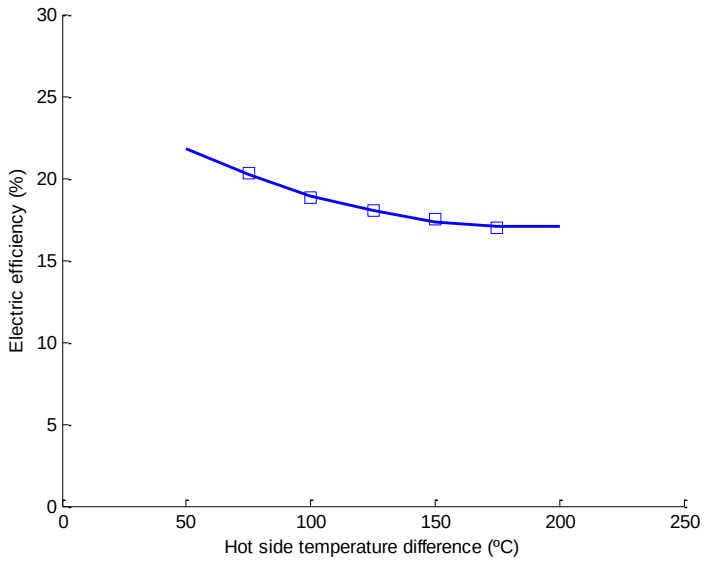

Fig. 32 Electric efficiency of the EFGT at different hot side temperatures (HTHE).

The parameter analyzed is the hot size temperature difference, ΔT_{hs}, which is the subtraction between combustion gases temperature (pipe 8, in Fig. 4) and temperature inlet air (pipe 5). It is found that the electric efficiency decreases (20.3%e17%) when the ΔT_{hs} rises from 50 °C to 200 °C, this is due to the reduction of the total heat transmitted between both fluids in the heat exchanger. It must be noticed that, for a given turbine inlet temperature, the increase of ΔT_{hs} also requires higher temperatures at the combustion chamber outlet (the furnace temperature is fixed by control valve, block 9). In our case, for a turbine inlet temperature of 1000 °C and a ΔT_{hs} of 200 °C requires the availability of material. suitable for 1200 °C and this option could result a very critical operation point [138]. Finally, it should be noticed the ΔT_{hs} is an important parameter in the size and plant cost. According to [112],a ΔT_{hs} of 100 °C requires a heat exchanger size around 150 m^2 of surface and 8 m of tube length. Whereas, for ΔT_{hs} of 200 °C the heat exchange size decreases considerably (80 m^2 and 4.5 m). To conclude the EFGT study, Fig. 33 presents the exergetic analysis of the plant. The fraction of the input exergy (biomass chemical exergy, 170.6 kW) is converted into electric power (30 kW) and exergy out (19.6 kW) for thermal applications.

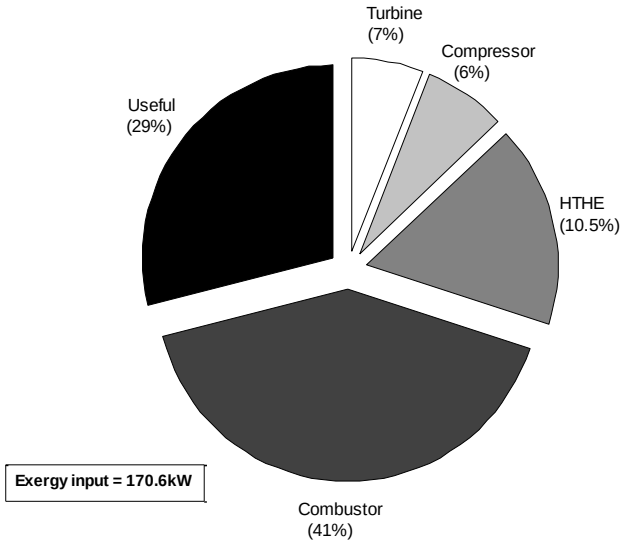

Fig. 33 Exergy balance of the EFGT plant

Both streams represent the useful exergy of the EFGT cycle (29%). The remaining part of the biomass input exergy is either lost in the exhaust heat or destroyed through irreversibilities in various components. It is observed that the major exergy destruction takes place in the combustion chamber (41% of exergy input) and the HTHE (17%), while the exergy

destruction in the turbine and compressor are much lower (7% and 6% respectively). The relatively lower exergetic efficiency in the combustion chamber (about 70%) is attributed to the irreversibility pertaining to the chemical reactions occurring there. Increasing the outlet temperature in the combustion gases (pipe 8, in Fig. 24) decreases the exergy destruction in the combustor. Otherwise, exergy destruction in the HTHE increases with the ΔT_{hs}.

5.4. Comparison between conventional GT and EFGT. Conclusion

The optimum performance parameters for the two CHP systems are listed in Table 12. It can be observed that the net electric efficiency and overall efficiency is higher in EFGT (19.1% and 59.3%) than in the gasification system (12.3% and 45.4%, respectively). This is mainly due to the compression stage (block 15, Fig. 23) reduces electric efficiency in 3.5%. The biomass consumption is also higher in gasification system than EFGT system. Moreover, because across the turbine only circulates hot air, the system allows using of dirty and low calorific value fuels without having to install complex cleaning systems, as in the gasification system. However, the optimal performance and maintenance of the HTHE, as well as their size, are the key parameters for choosing the EFGT system.

	Gasification system (FBG-GT)	EFGT system
Gross electric power (kW)	30	30
Net electric power (kW)	22.3	28.6
Thermal power (kW)	60	60
Gross electric efficiency (%)	16.5	20.1
Net electric efficiency (%)	12.3	19.1
CHP efficiency (%)	49.7	60.2
Overall efficiency (%)	45.4	59.3
Biomass consumption (kg/h)	40	33
Optimum pressure ratio (bar)	3.8	4
Air ratio (-)	6.38	6
Electric exergy efficiency (%)	11.1	16.9
Turbine inlet temperature (°C)	830	830

Table 12 Optimum operating parameters for CHP systems

Chapter 6. Study of a downdraft gasifier and gas engine fueled with olive oil industry wastes

Chapter 6. Study of a downdraft gasifier and gas engine fueled with olive oil industry wastes

A downdraft gasifier was chosen for the valorization of not only leaves and prunings, but olive stones as well following the reasons described in Martínez et at., 2012 [143],. During gasification, four different processes take place in the reactor: drying, pyrolysis, oxidation and reduction [72]. The model and simulation of the gasifier, gas cooling and cleaning stage have been prepared with the Cycle-Tempo® software [137] (Fig. 46) .

6.1. Plant description

As described before, the system consists of a downdraft gasifier, gas cooling and a cleaning stage where the gas impurities are removed. When the gasifier operates in steady state conditions, the producer gas can be burned in a SI engine to produce 70 kW_e and 110 kW_{th}. A thermodynamic and mechanical model of the gas engine, electric generator, electric transformer and transmission line have been developed in order to study the performance of the CHP plant connected to the grid.

The global gasification reaction can be written as follows:

$$CH_aO_bN_cS_dSiO_2Al_2O_3 + wH_2O + \lambda(O_2 + 3.76N_2) \rightarrow x_1H_2 + x_2CO + x_3CH_4 + \\ + x_4CO_2 + x_5N_2 + x_6H_2O + x_7NH_3 + x_8H_2S + x_9char + x_{10}ash \quad \text{Eq. 12}$$

where *a, b, c, d* are the number of atoms of hydrogen, oxygen, nitrogen and sulfur, respectively. Values from x_1 to x_{10} (producer gas molar composition, kmol) have been calculated using Cycle-Tempo [137]. The producer gas leaves the reactor at 950-990 °C (block 7) and enters in the second section of the model: gas cooling and cleaning process. This stage consists of:

- Cyclone (block 8): dust and particulates are removed from the producer gas.

- Venturi Scrubber (block 10): pulverized water is injected to decrease the producer gas temperature up to 75 °C. Other organic impurities (H_2S, NH_3) are also removed in this stage.
- Heat exchanger (block 14): where the water content of the producer gas is disposed. The gas temperature is also reduced up to 25-30 °C.
- Finally, the producer gas passes through several fine filters (block 17) where small particulates of carbon and water steam are removed.

In Table 13, the operating parameters of the gasifier assumed in the Cycle-Tempo® simulation are summarized. The performance parameters according to a real downdraft gasifier feeding with wood chips have been used to validate the model [144].

Firstly, the biomass tested (block 1 in Fig. 34) is introduced into the reactor reaching the drying and pyrolysis process. In this stage (block 3), the reactor temperature reaches values between 200 °C and 500 °C, and the biomass moisture content is released in steam. In the same stage, char and other volatile species such as CO, CO_2, H_2, CH_4 and tar are also formed. Later, these products enter in the combustion-reduction zone (block 6) reaching temperatures above 1000 °C. An accurately controlled amount of air is continuously supplied to the reactor in this zone (block 87). During the combustion-reduction process, the tar cracking and gas (composed of CO, H_2, CH_4, N_2, CO_2 and H_2O) are produced. The gasifier has an automatic system to remove ash and unconverted char generated during the process (pipe 24 and block 4).

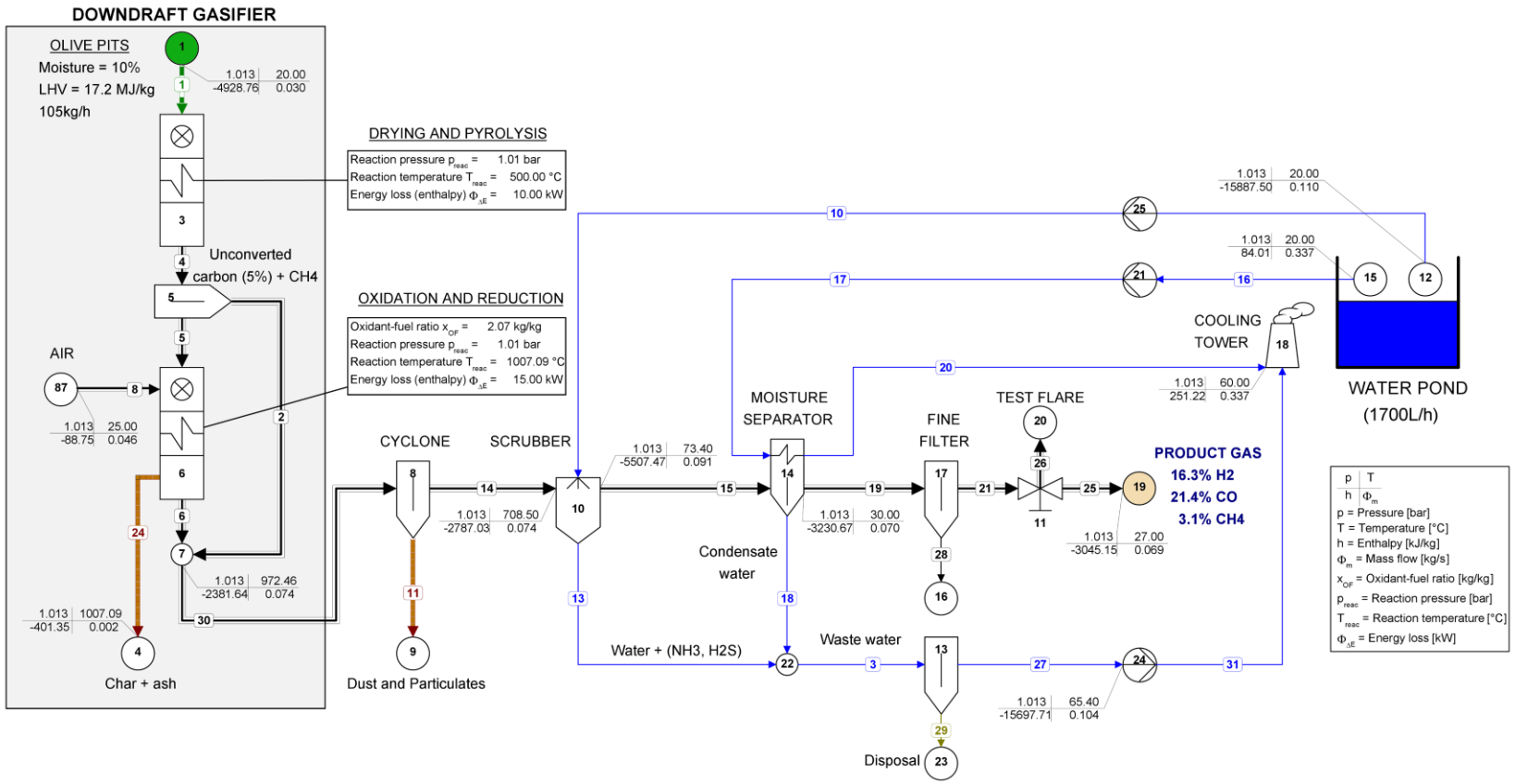

Fig. 34 Cycle-Tempo® Simulation of the downdraft gasifier, gas cooling and cleaning stages.

Operating Pressure (bar)	Gasification Temperature (ºC)	Moisture Content (%)	Rated gas flow (Nm3 h-1)	Producer gas LHV (MJ kg-1)	Biomass Consumption (kg h-1)	Main Producer gas Composition (Mole %)
1.013	1000-1100	<20%	250-300	>4.5	96-110	CO: 19 ± 3% H2: 18 ± 2% CH4: 1-3%

Table 13 Performance parameters of the gasifier.

The basic assumptions during the simulation are the following:

- Pyrolysis temperature is fixed at 500 °C [145].
- The oxidant agent (air) is sufficient to convert all carbon in producer gas. A part of this carbon is removed from the gasifier system representing the losses that usually occurring in gasifiers (char). Here, it is assumed 5% of unconverted carbon (block 5 in Fig. 3) [134,146].
- A fraction of CH_4 formed during the pyrolysis process is not included in combustion-gasification stage. In general, the producer gas does not achieve complete equilibrium composition in the gasifiers (as indicated by the presence of methane). For this reason, 3% of methane (mole %) is bypassed (block 5 in Fig. 3) to the gas outlet [147,148].
- Tar yield is neglected during the combustion-gasification stage, x_{OF} is regulated to set the temperature above 1000 °C. In these conditions, the tar cracking is produced [143].
- It is assumed that 5% of the biomass energy input is released (heat losses) through the gasifier walls [145].
- Ash is mainly composed of SiO_2 and Al_2O_3 [47]. The gasification efficiency can be expressed as cold-gas efficiency, η_{cg} (measured in pipe 25 in Fig. 3) or hot-gas efficiency, η_{hg}, taking into account the sensible heat of the producer gas (measured in pipe 30). These can be showed as follows [19] :

$$\eta_{cg} = \dot{m}_{pg} LHV_{pg} / \dot{m}_b LHV_b \quad \text{Eq. 13}$$

$$\eta_{hg} = \frac{\dot{m}_{pg} LHV_{pg} + \dot{m}_{pg} Cp_{pg} [T_{pipe30} - T_0]}{\dot{m}_b LHV_b} \quad \text{Eq. 14}$$

Where $\dot{m}_{pg}$ and $\dot{m}_b$ is the producer gas and biomass mass flow respectively (kg s^{-1}); LHV_{pg} and LHV_b the lower heating value (kJ kg^{-1}) of the producer gas and biomass tested; $C_{p_{pg}}$ the specific heat capacity of the producer gas (kJ $kg^{-1}K^{-1}$); T_{pipe30} is the producer gas temperature at gasifier outlet (in pipe 30, fig. 3) and finally, T_0 the ambient temperature (25°C).

Cycle-Tempo® uses an iterative approach to obtain the producer gas composition: first, the biomass inlet characteristics (atomic composition, LHV, moisture, biomass flow and temperature), environmental conditions (temperature and pressure), oxidant characteristics (temperature, atomic composition, oxidant/fuel ratio) and other parameters (gasifier operating pressure, heat loss) are introduced in the program. In a second stage, the product gas composition is estimated by a non-stoichiometric equilibrium model (minimization of the Gibb's free energy method). Details of these models are available in the Cycle-Tempo® manual and other similar works [131,146,149].

6.2. Gas engine and network connection model

A gas engine fueled by producer gas has been modeled in order to demonstrate the viability of the gasifier and its performance when it is connected to the grid. A general scheme of the plant can be observed in Fig. 35. Olive wastes feed a downdraft gasifier working at atmospheric pressure and high temperature (above 1000 °C). Basically, the producer gas enters in a modified carburetor and the mixture is used to run a gas engine connected to an electric generator. This system can produce 70 kWe and 105 kWt. Thermodynamic and mechanical models of the gas engine have been carried out using three Matlab®/Simulink® toolboxes [150]:

1. The thermodynamic model has been carried out with Thermolib® [151]. The toolbox provides a Simulink® blockset for system simulations and a set of Matlab® command line functions for thermodynamics calculations and balancing of the simulated models. The blockset includes Simulink® blocks for components such as heat exchangers, compressors, thermodynamic state changes, valves, chemical reactors, burners, etc. Thermolib® also provides an extendable thermo-physical properties database.
2. The mechanical model of the gas engine has been developed with the SimDriveline® toolbox [150]. It is assumed a SI gas engine.
3. The connection to the grid (electric generator, transformer and transmission line) has been carried out using SimPowerSystem® toolbox [152].

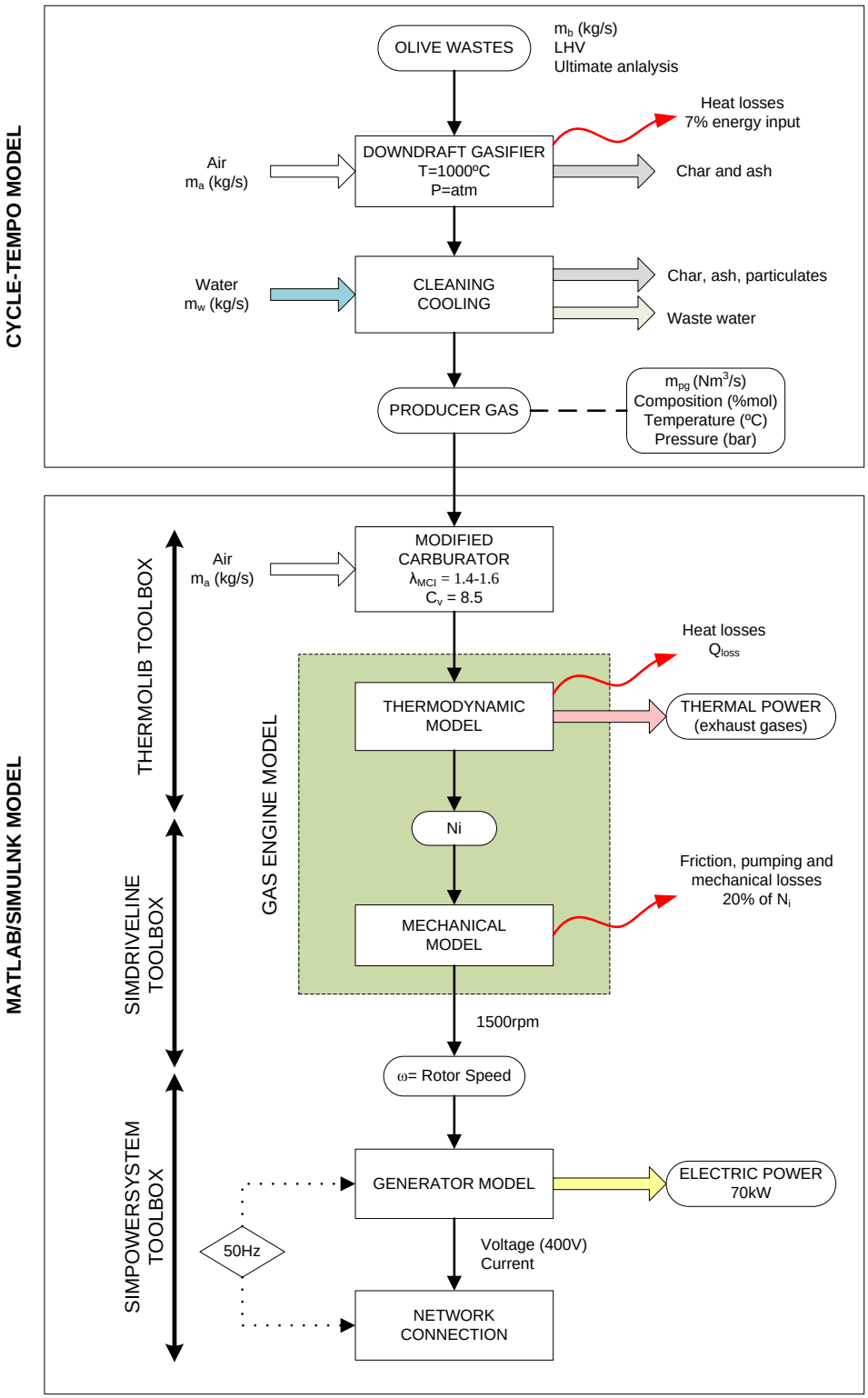

Fig. 35 General scheme of the plant.

Fig. 36 shows the Simulink® layout of the gas engine connected to the grid. The producer gas properties (molar composition, pressure, temperature and volumetric flow) obtained with Cycle-Tempo® software have been introduced in the Simulink® model through thermolib "mixture source" block (Fig. 37) [151]. In a real case, the simulation starts when the gasifier reaches steady state conditions (around 15-20 min, [73]).

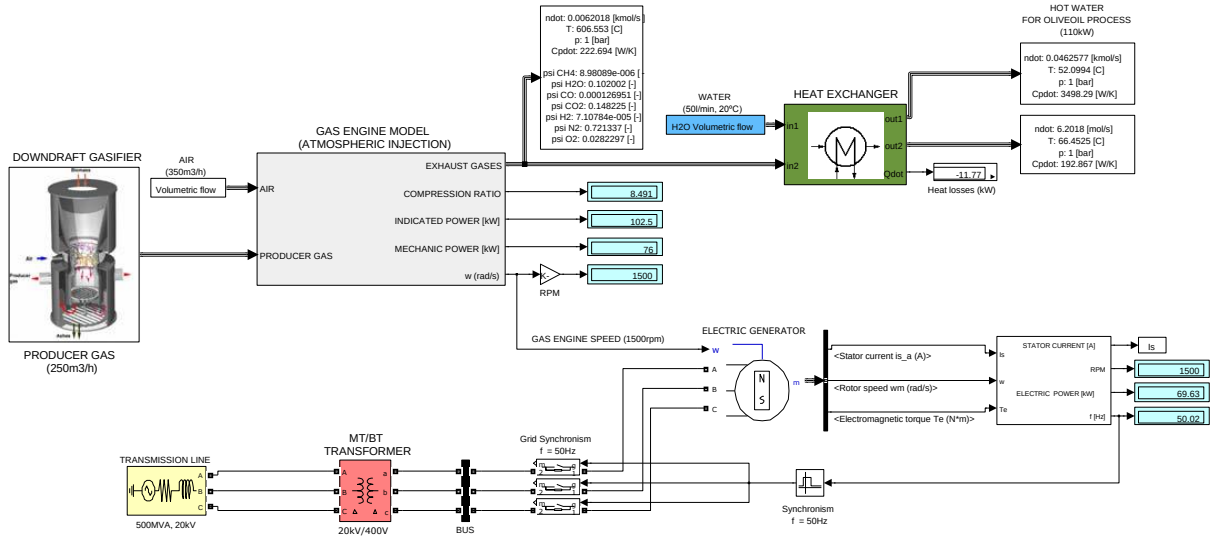

Fig. 36 Gas engine and network connection model (Matlab®/Simulink).

The producer gas and air enter in the gas engine carburetor setting the airefuel ratio at 1.6 (according to the operation manual 250 m^3 h^{-1} of producer gas and 350 m^3 h^{-1} of air). In this paper, a commercial natural gas engine (spark ignition) model Cummins G855G has been chosen [153]. The technical parameters of the gas engine are depicted in Table 14.

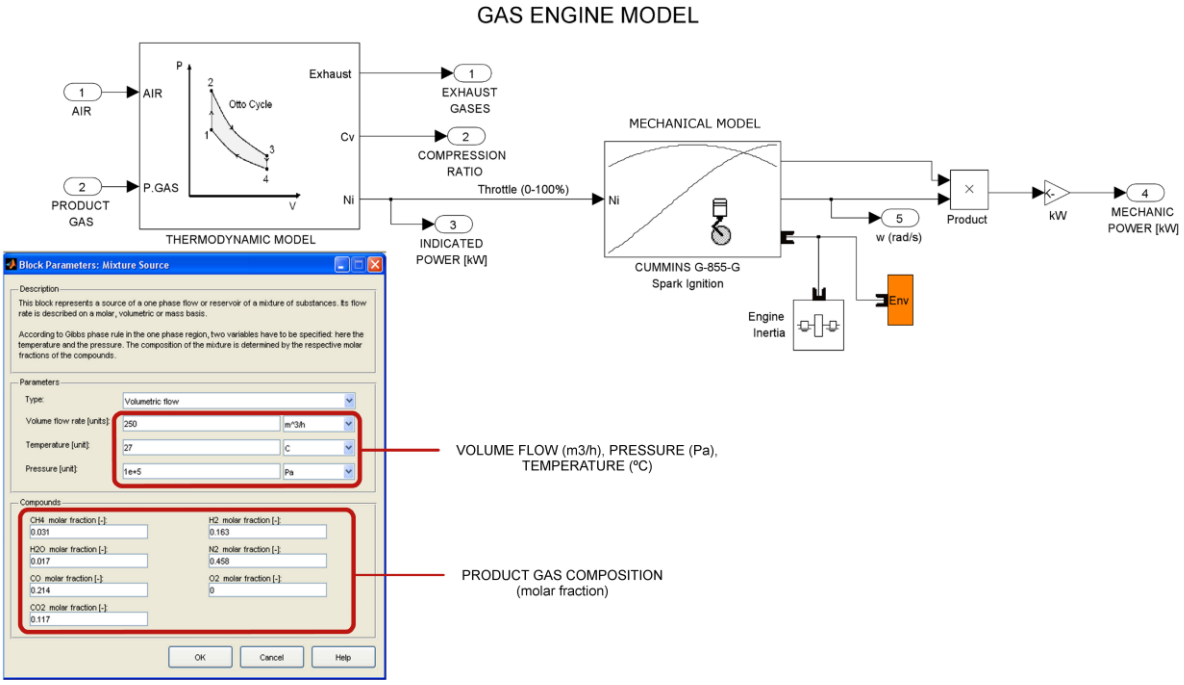

Fig. 37 Gas engine sub-model and mixture source book.

Engine Model	Cummins G - 855 -G
N° of cylinders	6
Aspiration	Naturally aspirated
Bore x Stroke	140x152
Displacement volume-liter	14.0
Engine output prime, kW (operating with natural gas)	125
Engine speed, rpm	1500
Compression ratio	12

Table 14 Technical parameters of the gas engine.

The thermodynamic model of the gas engine involves a producer gas-air mixture developing a real Otto cycle (4 strokes) [154,155]. Previously, the carburetor has been modified to operate with this kind of mixture. Thermolib® provides Simulink blocks where any mixture can develop any thermodynamic state change. The model outputs are the indicated power (N_i), compression ratio (C_v) and the composition and properties of the exhaust gases.

In the first stroke, the mixture volume is compressed up to set the maximum compression ratio (C_v=8.5). Then, the mixture compressed develops the thermodynamic changes related to Otto cycle [154]. The power stroke is the only thermodynamic process in which the engine operation is modified respect to the NG behavior. In this state, the compressed mixture is burned by a spark plug with the following combustion reactions:

$$CH_4 + 2O_2 \rightarrow CO_2 + 2H_2O \qquad \text{Eq. 15}$$

$$H_2 + 0.5O_2 \rightarrow H_2O \qquad \text{Eq. 16}$$

$$CO + 0.5O_2 \rightarrow CO_2 \qquad \text{Eq. 17}$$

These combustion reactions are introduced through an equilib- rium reactor block from Thermolib® toolbox. Any chemical reaction can be formulated and include other parameters as the energy loss to the environment, pressure loss, reaction surface, etc. The outgoing flow is at chemical and thermodynamical equilibrium.

The Second Law of Thermodynamics has been used to calculate the thermal power developed inside the cylinder (closed system). According to [101], the work of an Otto cycle (W_{cycle}) is expressed as the difference between expansion work and compression work.

$$W_t = W_{cycle} = W_{exp} - W_{comp} = (u_3 - u_4) - (u_2 - u_1) \quad \text{Eq. 18}$$

Where $u_3 - u_4$ and $u_2 - u_1$ are the internal energy variation during the expansion and compression strokes, respectively.

The power developed inside the cylinder according to Otto cycle is called indicated power, N_i (eq. 20). Losses during the expansion and compression strokes and heat losses (Q_{loss}) are included in this power. The power losses due to heat transfer through the cylinder wall is given by eq. 21. [154,156]. The values of constants and parameters used in the thermodynamic model are summarized in Table 15 [154,155].

$$N_i = (\eta_{exp}\dot{W}_{exp} - \eta_{comp}\dot{W}_{comp}) - \dot{Q}_{loss} \quad \text{Eq. 19}$$

$$\dot{Q}_{loss} = \dot{m}_{mix} B (T_c + T_e) \quad \text{Eq. 20}$$

The waste heat could be used during the olive oil extraction process. Therefore, the composition and characteristics of the exhaust gases have been also modeled. A heat exchanger (counter current) has been modeled in order to simulate a water stream of 50 L min^{-1} at 50 °C (around 110 kW_{th}).

Parameter	Units	Value
Thermodynamic model (gas engine)		
Constant related to heat transfer, *B*	*kJ kg^{-1} K^{-1}*	0.71
Producer gas LHV	*MJ kg^{-1}*	5000
Air-fuel ratio *(kg air/kg p. gas)*	-	1.6

Compression efficiency	*%*	0.97
Expansion efficiency	*%*	0.97
Combustion efficiency	*%*	0.98
Compression ratio, C_v	-	8.5
Intake temperature	*ºC*	25
Heat exchanger efficiency	*%*	85
Mechanical model (gas engine)		
Losses (friction, pumping, distribution, etc.)	*%*	20
Rotor speed, *w*	*rpm*	1500
Throttle valve position	*%*	100
Electric generator		
Output voltage	*V*	415
Nominal frequency	*Hz*	50
Power factor	-	0.8
Maximum active power, P_e	*kW*	100
Number of phases	-	3
Electric transformer		
Windings connection	-	Delta
power	*KVA*	250
Primary/secondary voltage	*kV*	20/0.4
Transmission line		
Base voltage	*kV*	20
3-phase short-circuit level at base voltage	*MVA*	500
X/R ratio	-	5

Table 15 Constants and parameters used in overall Matalb®/Simulink® model.

The indicated power obtained in the thermodynamic model, N_i, is the input of the mechanical model. The mechanical model of the engine has been carried out using a SimDriveline® Simulink block [152]. This block represents a SI engine with a speed governor where the input is a throttle signal, this can oscillate from 0% (no load) to 100% (full load). In this paper, the performance of the gasification plant in steady state conditions has been studied, i.e., the engine operates at full load and constant speed (stationary engine). Thus, N_i represents a throttle signal with a value of 100% (full load). The throttle

signal directly controls the output torque that the engine generates and indirectly controls the speed at which the engine runs.

The mechanical torque (T_m) and the angular velocity (w) signals are the outputs of the mechanical model. In Matlab®, the instantaneous mechanical power can be determined as follows:

$$P_m(t) = w(t)T_m(t) \quad \text{Eq. 21}$$

The total friction loss (N_f) consists of three major components: pumping work, rubbing friction work and accessory work [156]. In this thesis, it is assumed that the total friction loss when the gas engine operates at full load is 20% of the indicated power, N_i, [134], [153].

The gas engine is connected (in the same shaft) to an electric generator and the angular speed will be the signal input. When the gasifier reaches the steady state conditions (15-20 min of operating [157]), the gas engine increases the angular velocity up to 1,500rpm and the mechanical torque (the electric generator rotor speed increases at the same time). The network connection occurs when the electric generator frequency is set around 50 Hz. To avoid important transitory changes, the electric generator is connected to an infinite grid. In this work, the electric power, frequency, current harmonic distortion and dynamic performance of the CHP plant have been analyzed. Table 4 describes the simulation parameters used in the mechanical model, electric generator and grid connection (transformer and transmission line), [153], [154], [156].

6.3. Results

Firstly, the simulation of the gasification plant (downdraft gasifier and gas cooling-cleaning stage) has been carried using Cycle-Tempo® [137]. This software determines the gasifier behavior and producer gas characteristics in steady-state conditions. The downdraft gasifier has been fed with olive wastes: olive stones and small branches and leaves described in Table 13 and in Table 5. In the simulation, x_{OF} is regulated to set a combustion-gasification temperature above 1000°C (block 6, Fig. 34). Because of this, tar cracking is reached and its

yield is negligible. Tar causes severe problems to all mechanical parts of the equipment used after the gasifier and in specific the gas engine (corrosion).

Fig. 38 presents the producer gas composition in function of x_{OF} before it reaches the cleaning and cooling system (pipe number 30 in Fig. 34). In equilibrium conditions, it can be observed that the CH_4 formation is practically constant (around 3%) and H_2 decreases with air-biomass ratio. The effect of the gasification temperature (increasing x_{OF}) in the producer gas composition shows a reduction in the percentages of H_2 and CO. Moreover, an increase of x_{OF} (air amount supplied) brings a larger presence of N_2 in the fuel gas composition. The H_2 reduction with the increase of x_{OF} is attributed to the higher H_2O formation in the composition [146].

In equilibrium conditions, methane is not expected to be present in the producer gas. In

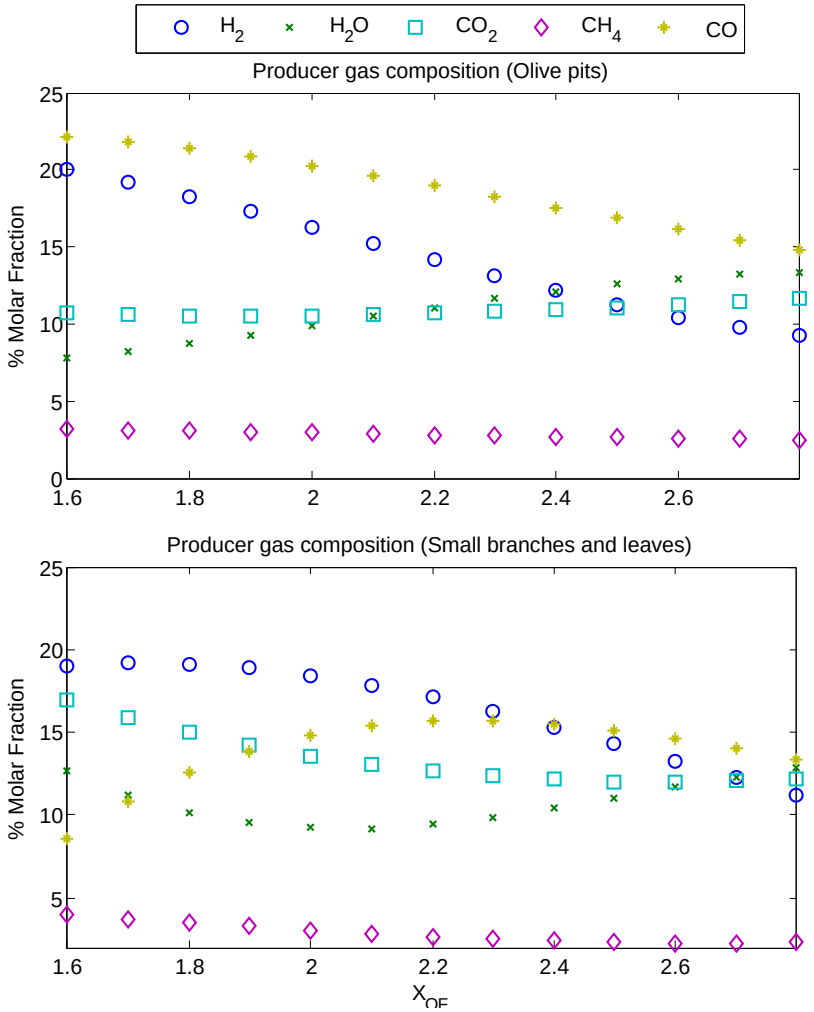

Fig. 38 Producer gas composition at gasifier outlet.

general, the producer gas does not achieve complete equilibrium composition in the gasifiers (as indicated by the presence of methane). For this reason, a part of methane is bypassed in the gasification reactor up to get around 3% of methane (block 5 in Fig. 34) [144].

It can be observed that the CO and H_2 yields are higher when the gasifier is fed with stones than branches and leaves. Because of this, the gasification of olive stones provides a producer gas with higher calorific value than the obtained with branches and leaves (fig. 7). The CO_2 and CH_4 formation is practically constant when x_{OF} is increased. According to the assumptions described in 6.1, a gasifier reaction temperature above 1000 °C has been fixed. In this case, x_{OF} is 2.07 and $LHV_{p.gas}$ is 4.8MJ kg^{-1} (operating with olive stones). The calorific value of the producer gas increases slightly after gas cooling and cleaning stage up to 5.1kJ kg^{-1} (Table 16)

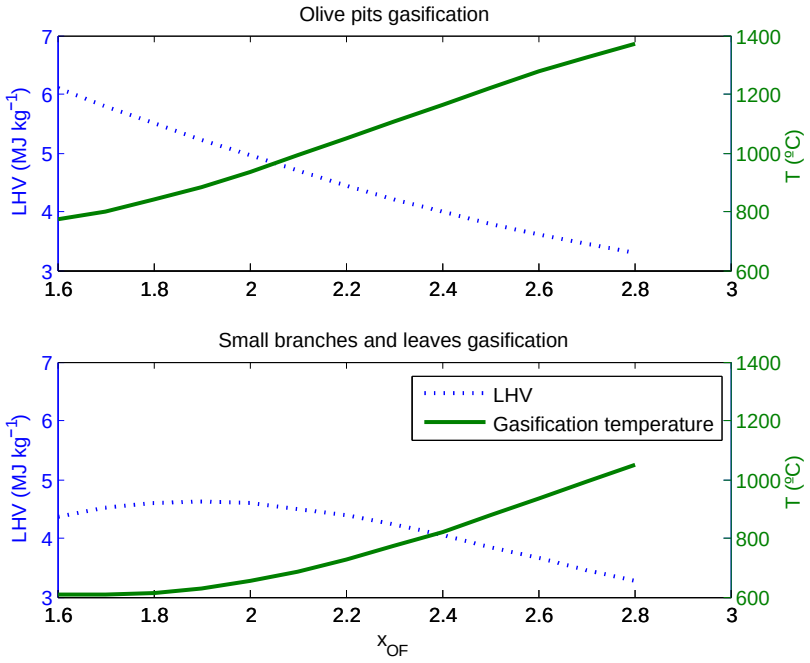

Fig. 39 Calorific value and temperature of the producer gas.

Fig. 39 also shows that the gasification temperature reached with branches and leaves is higher than in the gasification of olive stones, the reactor needs more quantity of air

supplied to reach 1000°C during combustion-gasification stage. This is another reason for the lower calorific value obtained with branches and leaves.

Biomass	Producer gas composition (% molar fraction)						LHV (MJ kg^{-1})	x_{OF}	Gas flow (m^3 h^{-1})
	H_2	CO	CH_4	CO_2	N_2	H_2O			
Olive pits	16.8	21.6	3.1	11.6	45.2	1.7	5.1	2.07	250
Branches and leaves	13.5	15.6	2.6	13.6	52.8	1.3	3.7	2.72	260
Gasifier specifications (wood biomass)	18±2	19±3	1-3	10±3	45-50	1-2	4.4-5.4	1.8	260

Table 16 Producer gas composition after gas cleaning and cooling stage.

The characteristics of the producer gas depend on the gasifier operating conditions and biomass properties: size, density, moisture content, proximate and ultimate analysis. Table 16 presents the producer gas properties obtained from Cycle-Tempo® in steady state conditions after gas cooling and cleaning stage (pipe 25 in Fig. 34). These results have been compared with the experimental gas composition of a commercial gasifier (working with wood chips) [144]. In this table, the producer gas composition, calorific value, x_{OF} and gas flow rate obtained for 100-105kg h^{-1} of biomass consumption is summarized. The gasification of olive stones provides a gas with high energy density (5.1 MJ kg-1) and similar properties than wood gas. However, the gasification of small branches and leaves has the lowest calorific value (3.7 MJ kg^{-1}) mainly due to the high x_{OF} (increasing the N_2 formation) and high ash content (8.71%). According to [74], each 1% increase in ash content translates roughly into a decrease of 0.2MJ/kg of the heating value. It can be observed that ash content of the branches and leaves is considerably higher than for the olive stones (Table 13). In both cases, the gas flow rates are practically the same.

It must be noticed that a biomass source with high ash content (commonly above 5%) is not desirable and it can produce severe problems in the gasifier and furnace systems [47], [158]: slagging and ash agglomeration due to fusion, corrosion and formation of clinkers.

Table 17 depicts the performance parameters of the gasification plant achieved for the olive wastes tested. It is found that the producer gas calorific value and gasification efficiencies

achieved with small branches and leaves is lower. This is due to the fact that the gasification process (with olive stones) yields a producer gas with higher calorific value (5.1 MJ kg^{-1} respect to 3.7 MJ kg^{-1}). The char and ash yield with small braches and leaves gasification (13.3 kg h^{-1}) is much higher than olive stones (6 kg h^{-1}) due to the high ash content in the feedstock. To conclude this section, the water needed for cooling and cleaning stage is different depending on the feedstock.

Parameter	Olive pits	Small branches and leaves
Biomass calorific value *(MJ kg^{-1})*	17.2	14.6
Biomass consumption *(kg h^{-1})*	105	105
Air-biomass ratio, x_{OF} *(-)*	2.07	2.72
Producer gas mass flow *(m^3 h^{-1})*	245	260
$LHV_{p.gas}$ *(MJ kg^{-1})*	5.1	3.7
Gasification temperature *(ºC)*	1007	1005
Hot-gas efficiency, η_{hg} *(%)*	89	87.5
Cold-gas efficiency, η_{cg} *(%)*	71.2	63.1
Gasification losses, *(kW)*	25	25
Char &Ash production, *(kg h^{-1})*	6.0	13.3
Water needed, *(L h^{-1})*	1700	1800

Table 17 Gasification performance parameters.

Secondly, the gas engine is started when the gasifier operates in steady state conditions. Around 250m^3 h^{-1} of producer gas is mixed in a modified carburetor with 350m^3 h^{-1} of atmospheric air. Due to the higher calorific value of the producer gas and low ash content, olive stones as a feedstock for gasification has been chosen to run the gas engine.
In this work, a commercial natural gas engine (spark ignition) model Cummins G855G has been used [153]. The technical parameters of the gas engine are depicted in Table 14.

Fig. 40 shows the frequency, mechanical and electrical power (P_m and P_e) developed for the gas engine shaft (76kW) at full load. In steady state conditions (after 4s), the angular velocity is 1,500rpm and the mechanical torque 484Nm (the electric generator rotates at the same speed that the gas engine). To avoid high harmonic injection inside the grid, the electric generator is connected to an infinite transmission line when the frequency reaches around 50Hz (it is produced around 3s.). In this way, the electric generator is connected to the grid producing 70kW of electric power. On the other hand, the gas engine also produces

130kW of thermal energy through exhaust gases at 600°C roughly. This waste energy is used in a heat exchanger in order to generate a water flow of 50L min^{-1} at 52°C (110kW_{th}). Finally, the hot water obtained in the process will be used in the mill during the olive oil extraction process.

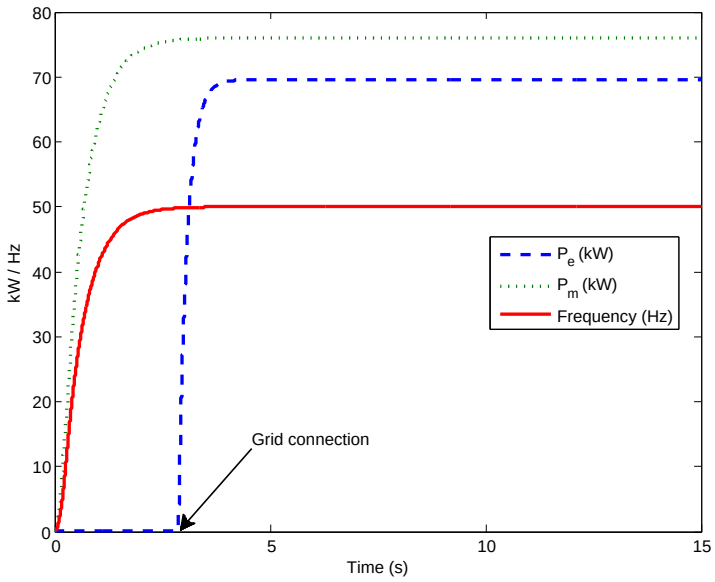

Fig. 40 Frequency, mechanic and electric power.

Table 18 shows the optimum performance parameters of the gas engine achieved with producer gas and a comparison for NG [153]. Due to the high calorific value of the natural gas (41MJ kg^{-1}), it can be observed that the mechanical and electrical power are much higher when using NG instead of producer gas. This is the reason why the gas-to-shaft and electric efficiency achieved with NG is respectively 33.8% and 27% compared to 21.1% and 19.5% when the gas engine is fed with producer gas.

Parameter	Producer Gas	Natural gas (NG)
P_m, *kW*	76	125
P_e, *kW*	70	100
Energy input, *kW*	360	370
Maximum compression ratio	8.5	12
Fuel consumption, m^3h^{-1}	250	40
Air-fuel ratio, *kg air/kg fuel*	1.6-1.7	15-16
Gas-to-shaft efficiency, *%*	21.1	33.8
Electric efficiency, *%*	19.5	27
Exhaust gas temperature, *ºC*	606	660

Table 18 Gas engine performance parameters.

In both cases, the exhaust gas temperature and combustion air (around $350m^3h^{-1}$) are practically the same. Noticed that more than 50% of the producer gas composition is composed of non-combustible gases like N_2, CO_2 and Ar, because of that, the air amount needed is much lower. Thus, the low calorific value of the product gas explains the very high fuel consumption ($250m^3\ h^{-1}$). The low air amount needed explains the air-fuel ratio decrease (1.6-1.7).

To conclude, Fig. 41 shows the three-phase electric current produced by the generator feeding the gas engine with producer gas.

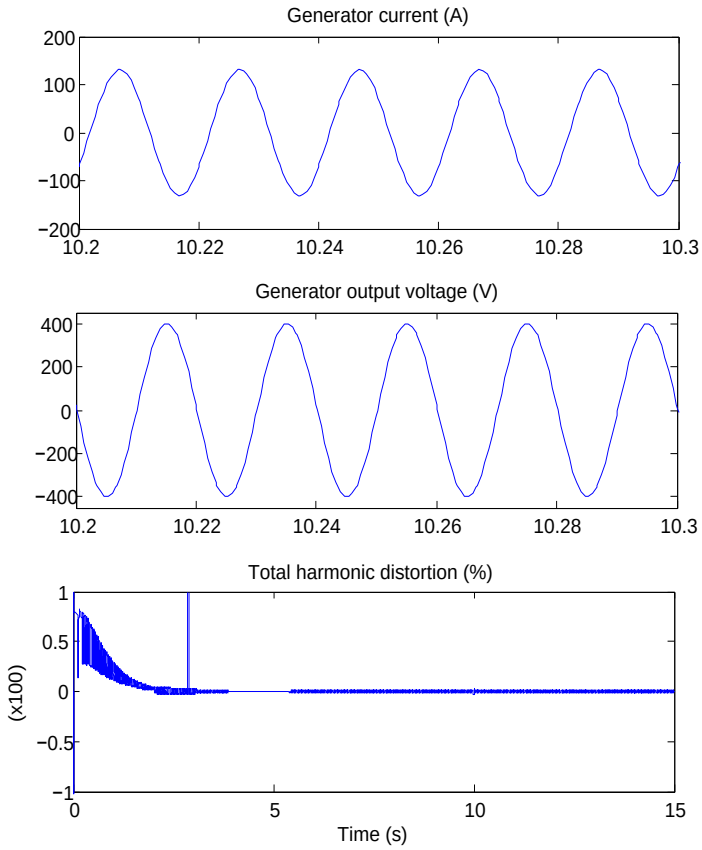

Fig. 41 Current generated, voltage output and total harmonic distortion injected to the grid.

The generator output voltage (V) and the total harmonic distortion (%) of the current signal injected to the grid can be seen in the rest of figures. It is observed that there is a very high harmonic distortion before the connection of the gas engine to the grid (from 0s to 3s). In steady state conditions (after 4s) this value decreases up to 0.6%.

Chapter 7. Updraft gasifier and ORC systemfor high ash content biomass: A modelling and simulation study

Chapter 7. Updraft gasifier and ORC system for high ash content biomass: A modelling and simulation study

In this thesis, the modelling and simulation of an updraft gasifier and ORC is carried out to complete the comparison between technologies that can prove to be a clear advantage for the valorization of olive tree and mills by-products. This novelty CHP plant can be fed by materials with a high ash and moisture content, i.e. olive leaves, switch grass, rice straw, lucerne, etc. In this work the olive leaves that remained in the mills after the olive oil extraction process have been tested as biomass feedstock. The system can produce electrical and thermal energy for the mill necessities collaborating to eliminate their difficult disposal problems for the owners.

Fig. 42 a) Olives with leaves reception; b) Leaves separation before the olive oil extraction process; c) Olive leaves storage at the mill proposed; d) Olive leaves sample.

7.1. Biomass and mill description

In this work, the CHP plant is fed with olive leaves. This by-product is also composed of a small quantity of branches improving the lower calorific value slightly (LHV_b). As it has been discussed in Chapter 2, the olive leaves cannot be burned currently in an uncontrolled manner and represent a concern for the mill owners, as they take up plenty of space at the mill, Fig. 42(c). Thus, ways to valorize this by-product are needed and most welcome. It is important to notice that the amount of leaves available at the mill is around 10% of the weight of olives processed yearly, [56].

A medium-size olive oil mill located in Andalusia (Spain) was selected as a reference for the present study. Fig. 43 presents a flow chart of the olive oil extraction process for the mill selected, around 25,000-35,000 olive tons (depending on the harvest) are processed yearly, producing around 2,000-3,000 tons of leaves. The electrical and thermal power demanded by the mill are 300kW$_e$ and around 750kW$_{th}$, respectively.

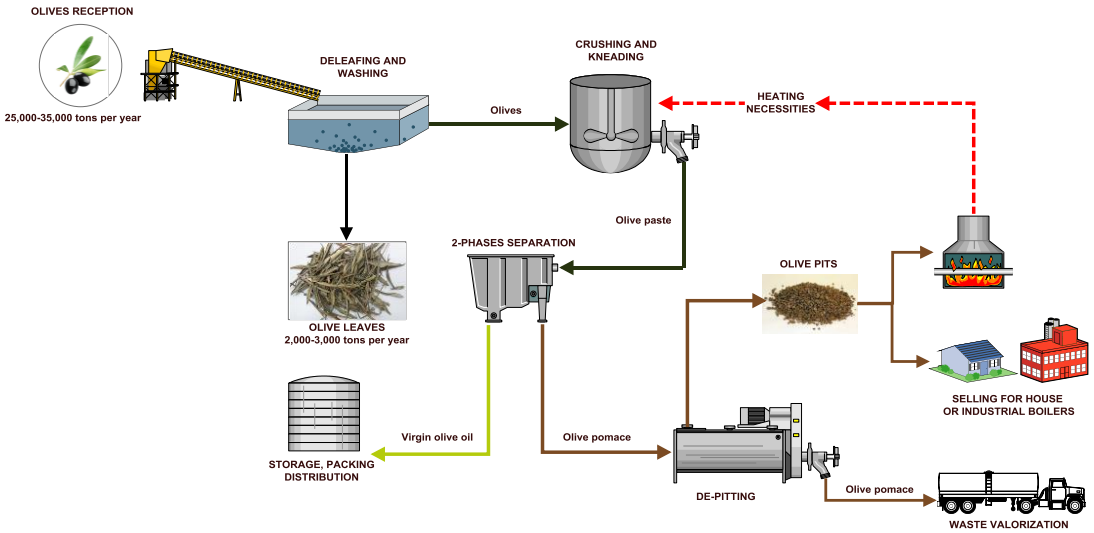

Fig. 43 Olive oil extraction process (2-phases) and by-products generated in a typical Spanish mill.

The proximate and ultimate analyses and other thermo-physical properties of the olive leaves are presented in Table 19 .

Proximate analysis (wt%)	
Moisture content (*ar*)	8.5
Ash content (*db*)	8.6
Volatile matter (*db*)	71.41
Fixed carbon (*db*)	19.88
Ultimate analysis (wt%, db)	
C	45.08
H	5.89
N	0.52
S	0.09
O (by difference)	39.7
Other properties	
LHV_b (*MJ/kg*)	13.0
Ash fusion (*°C*)	>1,200
Bulk density (kg/m^3)	108
Average particle size (*mm*)	20-40

Table 19 Proximate and ultimate analysis of the olive leaves (*ar*: as received; *db*: dry basis).

7.2. Plant configuration

This innovative system consists of an updraft gasifier, an external combustion chamber and an ORC machine as a power generation unit. It is capable of producing 100kW of net electrical power and around 435kW of thermal power, consuming 0.08 kg/s of olive leaves (approximately 290 kg/h). The main innovation of this hybrid system is that the gasifier can be fueled with high ash and moisture content biomasses.

The modelling and simulation of the power plant was performed in Cycle-Tempo® software, [159]. In this work, the following general considerations are defined:

1) The feedstock is composed exclusively of olive leaves (Fig. 42)
2) The environmental reference state is fixed at 25°C and atmospheric pressure
3) Finally, the CHP plant is operating in steady state conditions and connected to the electrical grid.

The main features of the updraft gasifier, external combustion chamber and ORC sub-systems are described in the following sub-sections

7.2.1. Updraft gasifier model

In this section, the thermodynamic modelling of the updraft gasifier was carried out according to the performance characteristics depicted in Table 20, [17]. The producer gas composition will mainly depend on the biomass composition, gasifier reactor and operating conditions, [17].

Performance parameters (for wood)	Updraft	Downdraft	Crossdraft
Maximum moisture content (%)	60	25	20
Maximum ash content (%)	25	6	1
Ash melting temperature (ºC)	>1,000	>1,250	-
Particulate size (mm)	5-100	20-100	5-20
Reaction temperature (ºC)	700-1,000	1,200-1,400	>1,500
Producer gas exit temperature (ºC)	200-400	700	1,250
Tar (g/Nm^3)	30-150	0.015-3.0	0.01-0.1
Producer gas LHV (MJ/Nm^3)	5.0-6.0	4.5-5.0	4.0-4.5
Gasification efficiency (%)	90-95	85-90	75-90

Table 20 General characteristics of fixed bed gasifiers.

Many researchers proposed the thermodynamic equilibrium model to predict the final composition of the producer gas in downdraft fixed bed reactors, [126,160–163]. Melgar *et al.*, [126], used a model which combines the chemical equilibrium and the thermodynamic equilibrium of the global reaction, predicting the final composition of the producer gas as well as the reaction temperature. Prins *et al.*, [162], developed a thermodynamic equilibrium

model based on several assumptions in better agreement with specific types of reactors. Also, Loeser *et al.*, [160], assumes an equilibrium model that provides the realistic chemical properties of the resulting streams, especially for fixed bed downdraft gasification systems. However, when applied to updraft fixed gasifiers, equilibrium models lead to large uncertainties in the reaction temperature, even though reactants residence time inside the gasifier is higher than reaction time, insofar as biomass is heated by producer gas, through countercurrent heat transfer. As can be observed in Fig. 44 the biomass drying, devolatilization and pyrolysis processes in updraft gasifiers take place in the heat transfer zone at a lower temperature than in the gasification and combustion zone; consequently, moisture and volatiles are not generally involved in the gasification and combustion reactions since they are released before reaching the reaction zone, [164,165].

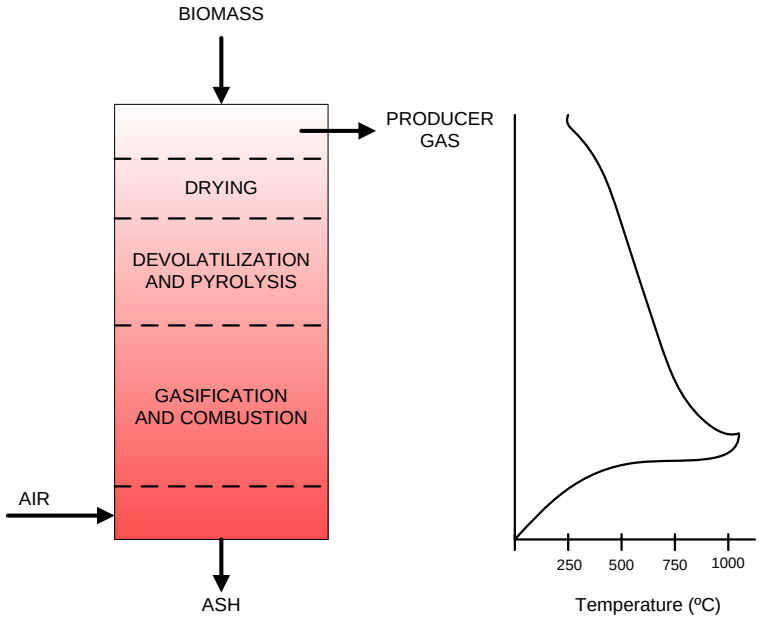

Fig. 44 Gasification stages and temperature profile in an updraft reactor.

In this study, the thermodynamic model of the updraft gasifier has been adapted from the work performed by Cau *et al.*, [164]. This steady state model calculates the mean temperature in the gasification-combustion zone as a function of air-biomass ratio (AB), biomass composition and temperatures of main inflows (biomass and air). This model also provides the thermodynamic characteristics of the producer gas and ash exiting the gasifier. The present model previously needs to accurately characterize the biomass volatile matter since as much as more than 50% of the biomass mass can be lost in the devolatilization process. As can be observed in the previous Fig. 44, the devolatilization process occurs in

the top of the reactor, being carried away by the hot producer gas going up countercurrent, as they are released from biomass without being affected by the gasification and combustion zone. In consequence, the producer gas composition absolutely depends on the devolatilization process.

Fig. 45 presents the updraft gasification scheme divided in different sections: biomass drying, decomposition-devolatilization and char gasification-combustion, this model has been developed in PRO/II software. As can be observed, biomass enters at the gasifier top and is preheated by the exiting producer gas releasing its moisture. This drying process is modeled as fictitious countercurrent heat exchanger (DRYING) by the hot producer gas leaving the gasifier. Water vapor from the drying zone is mixed with the hot producer gas increasing the final moisture content. The simulation of the whole devolatilization process requires a reactor (BIOMASS DECOMPOSITION) where exhausted biomass is decomposed in the three main components of the proximate analysis (from Table 4): fixed carbon, ash and volatile matter. The volatile matter is further decomposed into volatile gases (CO, CO_2, CH_4 and H_2), water vapor and tar through a mass balance calculation with chemical reactions, imposing a suitable production of tar and water in the volatile matter composition, [164–166], the mass balance is carried out through DEVOLATILIZATION module in Fig. 45. Water vapor and volatile gases released from the volatile matter are also mixed with the producer gas which leaves the gasification zone. A part of the tar produced during the devolatilization, ash and fixed carbon are heated and mixed forming the char that feeds the gasification section. In this zone, char is heated in series by the hot producer gas through fictitious heat exchanger imposing a suitable minimum temperature difference. Finally, the gasification and combustion processes take place in the same block fed by atmospheric air and char. In this zone, the thermodynamic equilibrium is achieved with the minimization of Gibb's free energy. More information about the minimization of Gibb's free energy method is reported in the literature, [47,163,167].

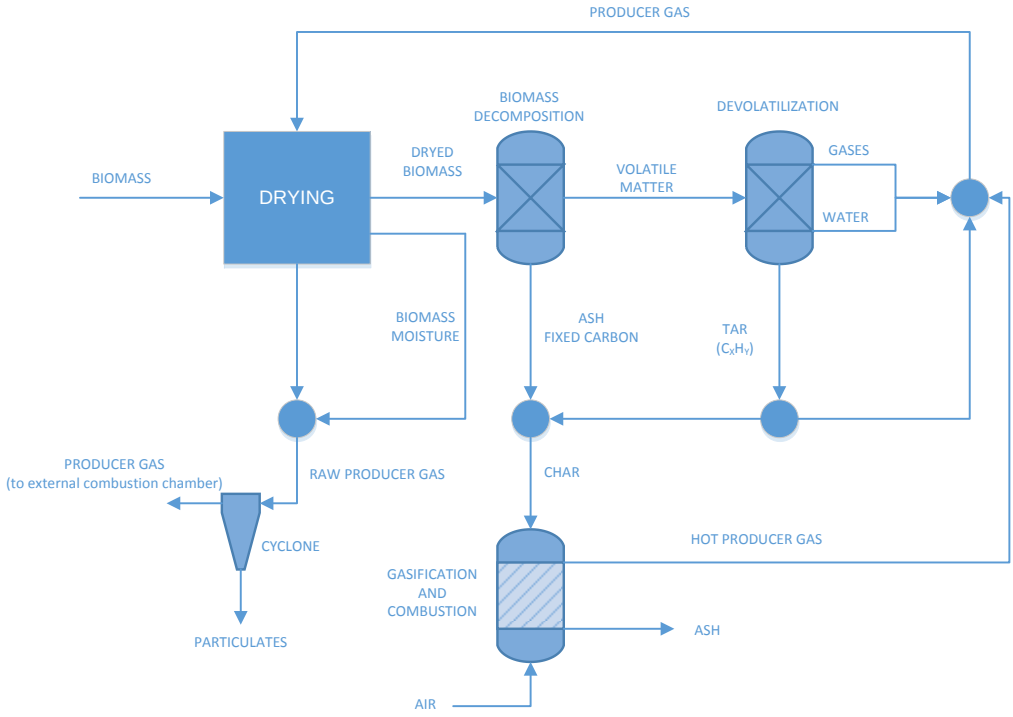

Fig. 45 Simplified scheme of the updraft gasification model in PRO/II software.

The main model assumptions of this steady state model of the updraft gasifier are depicted as follows:

- All the gasification stages operate at the same pressure (1.013bar), and therefore the pressure drops are neglected.
- Devolatilization process is assumed to occur instantaneously, in fixed-bed reactors this assumption is justified by the large biomass residence time compared to devolatilization time, [164].
- The model supposes that nitrogen and sulphur are included in fixed carbon composition while oxygen and hydrogen are fully contained in the volatile matter.
- During the devolatilization process a CO/CO2 mole ratio in the volatile gases is assumed equal to 2, [164]. Also, tar and water vapor mass content of 10% and 20%, respectively, is assumed after the biomass devolatilization, [164–166].
- Due to corrosion problems related to the tar dew point, a minimum exit temperature of the producer gas of 250°C is assumed. Tar from biomass gasification is mainly composed of benzene, toluene, 1-2-3-ring aromatic hydrocarbons, naphthalene and others, [17], then according to the Energy research Centre of the Netherlands (ECN)

the tar dew point for this composition is around 200-250°C, [168]. In this work, tar is assumed to be composed of 90 wt% by carbon and 10 wt% by hydrogen, [164].

- The ash composition of the biomass (olive leaves) cosists mainly of CaO, SiO2 and Al2O3, [169].
- The gasification agent is humid atmospheric air, with the following molar composition: oxygen 20.75%, nitrogen 77.29%, argon 0.92%, carbon dioxide 0.03% and water 1.01% (relative humidity is 60%). Here, it is assumed that a part of the air mass (10%) does not react during the gasification and combustion process.
- The oxidant agent (air) is sufficient to convert all carbon into producer gas. However, a part of the biomass carbon content is removed from the gasifier system reaching a carbon conversion efficiency of 95%, [170]. In fixed bed gasifiers, this is the fraction of solid carbon which does not get converted in the gasification reaction and gets removed from the bottom of the reactor together with ash (also called charcoal).

A summary of the gasification performance parameters and other minor assumptions are reported in Table 21, [17,135,170].

Parameter	Value
Gasifier	
Type	Fixed bed: updraft
Reaction pressure (bar)	1.013
Gasification agent	Air
Inlet air temperature (°C)	25
Heat exchangers efficiency, (%)	85
Gasifier heat losses (%)	5
Carbon conversion efficiency (%)	95
Unreacted air mass flow (%)	10
Biomass requirements	
Max. Moisture content (%)	60
Max. Ash content (%)	25
Average size (mm)	5-100
Producer gas requirements	
Minimum producer gas exit temperature (°C)	250

Table 21 Performance parameters of the updraft gasifier.

In this case, the producer gas is burned in an external combustion chamber without being previously cooled down, reaching in this case greater energy utilization. Therefore, by taking into account the high temperature of the producer gas at the gasifier outlet, the gasification efficiency (η_g) can be expressed as follows, [17]:

$$\eta_g = \frac{\dot{m}_{pg} LHV_{pg} + \dot{m}_{pg} Cp_{pg} (T - T_0)}{\dot{m}_b LHV_b} \quad \text{Eq. 22}$$

Where the subscript *pg* means producer gas, *b*: biomass, *g*: gasification, *0*: ambient or reference conditions.Therefore, the total energy content of the producer gas will be composed of a chemical stream which depends on the heating value of the fuel (LHV_{pg}) and a thermo-mechanical energy stream due to the producer gas exit temperature. This efficiency is usually named "hot-gas-efficiency".

7.2.2. External combustion chamber

One of the key components of this novel CHP system is the external combustion chamber; this connects the gasifier and the ORC sub-system (Fig. 45). The best advantage of the direct-combustion is the very low tar and particulate requirements in comparison with internal combustion engines, gas turbines, fuel cells and pipeline transport over long distances, [17].

Fig. 46 presents the simulation layout of the external combustion chamber and ORC subsystems carried out in Cycle-Tempo® software.

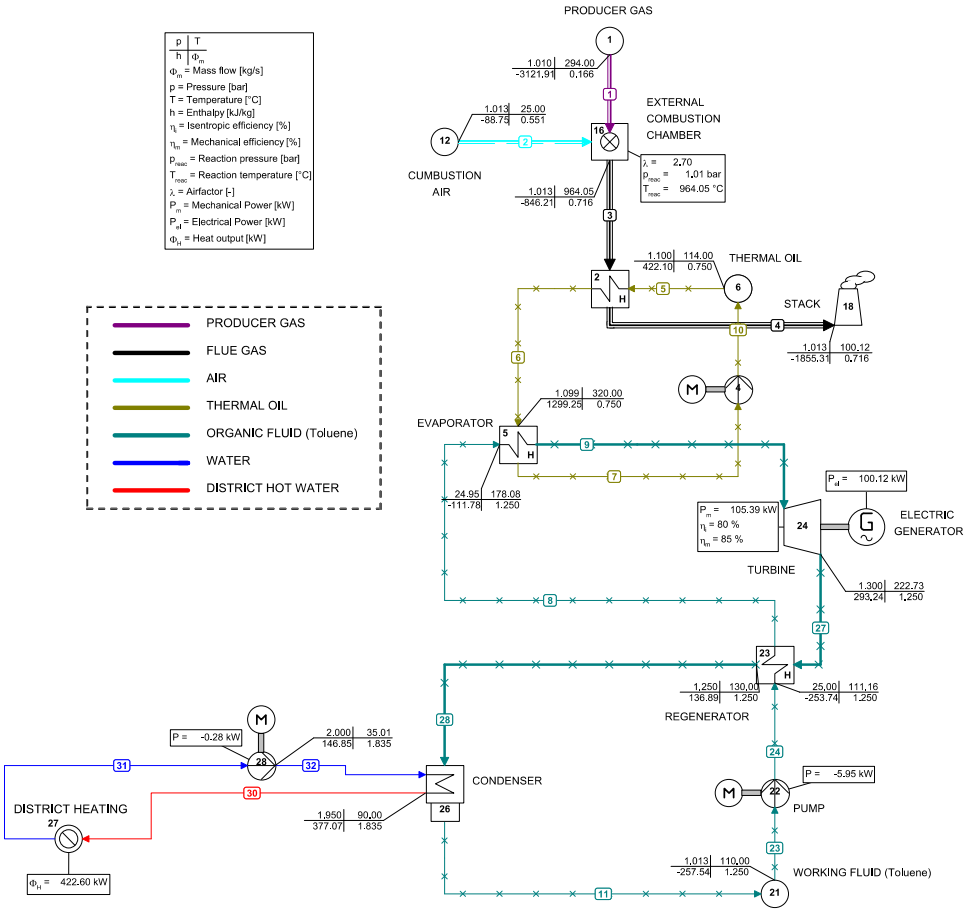

Fig. 46 External combustion chamber and ORC scheme in Cycle-Tempo software.

The producer gas leaves the reactor at 294°C (pipe 1, in Fig. 46) and feeds the external combustion chamber (block 16). In this stage, the combustion process is carried out at atmospheric pressure and a temperature higher than 950°C. The air amount is controlled by the air-fuel ratio (λ) and it must be sufficient to complete the combustion process. Then, the thermal energy of the flue gases is transferred to thermal oil through a high temperature heat exchanger (block 5), this thermal oil will be the future exchange medium of the ORC unit. It is important to highlight that the thermal oil target will be to avoid the local overheating and chemical instabilities of the organic (or working) fluid, [90]. After the turbine expansion (block 24), the working fluid is recovered in a low temperature heat exchanger or regenerator (block 23) to enhance the whole ORC efficiency. At last, the

working fluid passes through a condenser (block 26) producing the thermal energy necessary for the olive oil process and other heating necessities (412.6kW).

The external combustion chamber is one of the key components of this novelty system; this connects the updraft gasifier and the ORC sub-system. The best advantage of the direct-combustion is the very low tar and particulate requirements in comparison with internal combustion engines, gas turbines, fuel cells or pipeline transport over long distances, [17]. In the direct-combustion, the producer gas is burnt directly in a nearby unit (block 16 in Fig. 46) according to the following equations:

$$CH_4 + 2O_2 \rightarrow CO_2 + 2H_2O \quad \text{Eq. 23}$$

$$H_2 + 0.5O_2 \rightarrow H_2O \quad \text{Eq. 24}$$

$$CO + 0.5O_2 \rightarrow CO_2 \quad \text{Eq. 25}$$

$$C_mH_n + (m + n/4)O_2 \rightarrow mCO_2 + (n/2)H_2O \quad \text{Eq. 26}$$

Co-firing of gasified biomass in fossil-fuel-fired boilers is an example of direct-combustion applications; also industrial units like ovens, furnaces, and kilns are good examples. In fact, some power generation units use direct-combustion furnaces such as ORC, Stirling engines and EFGTs. In such applications, it is not necessary to cool down the producer gas and it can be directly burnt in a burner. However, one of the major problems of this hot gas is the small chance of tar condensation. Thus, the pipeline between the gasifier exit and the external burner inlet (pipes 12 and 17) should be insulated in such way that the gas does not cool down below the tar dew-point. If that happens, tar deposition might clog the pipes, leading to hazardous conditions and future corrosion problems. In applications where the producer gas is burnt directly without cooling (current work), there is no need for cleaning in depth. Such systems have no restrictions on the amount of tar and particulates as long as the gas travels freely to the burner, and as long as the burner design does not impose any restrictions of its own.

Table 22 presents the performance parameters of the external combustion model carried out in Cycle-Tempo® software, [47,139].

Parameter	Value
Reaction pressure (bar)	1.013
Maximum temperature outlet (ºC)	940
Combustion chamber efficiency (%)	94
Inlet air temperature (ºC)	150
Heat exchanger efficiency (%)	90
Pressure losses (%)	1

Table 22. Performance parameters of the external combustion chamber.

According to the power system conditions, three dry organic fluids (toluene, decane and cyclohexane) could be used for the aim of this work due to their high operating temperatures (>900°C) and the possibility for CHP applications, consistent with the requirements of the gasification plant described in Fig. 45. Table 23 depicts some thermodynamic properties of these organic fluids, [86].

Thermo-physical properties	Cyclohexane	Decane	Toluene
Critical pressure, (bar)	40.75	21.03	41.26
Critical temperature, (°C)	280.49	344.55	318.60
Condensation pressure, (bar)	1.75	0.10	0.74
Condensation temperature, (°C)	80.40	100.00	100.00
Pump specific work (superheated conditions), (kJ kg^{-1})	4.61	0.92	2.52

Table 23 Thermodynamic properties of the organic fluids proposed for high temperature sources.

As described by Bahrami *et al.*, [171], toluene presents the highest critical pressure and condensation temperature (100°C), together with a low condensation pressure and medium pump specific work. Cyclohexane presents similar critical properties as toluene, however its condensation temperature is quite lower (80°C) together with a larger pump specific work. Finally, decane presents the lowest critical and condensation pressure, the same condensation temperature than toluene and the least specific work, leading to the smallest size of utilities, equipment and pump consumption. In this work, superheated conditions

have been adopted to avoid the presence of liquid traces during the expansion work (the existence of water could be dangerous for turbine blades, [86]. For superheated conditions, Algieri and Morroe found cyclohexane as the most efficient working fluid followed by toluene, [90]; however, the relative low condensation temperature of cyclohexane (80°C) does not satisfy the heating network necessities (around 90°C) and other low heat applications of the mill (cooling through absorption chillers and sanitary hot water). Thus, toluene has been selected as working fluid, the performance parameters of the ORC sub-system is presented in Table 24 ,[47,171–173].

Performance parameters	Unit	Value
Turbine and pump isentropic efficiency	%	80.0
Compressor isentropic efficiency	%	85.0
Electro- mechanical efficiency for pumps and compressors, $\eta_{e\text{-}m}$	%	80.0
Evaporator efficiency	%	95.0
Condenser efficiency	%	85.0
Regenerator and rest of heat exchangers efficiency	%	90.0
Evaporator pinch point, ΔT	°C	10.0
Maximum thermal oil temperature	°C	350.0
Temperature design of district heating	°C	90.0
Pump operating pressure (Π_p)	bar	25
T/T design	°C	300

Table 24 Performance parameters of the ORC sub-system.

The maximum ORC working pressure and turbine inlet temperature (*T/T*) are limited to 25bar and 300°C, respectively, to reduce safety measures, materials expenses and avoid critical operating conditions, [91]. Finally, it is assumed an energy efficiency of 90% and pressure drop of 2% for the rest of heat exchangers.

The net electrical and CHP efficiency of the whole plant can be defined as follows:

$$\eta_e = \frac{P_t - P_p - P_{aux}}{\dot{m}_b LHV_b} \qquad \text{Eq. 27}$$

$$\eta_{CHP} = \frac{(P_t - P_p - P_{aux}) + P_{DH}}{\dot{m}_b LHV_b} \quad \text{Eq. 28}$$

$$P_{DH} = \dot{m}_w Cp_w \Delta T \quad \text{Eq. 29}$$

Where the subscript *b* means biomass, *e:* electrical, *aux*: auxiliary components, *CHP*: combined heat and power, *DH*: district heating and *w*: water.

7.3. Results

Firstly, the effect of the air-biomass ratio (*AB*) is presented in Fig. 47. As can be observed, the air-biomass ratio strongly decreases the molar production of CO and, in a minor rate, the CH_4, H_2, and H_2O; in contrast, the mole percentage of CO_2 increases with the air-biomass ratio due to the air increase inside the reactor (the N_2 yield also increases). It is important to notice the molar yield of H_2O, H_2, and CH_4 directly depend on the volatile matter composition of the biomass that it is only involved in the devolatilization process, and not in the gasification-combustion process (Fig. 46). Thus, the main reason in the reduction of these mole percentages in producer gas composition is the increase of the air mass flow in the gasification-combustion process. Otherwise, the strong reduction of CO is attributed to the higher presence of the char combustion reaction releasing CO_2 instead of CO (Table 25); thus, the lower calorific value (LHV_{pg}) and the cold gas efficiency (η_g in equation 1) decrease considerably. This effect can be observed in Fig. 48, the LHV_{pg} decreases around 37.47% (from 5.53 MJ/kg to 3.46 MJ/kg) and the cold gas efficiency from 92.72% to 76.87%. The O_2 increase inside the reactor promotes the exothermal combustion reactions increasing the temperature and reducing the LHV_{pg}. The minor decrease of the hot gas efficiency in Fig. 48 is attributed to the sensible heat of the producer gas at the gasifier outlet, in this case, despite of the chemical energy of the producer gas (LHV_{pg}) decreases, the thermo-mechanical energy increases with the producer gas exit temperature.

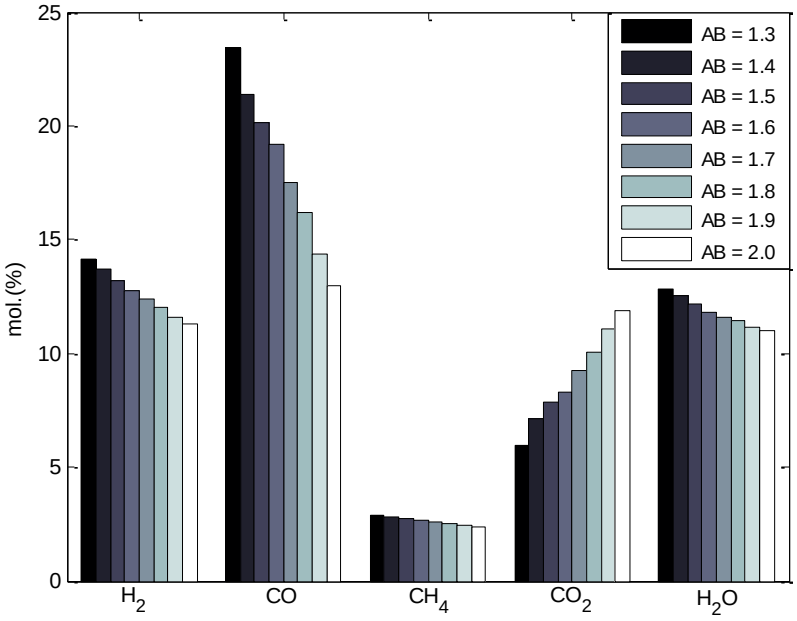

Fig. 47 Producer gas composition as a function of air-biomass ratio *(AB)*

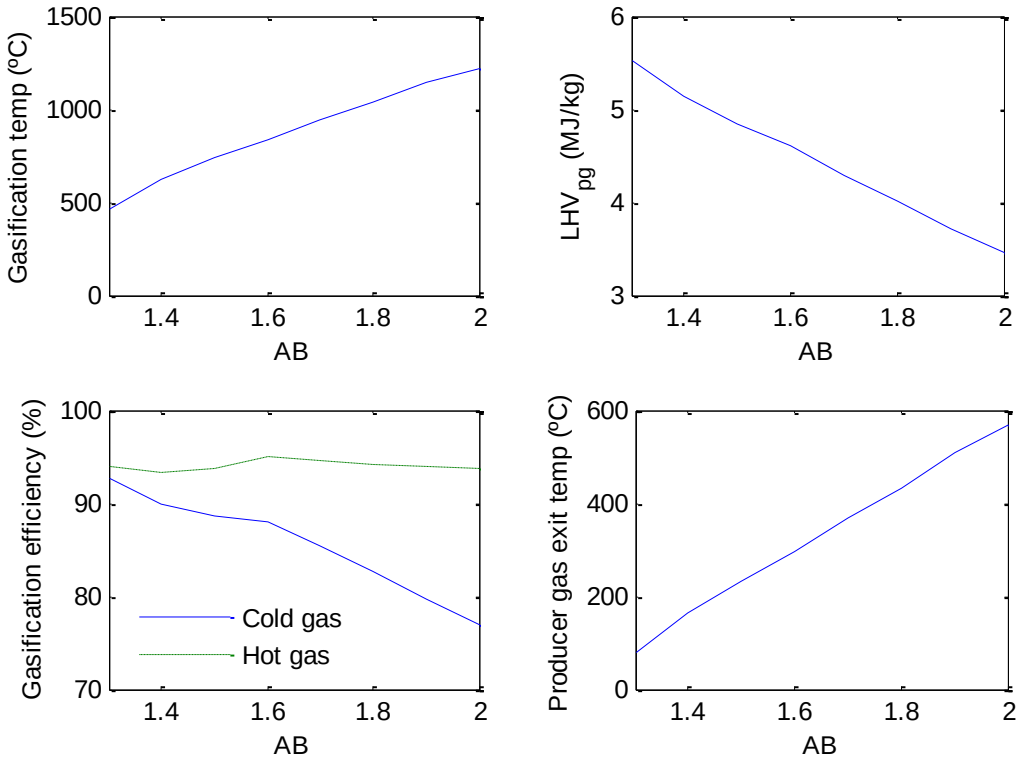

Fig. 48. Mean temperature in the gasification-combustion zone, producer gas calorific value (LHVpg), gasification efficiency and producer gas exit temperature as a function of air-biomass ratio (AB).

Fig. 48 also presents the variation of the producer gas exit temperature as a function of *AB*. It is observed as this temperature increases from 77°C (for *AB* = 1.30) to 570°C (for *AB* = 2.00) as a consequence of the gasification-combustion temperature increase from 500°C to 1220°C. As it was explained above, this effect reduces considerably the LHV_{pg} and the cold gas efficiency; in contrast, the hot gas efficiency is practically constant, reaching a maximum value of 95% for *AB* = 1.60. According to the assumptions cited in the section: *updraft gasifier model*, the exit temperature of the producer gas must be higher than 250°C to avoid future corrosion problems in pipes and auxiliary elements due to the effect of the tar condensation.

According to the present gasification model and the assumptions depicted in Table 21, the optimum performance parameters of the gasifier are achieved for an air-biomass ratio of 1.60. At these operating conditions, the producer gas composition (in mole fraction) is the following: 12.8% H_2, 19.2% CO, 2.6% CH_4, 8.3% CO_2, 11.8% H_2O, 42.1% N_2, 1.71% Tar (C_xH_y) and the rest Ar, O_2, H_2S, dust and particulates. The gasification-combustion temperature is 830°C, the producer gas reaches a lower heating value of 4.6 MJ/kg, a temperature of 294°C at the gasifier exit and a hot and cold gasification efficiencies is 95% and 88.1%, respectively. The biomass consumption during the optimum operating conditions is 0.066 kg/s (around 240 kg/h) and the producer gas mass flow 0.166 kg/s.

Reactor zones	Reactions	Heat of reaction* (kJ/mol)
Drying	Wet biomass → Dry biomass + H_2O	-
Devolatilization	Dry biomass → Char (C) + ash + volatiles	-
Gasification	C + CO_2 ↔ 2CO (Boudouard)	+172.0
	C + H_2O ↔ CO + H_2 (Watergas)	+131.0
	CO + H_2O ↔ CO_2 + H_2 (Shift)	-41.2
	C + 2H_2 ↔ CH_4 (Hydrogasification)	-74.8
Combustion	C + O_2 → CO_2	-394.0
	C + 0.5 O_2 → CO	-111.0

Table 25 Main reactions in the updraft gasifier.

* Positive symbol ("+") represents an endothermic reaction and "-" an exothermic reaction.

ER (equivalence ratio) is an important design parameter for a gasifier, it is the ratio of the actual air-fuel ratio to the stoichiometric air-fuel ratio, [17]. According to Karamarkovic and Karamarkovic, [141], this parameter can be calculated as follows:

$$ER = \frac{0.21 n_{air}}{n_C + 0.5 n_H - n_O} \qquad \text{Eq. 30}$$

Where n_{air} represents the air molar flow and n_C, n_H and n_O the molar flow of carbon, hydrogen and oxygen, respectively, in the biomass.

As it has been discussed in the previous sections, the updraft gasifier behavior directly depends on the feedstock's physical-chemical properties, volatile matter content (the final producer gas composition strongly depends on the devolatilization process) and the equivalence ratio (*ER*). It can be observed in thus study as the optimum performance parameters are reached at *ER*=0.30, under these conditions the hot gasification efficiency and LHV_{pg} is maximized keeping a producer gas exit temperature above 250°C. The results presented by Chen *et al.*, [174], and Lui *et al.*, [175], describe experimental studies with updraft reactors for three biomass types: mesquite, juniper and pine sawdust, as well as working characteristics depending on *ER*. It can be observed these studies show a

gasification behavior similar to the one presented: the gasification temperature and the producer gas yield increase with the *ER*, while, the LHV_{pg} decreases. According to the producer gas composition (on dry basis) the main deviation is presented in H_2 composition. This is largely due to the lower calorific value of the olive leaves (13.0 MJ/kg) compared to mesquite, juniper and pine sawdust (15.3, 17.7 y 16.6 MJ/kg, respectively). When the biomass has a higher LHV_b presents higher fixed carbon content and, in consequence, lower volatile matter content, thus during the devolatilization process the amount of H_2 released is much lower. The results presented by Liu *et al.*, [175], for pine sawdust show production ratios similar to those obtained in the present study.

The works published by Gunarathne *et al.,* [176], and Seggiani *et al.,* [177], evaluate the gasification of different types of pellets (black, grey and wood pellets) in updraft reactors. The experimental analyses show that the composition of the producer gas (in dry basis) for the gasification of grey pellets presents a mole composition similar to those obtained for olive tree leaves. However, their calorific value (LHV_{pg}) and *ER* are different as a consequence of the high calorific value of the pellets in comparison with the olive tree leaves, especially in the gasification of black pellets (LHV_b = 19.3 MJ/kg; LHV_{pg} = 7.3 MJ/Nm^3). When the biomass has a higher LHV_b, the energy liberated in the gasification-combustion process will be higher, and the amount of gasification air required (*ER*) will be lower to achieve the same gasification temperature. On the other hand, it is important to highlight that black pellets are obtained by dry torrefaction of grey pellets, showing then a higher calorific value (LHV_{pg}) and better producer gas characteristics; however, at lower gasification temperatures (<700°C), they exhibit a high tar content (around 5% mole), thus increasing the economic cost of the cleaning and cooling systems. It needs to be emphasized that the relation of producer gas yields for black and grey pellets (2.0 and 2.1) are close to those obtained in the present study (1.9-2.4).

To conclude this section, the experimental results of updraft gasification found in the literature show a high variability and depend strongly of two essential parameters: the lower calorific value of the biomass (LHV_b) and the volatile matter composition (from the ultimate analyses), the last one is directly related with the final H_2 content in the producer gas.

Researching study		Present work	Chen et al.		Gunarathne et al.		Lui et al.	Seggiani et al.
Biomass		Olive leaves	Mesquite	Juniper	Black pellets	Grey pellets	Pine sawdust	Wood pellets
ER **(-)**		0.24-0.38	0.24-0.37		0.20	0.20	0.10-0.50	0.25
LHV $_b$ **(MJ/kg)**		13.0	15.3	17.7	19.3	16.6	16.6	16.7
Ash (mass %)		8.5	1.7	1.9	0.9	1.9	0.83	0.7
Producer gas composition on dry basis (mol. %)	CO	26.9-14.6	21.0-13.0	25.0-21.0	32.0	19.0	21.5-16.5	29.0
	H_2	16.2-12.7	3.0-1.6	3.3-2.6	12.0	16.0	10.0-7.6	6.0
	CH_4	3.3-2.7	1.5-1.2	1.7-1.5	4.5	2.5	6.0-3.8	1.9
	CO_2	6.8-13.3	15.0-11.0	11.0-9.0	9.9	14.5	8.1-18.7	9.1
	Tar	2.1-1.4	0.6-0.4	0.5-0.3	5.0	2.0	2.0-1.0	1.9
Gasification temperature (°C)		490-1,220	750-1,000	750-950	> 700	> 800	800	> 700
LHV $_{pg}$ **(MJ/Nm^3)**		5.5-3.4	3.5-2.4		7.3	6.0	7.2 – 4.1	5.8
Producer gas yield (Nm^3/kg)		1.9-2.4	1.4-2.4		2.0	2.1	1.3-2.8	1.6
Cold gasification efficiency (%)		92.7-76.9	-		75.6	75.9	-	59.7

Table 26 Gasification performance parameters for different updraft reactors presented in the literature.

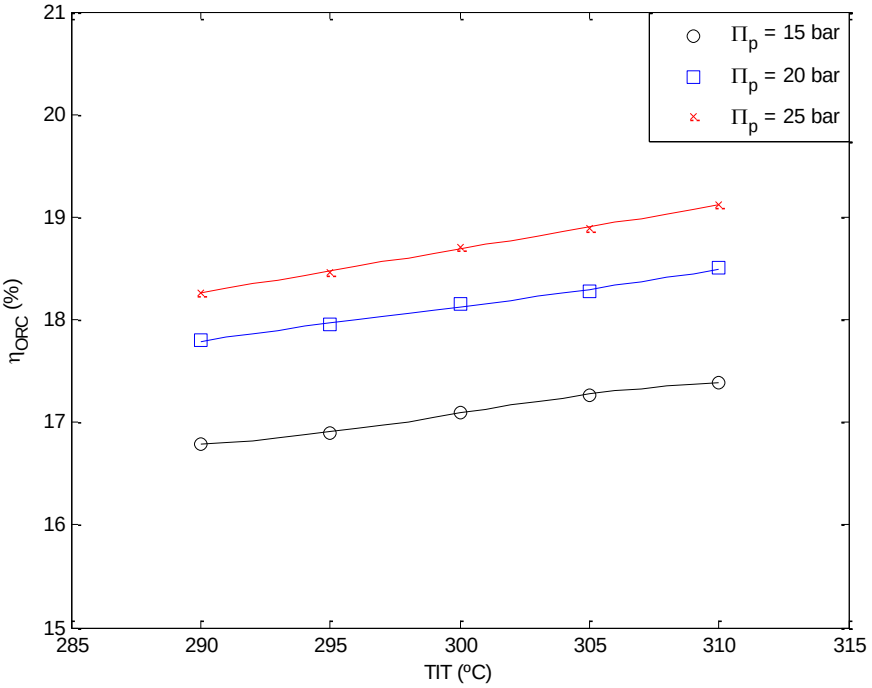

Fig. 49 ORC efficiency for different *TITs* and pressure ratios (Π_p).

After analyzing the optimum parameters of the gasification system, the study of the ORC cycle is presented. Fig. 49 shows the efficiency of the ORC cycle (η_{ORC}) for different turbine inlet temperatures (*TIT*) and pump pressure ratios (Π_p). It can be seen as η_{ORC} depends mainly of the working pressure of the organic fluid and, at a lesser extent, of *TIT*, which shows a practically linear growth for each Π_p analyzed. Following the results obtained during the simulation and equation 10, the maximum η_{ORC} can be reached for the highest Π_p evaluated (25) and maximum *TIT* (310°C), under these conditions, η_{ORC} reaches a value of 19.1%. From a thermodynamic point of view, the ORC cycle can operate under pressures and temperatures close to the critical values tolerated by the organic fluid (41.26 bar and 315.8°C for toluene, Table 23); however, in this paper maximum working pressure and *TIT* have been set at 25 bar and 300°C respectively, thus ensuring that the ORC cycle will work under safe operating conditions, avoiding higher costs at the facility and critical operation conditions, under which the thermodynamic behavior of the organic fluid becomes unstable. Finally, it can be seen in Fig. 49 how the η_{ORC} reached is 18.7% for the predefined operating conditions (Π_p = 25; *TIT* = 300°C).

The distribution of the power losses, net electricity and heat generated are presented in Fig. 50. It can be seen how the chemical energy content in the biomass is converted into electrical and thermal power (93.8kW and 412.6kW, respectively); the useful heat is more than four times the net electricity generated, being this novelty system an attractive solution for CHP applications. Regarding the power losses distribution, the major leak is located in the combustion chamber (158.7kW), followed by the updraft gasifier (104kW) and the ORC subsystem (98kW). It is observed as the higher losses in the combustion chamber are produced in the heat exchanger; here, the energy content of the flue gases is transferred to the thermal oil, releasing 63.5kW to the environment as heat transmission losses (representing around 40% of the total energy losses in the combustion chamber). Other losses of this subsystem are originated in the external combustion chamber (27%) and delivered through the stack (33%).

The power losses in the ORC subsystem are mainly attributed to the three heat exchangers (blocks 5, 23 and 26 in Fig. 46. The highest energy losses are produced in the condenser (32% of the total losses), followed by the evaporator (29%) and regenerator (18%). Other minor losses are located in the steam turbine - electrical generator (15%) and pump (6%).

Finally, the most important power loss in the updraft gasifier is attributed to the charcoal produced after the gasification process. According to the simulation results, this waste has a carbon content of 46.3% (in mole fraction) and 53.7% of ashes, representing a chemical power stream of 43.7kW (around 42% of the total gasifier losses, Fig. 50). It is important to consider that this waste could be a feasible option for the production of activated carbon. Additional losses in the gasifier subsystem are the heat transmission losses from the reactor to the environment (42%) and the minor losses attributed to the carbon particulates removed in the cyclone (17%).

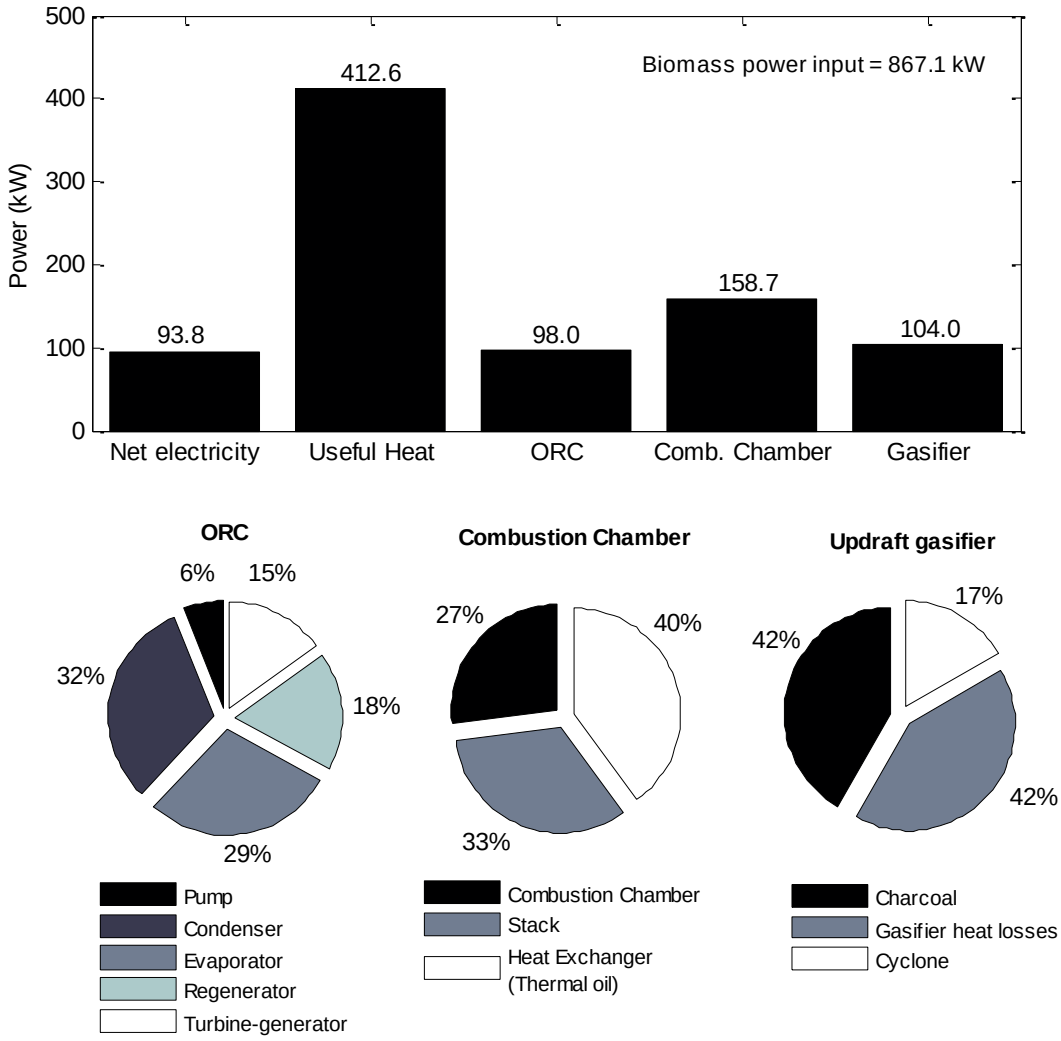

Fig. 50 Power losses distribution of the plant.

To conclude this section, Table 27presents the optimum performance parameters achieved in this study and the comparison with other similar technologies, [94,178].

The work presented by Huang *et al.*, [178], evaluates the gasification and pyrolysis of two poultry litter (PL) samples, characterized by their high ash content, for obtaining two final products: charcoal and energy (this last one, through an ORC cycle). The results achieved with PL were also compared with a high quality biomass: willow chips (with a lower ash content and higher LHV). It is observed in Table 27 that the results achieved in the present work show better electrical and CHP efficiencies than the work of Huang *et al.*, [178]. This is due to the fact that one of the objectives of the work of Huang et al. was the joint

production of charcoal and energy; while in the present work, only energy production has been maximized (both electrical and thermal). It can be also observed as the olive leaves gasification shows a LHV_{pg}, 4.60MJ/kg, higher than the one obtained in the gasification of PL: 4.15 MJ/kg for sample #1 and lower for sample #2 (4.81MJ/kg).

Alternatively, Kalina introduced a simulation work based on the gasification of spruce chips for the production of electrical energy by means of a combined cycle with a gas motor and an ORC cycle (as bottoming unit), [94]. The results obtained by Kalina showed a higher electric performance than the one obtained in the present work (23.80% against 10.82%, respectively). This is principally due to two reasons: the first and most important is that the main objective of Kalina's work was to maximize the electrical energy produced through two power units: a motor gas which uses the producer gas from gasification and a ORC which uses the residual heat from the exhaust gases from the motor to maximize the electrical energy generated. In this case, the electrical energy produced is higher, however, there is no thermal energy produced, and the system used by Kalina cannot be used for cogeneration applications. The second reason is that the biomass used in Kalina's work shows better qualities than olive leaves, namely lower ash content and higher LHV_b. As a consequence, the producer gas obtained from the gasification of spruce woodchips presents a higher LHV_{pg} (5.26MJ/kg against 4.60MJ/kg), and therefore, the electricity production per kg of biomass consumed is higher. Finally, it can be observed that the cold gasification efficiency reached in the present work is superior to that obtained by Kalina (88.10% and 59.96%, respectively). This is due as well to two main reasons: the first one lies in the fact that the work of Kalina used a downdraft reactor, against the updraft reactor used in the present study. Downdraft reactors are characterized by the cleaner producer gas obtained (with a low particle and tar content). However, the performance of these reactors is lower than that of the updraft, [17]. The second reason is that the producer gas obtained in Kalina's work feeds a gas motor, and therefore it must be cooled down to ambient temperature and must have low content in water steam and other impurities which could damage the combustion engine. For this reason, this cleaning and cooling process diminishes the energetic content of the producer gas at the gasifier's outlet and therefore, the gasification efficiency (also named cold gas efficiency). It is important to highlight that the performance of the ORC system reached in this work is higher and that the one

obtained by Kalina (18.70% against 13.90%). Toluene allows working with high temperature heat sources, while R123 is used for waste heat at low temperature (as well as R245fa), this allows work at higher temperatures and operating pressures, and therefore, to maximize the ORC performance, [86].

Performance parameter	Units	Present work	Huang et al.		Kalina work
Biomass source	-	Olive leaves	PL sample 1 (option 4)	PL sample 2 (option 4)	Spruce chips (Config. No. 2)
Ash content	wt%	8.50	22.4	17.30	1.50
LHV_b	MJ/kg	13.00	17.23	16.02	18.29
LHV_{pg}	MJ/kg	4.60	4.15	4.81	5.26
Biomass consumption	kg/h	240.0	1500.0	1500.0	194.7
Net electrical power	kW	93.8	376.0	388.0	242.1[b]
Thermal power	kW	412.6	1777.0	1831.0	n.a.
Net electrical efficiency	%	10.82	5.23	5.81	23.80
CHP efficiency	%	58.41	30.00	33.24	n.a.
Gasification efficiency	%	88.10[a]	n.a.	n.a.	59.96[c]
ORC efficiency	%	18.70	n.a.	n.a.	13.90
ORC working fluid	-	Toluene	R245fa	R245fa	R123

Table 27 Optimum performance parameters.

[a] Based on cold gas efficiency (updraft gasifier)

[b] 202.3kW (ICE unit) and 39.8kW (ORC unit)

[c] Based on cold gas efficiency (downdraft gasifier)

n.a.: not available

Chapter 8. Comparison and analysis of most appropriate uses for the technologies considered

Chapter 8. Comparison and analysis of most appropriate uses for the technologies considered

The works presented in the previous chapters has described the modelling of four different systems for the valorization of olive grove and olive mill residues, namely:

- A biomass combustor coupled with an externally-fired gas turbine
- A downdraft gasifier with a microturbine
- A downdraft gasifier with a gas engine
- An updraft gasifier coupled with an ORC

Each of these presents different advantages and disadvantages for their use. Given the diversity in olive by-products that can be valorised and the heterogeneity in the size and production of olive mills throughout Europe, it is anticipated that certain technologies will be more suitable for their use in a certain type of mill than others.

The first system considered, the biomass combustor coupled with an EFGT, is more efficient than the combination of a gasifier and a microturbine, and the one system for which the net electric efficiency obtained is one of the highest (19.1% , Table 28). It achieves this value with a low biomass consumption (33 kg/h), and achieves an overall efficiency of 59,3%. It has the extra advantage of not requiring a complicated gas cleaning system, and it allows using dirty fuels, with a low calorific value. However, the optimization of the HTHE is a critical step in the design and operation of the this type of plant, which is not only expensive, but also affects efficiency. The size ofthe plant considered is also one of the smallest modelled in the present work.

The gasifier and microturbine plant have the same size as the EFGT system, 30 kW_e and 60 kW_{th}, and present in comparison to it a lower overall efficiency with higher restrictions for the type of fuel used and the gas cleaning stage required to avoid corrosion at the microturbine. For this reason the system with a microturbine would not be a direct recommendation for an olive mill willing to valorize their residues. In the current situation,

where olive stones have already a technically suitable and economically beneficial valorization pathway for domestic heating systems, other suitable by-products available require an intensive cleaning stage (wood, which must be free of leaves and young branches and chipped to a particle size adequate to the gasifier), as well as transport to the plant. For this reason, a gasifier combined with a microturbine would not be a recommendable system for valorization at the mill.

The system composed by a downdraft gasifier and a gas engine represents a medium-range and suitable solution, again for dedicated fuels. The system modelled has an electric power of 70kW$_e$ and thermal output of 110kW$_{th}$. The present thesis describes the results obtained with olive stones and with small branches and leaves, and shows that the best values are obtained whenever olive stones are used. The LHV_{pg} is higher for olive stones than for leaves and branches (5.1 MJ/kg vs 3.7 MJ/kg), and char and ashed produced are more than double for leaves and branches than for olive stones (13.3 and 6.0 respectively). The particle size required to achieve optimal operation is restrictive (20-100mm), and the fuels used should not exceed a maximum ash content of 6% or a moisture content of 25%. This explains the low performance obtained with leaves and branches. However, the values obtained for olive stones are promising, and this could be a system suitable for a region where the olive stones do not yet have an established valorization pathway, or olive wood from prunings is readily available in a clean, chipped form.

For the last system considered, the updraft gasifier coupled with an organic Rankine cycle presents the highest flexibility with regard to the fuel used: updraft gasifiers allow a higher moisture content (60% , compared to 20% maximum for downdraf gasifiers, used in the other technologies), ash content (25%, whereas the maximum for downdraf gasifiers is 6%), and particle size, which presents a wide range (5-100 mm), suitable for the use of coarse biomass. Especially the tolerance to higher moisture and ash contents indicate that this system is well suited for the valorization of olive leaves. The system modelled and discussed in Chapter 7 has in the external combustion chamber a key component, as it connects the gasifier and the ORC subsystems and gives the advantage of very low tar formation and particulate requirements in comparison to the rest of systems studied. For the ORC subsystem, the working pressure and *TIT* have been set at 25 bar and 300°C, which

allow safe operation conditions and yield an ORC efficiency still higher than those reported by other works, such as those by Kalina et al. Described in [94]. The net electrical efficiency is 10.82%, lower than the rest of technologies studied in the present thesis. The fuel used must however be considered: the valorization of leaves has shown problematic so far, and a reliable way of using them, like the combination of an updraft gasifier with an ORC presents a good oppotunity. With regard to the LHV_{pg}, the value obtained with this system is higher than the that obtained with the downdraft gasifier and gas engine: 4.60 MJ/kg compared to 3.7 MJ/kg. Biomas consumption is also the highest from the systems studied: 240 kg/h, which implies that this system could be a solution for large olive mills, which collect large amounts of leaves.

Table 28 below summarizes this comparison with the main results obtained:

	Biomass combustor+EFGT	Gasifier + microturbine	Downdraft gasifier+GE (olive stones)	Downdraft gasifier+GE (branches and leaves)	Updraft gasifier + ORC
Gross electric power (kW)	30	30	70	70	100
Thermal power (kW)	60	60	110	110	412.6
Biomass consumption (kg/h)	33	40	105	105	240
LHV_{pg} (MJ/kg)	*n.d.*	*n.d.*	5.1	3.7	4.60
Cold gas efficiency (%)	*n.d.*	*n.d.*	71.2	63.1	92.7 – 76.9
Net electric efficiency (%)	19.1	12.3	19.5	19.5	10.82
Advantages against other technologies	• High net electric efficiency • Can use dirty or low calorific value fuels, doesn't require gas cleaning stage		• High LHV_{pg}		• Fuel flexibility (high ash. High moisture biomass). Allows operation using exclusively leaves • At the conditions described, no tar does not represent clogging risks
Disadvantages against other technologies	• Requires careful optimization of HTHE	• Gas cleaning stage required	• Restrictive with respect to particle size • Large amounts of water required for cooling and cleaning stages	• Performance is much lower for lower-grade fuels	

Table 28 Comparison of the four technologies studied

Chapter 9. Conclusion and future works

Chapter 9. Conclusion and future works

As it has been discussed in the present work, there are a number of technologies suitable for the valorization of olive grove and olive mill by-products. The olive stones have already a marketable use, and for htis reason they are not the main concern whenever talking about the valorization pathways possible. The present thesis has focused on finding a solution for the valorization of olive tree prunings, especially small leaves and branches, which appear not only in the olive groves, but are also carried with the olives harvested to the olive mills (5-10% in weight of the whole received at the mill). Their disposal there is more problematic than at the olive grove, discards direct uses, such as spreading on soil, and implies an extra cost for the operation of the olive mill. Against this situation, there is the possibility of finding a technology that allows their valorization to cover the electrical and heat demands of the olive mill.

Four technologies have been studied in the present thesis with the aim of finding such solution. The results indicate that gasification is a technology suitable for the valorization of biomass from the olive grove, and that between the two gasifier types tested, the updraft gasifier presents the best features, especially for a high moisture and high ash substrate, such as the leaves. In the technologies for the use of biomass, both a gas engine and an ORC have yielded results that indicate an industrial valorization under real operating conditions is possible.

On the future works, after having studied the suitability of different technologies for the valorization of olive oil residues from a purely technical point of view, the economic and social aspects of the implementation of the best options need to be addressed. For this reason, the next works in this line will study the benefits of building different plants, considering the economic benefits they could imply (reduction of disposal and electricity costs) as well as the social benefits they could entail at a larger scale (employment creation, year-round employment in contrast to intermittent through the year, new skills to be

introduced to the staff at the mill). In this case, the obvious focus would be to compare the performances of a gasifier+ gas engine and a gasifier+ ORC.

Furthermore, the intrinsic complexities ofthe sector need to be addressed. There will not be a „one size fits all" solution for the valorization of olive mill by-products, due to the fact that the olive sector is very different in its structure in the different producer countries. The large cooperatives of Andalucía in Spain will need a valorization system that can cope with the large amounts of olives processed, and will probably be able to assume a larger investment than the smaller mills in Italy or Greece. These aspects need to be considered before issuing a strong recommendation on which technologies to implement.

Chapter 10. Curriculum Vitae

Chapter 10. Curriculum Vitae

Academic experience

01.2003 – 06.2004

MSc. In Landscape Planning

at the Universidad Politécnica de Madrid, Madrid (ES)

Escuela Técnica Superior de Ingenieros Agrónomos

09.1996 – 06.2002

BSc. In Biology

at the Universidad de Alicante Alicante (ES)

Work experience

07. 2011 – current

abc solution concepts GmbH

Co-founder and managing director (area International)

- Contract for GIZ: Development of a training program for entrepreneurs in industrial composting. Training of a group of 12 entrepreneurs in the Wilaya Tipaza (Algeria).
- Study for GIZ: Development of business ideas in valorization of organic waste in the Wilaya Tipaza (Algeria) as a pilot for the implementation of the green economy
- Preparation of project proposals for HORIZON 2020 in diverse thematic areas.
- Study for GIZ: Assessment of potential technology options for enhanced utilization of biomass residues in the food processing sector in Chittoor District, Andra Pradesh
- Development of a strategy for entering the Vietnamese market for the company PA-ID. Preparation of a research project proposal for the VHPS – VietHomePowerSystem project

- Development and execution of a course for coordinators of Horizon 2010 research projects
- Market study and strategy for market entry for a straw gasifier in the USA and Canada

06. 2010 – current

Technologie-Transfer-Zentrum Bremerhaven e.V. (ttz Bremerhaven)

Responsible for internal coordination of EU projects

- Strategy development and coordination of acquisition for the Water, Energy and Lanscape Management Institute at ttz Bremerhaven of international funds for a group of 15 project managers
- Troubleshooting in running projects
- Supervision of activity, financial reports and budgets
- Identification of new funding instruments
- Preparation of guidelines and tools for budget calculation and proposal preparation
- Carrying out contract negotiations with the European Commission

Summary of research work carried out

- Development of research plan and assessment of results in the project OPTIFERT (EU-funded project OPTIFERT, Development of an automatic irrigation and fertilization system. FP7)
- Integrated Sustainable Waste Management approaches for Asian countries in the frame of the EU-funded project ISSOWAMA, FP7 Gasification (EU-funded project RESOLIVE, FP7, waste-to-energy solutions for the olive oil sector)
- Anaerobic digestion (project RESOLIVE, assessment of the suitability of diverse agricultural residues for anaerobic digestion)
- Biomass co-firing (EU-funded project NETBIOCOF, FP6 assessment of current status of biomass co-firing in Europe and Central and Eastern Europe Countries, development of a roadmap for the development of biomass co-firing in Europe),

09. 2005 – 06.2010

Technologie-Transfer-Zentrum Bremerhaven e.V. (ttz Bremerhaven)

Project manager

- Scientific and Financial management of EU-funded research and cooperation projects at the Water, Energy and Landscape Institute of ttz Bremerhaven (6th and 7th Framework Programmes).
- Preparation of proposals for international research projects under various funding agencies (European Commission, UNDP, World Bank, BMBF)
- Consulting to companies, research centres and industrial associations for the acquisition of funds for research and development
- Planning and execution of training workshops for researchers, associations

08. 2003 – 08. 2005

CESPA Ingeniería Urbana, S.A. Madrid (ES)

Project manager

- Management of the Juan Carlos I park in Madrid, with resposibilities on staff management, working with teams of up to 10 gardeners.
- Preparation of proposals and quotations on management of public green areas and parks
- Preparation of evaluations of the biological and botanical state of green areas and parks
- Establishment of a GIS for Juan Carlos I park in Madrid

Education

Chapter 11. Contributions

Chapter 11. Contributions

11.1. JOURNAL CITATION REPORTS (JCR)

1. Vera D, Jurado F., **de Mena B.**, Schories G. "Comparison between externally fired gas turbine and gasifier-gas turbine system for the olive oil industry". Energy, 36 (2011) 6720-6730.

2. Vera D, Jurado F., **de Mena B.**, Schories G. "Study of a downdraft gasifier and gas engine fueled with olive oil industry wastes". Applied Thermal Engineering 51 (2013) 119-129.

3. **B. De Mena**, D. Vera, F. Jurado, M. Ortega. Updraft gasifier and ORC system for high ash content biomass: A modelling and simulation study. Fuel Processing Technology. (Accepted 27 September 2016).

11.2. BOOK CHAPTERS

1. Bolton, Kim, **De Mena, Bárbara**, Schories, Gerhard. „Sustainable Management of Solid Waste" Resource Recovery to Approach Zero Municipal Waste (Green Chemistry and Chemical Engineering). Eds. Mohammad J. Taherzadeh and Tobias Richards. 2015. CRC Press. 23-39. Print

Chapter 12. References

Chapter 12. References

[1] UNFCC, United Nations Framework Convention on Climate Change, Rev. Eur. Community Int. Environ. Law. 1 (1992) 270–277. doi:10.1111/j.1467-9388.1992.tb00046.x.

[2] EUROSTAT, Olives by production, 2016. http://ec.europa.eu/eurostat/tgm/table.do?tab=table&tableSelection=2&labeling=labels&footnotes=yes&layout=time,geo,cat&language=en&pcode=tag00122&plugin=0.

[3] R. Chiradeja, P. Ramakumar, An approach to quantify the technical benefits of disturbed generation, IEEE Trans. Energy Convers. 19 (2004) 764–773.

[4] P. Dondi, D. Bayoumi, C. Haederli, D. Julian, M. Suter, Network integration of distributed power generation (ABB), J. Power Sources. 106 (2002) 1–9. doi:10.1016/S0378-7753(01)01031-X.

[5] I. Olive, O.I.L. Council, Exportations Huiles D ' Olive - Olive Oils, 2015. http://www.internationaloliveoil.org/estaticos/view/131-world-olive-oil-figures.

[6] EUROSTAT, Crop statistics, 2016. http://appsso.eurostat.ec.europa.eu/nui/show.do?query=BOOKMARK_DS-600869_QID_-1CC13C8B_UID_-3F171EB0&layout=TIME,C,X,0;GEO,L,Y,0;STRUCPRO,L,Z,0;CROPS,L,Z,1;INDICATORS,C,Z,2;&zSelection=DS-600869CROPS,O1000;DS-600869INDICATORS,OBS_FLAG;DS-600869STRUCPRO,AR.

[7] International Olive Oil Council, World Olive Oil Figures, Int. Olive Counc. (2016).

[8] European Commission, EUROSTAT, (2016). http://ec.europa.eu/eurostat (accessed September 1, 2016).

[9] D. Vera, F. Jurado, N.K. Margaritis, P. Grammelis, Experimental and economic study of a gasification plant fuelled with olive industry wastes, Energy Sustain. Dev. 23 (2014) 247–257. doi:10.1016/j.esd.2014.09.011.

[10] International Olive Oil Council, Production Huiles D ' Olive - Olive Oils, 2015.

[11] A. para el A. de Oliva, Agencia para el Aceite de Oliva -, (n.d.).

[12] International Olive Oil Council, Production worldwide Olive Oils, 2015.

[13] Agencia Andaluza de la Energía, La biomasa en Andalucía, (2015) 40.

[14] I. Merriam Webster, ed., Merriam Webster Online English Dictionary, 2016. http://www.merriam-webster.com.

[15] J.M. Romero-Garc??a, L. Ni??o, C. Mart??nez-Pati??o, C. ??lvarez, E. Castro, M.J. Negro, Biorefinery based on olive biomass. State of the art and future trends, Bioresour. Technol. 159 (2014) 421–432. doi:10.1016/j.biortech.2014.03.062.

[16] J. Calatrava, J.A. Franco, Using pruning residues as mulch: Analysis of its adoption and process of diffusion in Southern Spain olive orchards, J. Environ. Manage. 92 (2011) 620–629. doi:10.1016/j.jenvman.2010.09.023.

[17] P. Basu, Biomass Gasification Design Handbook, Elsevier, 2010. doi:10.1016/B978-0-12-374988-8.00004-0.

[18] BISYPLAN web-based handbook, 2012. http://bisyplan.bioenarea.eu/Handbook-intro.html.

[19] P. Basu, Biomass Gasification and Pyrolisis. Practical Desing and Theory, Academic Press (Elsevier), Burlington, USA, 2010.

[20] R.C. Brown, ed., Thermochemical processing of biomass, 2011th ed., n.d.

[21] S.A. Channiwala, P.P. Parikh, A unified correlation for estimating HHV of solid, liquid and gaseous fuels, Fuel. 81 (2002) 1051–1063. doi:10.1016/S0016-2361(01)00131-4.

[22] B.. Jenkins, L.. Baxter, T.. Miles, T.. Miles, Combustion properties of biomass, Fuel Process. Technol. 54 (1998) 17–46. doi:10.1016/S0378-3820(97)00059-3.

[23] E. Christoforou, A. Kylili, P.A. Fokaides, Technical and economical evaluation of olive mills solid waste pellets, Renew. Energy. 96 (2016) 33–41. doi:10.1016/j.renene.2016.04.046.

[24] P. Bartocci, M. D'Amico, N. Moriconi, G. Bidini, F. Fantozzi, Pyrolysis of olive stone for energy purposes, Energy Procedia. 82 (2015) 374–380. doi:10.1016/j.egypro.2015.11.808.

[25] T. Miranda, J.I. Arranz, I. Montero, S. Román, C. V. Rojas, S. Nogales, Characterization and combustion of olive pomace and forest residue pellets, Fuel Process. Technol. 103 (2012) 91–96. doi:10.1016/j.fuproc.2011.10.016.

[26] RESOLIVE, Report on the results of chemical characterization of fuels and lab scale gasification tests, 2009.

[27] J. Capablo, Formation of alkali salt deposits in biomass combustion, Fuel Process. Technol. 153 (2016) 58–73. doi:10.1016/j.fuproc.2016.07.025.

[28] M. Campoy, A. Gómez-Barea, P. Ollero, S. Nilsson, Gasification of wastes in a pilot fluidized bed gasifier, Fuel Process. Technol. 121 (2014) 63–69. doi:10.1016/j.fuproc.2013.12.019.

[29] P. García-Ibañez, A. Cabanillas, J.M. Sánchez, Gasification of leached orujillo (olive oil waste) in a pilot plant circulating fluidised bed reactor. Preliminary results, Biomass and Bioenergy. 27 (2004) 183–194. doi:10.1016/j.biombioe.2003.11.007.

[30] A.A. Zabaniotou, G. Kalogiannis, E. Kappas, A.J. Karabelas, Olive residues (cuttings and kernels) rapid pyrolysis product yields and kinetics, Biomass and Bioenergy. 18 (2000) 411–420. doi:10.1016/S0961-9534(00)00002-7.

[31] V. Skoulou, A. Zabaniotou, G. Stavropoulos, G. Sakelaropoulos, Syngas production from olive tree cuttings and olive kernels in a downdraft fixed-bed gasifier, Int. J. Hydrogen Energy. 33 (2008) 1185–1194. doi:10.1016/j.ijhydene.2007.12.051.

[32] C. Pattara, G.M. Cappelletti, A. Cichelli, Recovery and use of olive stones: Commodity, environmental and economic assessment, Renew. Sustain. Energy Rev. 14 (2010) 1484–1489. doi:10.1016/j.rser.2010.01.018.

[33] A. Garcia-Maraver, M.L. Rodriguez, F. Serrano-Bernardo, L.F. Diaz, M. Zamorano, Factors affecting the quality of pellets made from residual biomass of olive trees, Fuel Process. Technol. 129 (2015) 1–7. doi:10.1016/j.fuproc.2014.08.018.

[34] D. Vera, F. Jurado, B. de Mena, G. Schories, Comparison between externally fired gas turbine and gasifier-gas turbine system for the olive oil industry, Energy. 36 (2011) 6720–6730. doi:10.1016/j.energy.2011.10.036.

[35] R. Ramos Casado, J. Arenales Rivera, E. Borjabad García, R. Escalada Cuadrado, M. Fernández Llorente,

R. Bados Sevillano, A. Pascual Delgado, Classification and characterisation of SRF produced from different flows of processed MSW in the Navarra region and its co-combustion performance with olive tree pruning residues, Waste Manag. 47 (2016) 206–216. doi:10.1016/j.wasman.2015.05.018.

[36] C. Buratti, S. Mousavi, M. Barbanera, E. Lascaro, F. Cotana, M. Bufacchi, Thermal behaviour and kinetic study of the olive oil production chain residues and their mixtures during co-combustion, Bioresour. Technol. 214 (2016) 266–275. doi:10.1016/j.biortech.2016.04.097.

[37] Regional Energy Agency of Central Macedionia, Market of Olive Residues for Energy, (2008) 1–66. file:///C:/Users/3042799/Downloads/Regional situation for olive-milling residues market (1).pdf.

[38] E. Christoforou, P.A. Fokaides, A review of olive mill solid wastes to energy utilization techniques, Waste Manag. 49 (2016) 346–363. doi:10.1016/j.wasman.2016.01.012.

[39] R. Thompson, R.B., Nogales, Nitrogen and carbon mineralization in soil of vermi-composted and unprocessed dry olive cake ("'orujo seco'") produced from two-stage centrifugation for olive oil extraction, J. Environ. Sci. Heal. (1999) 917– 928.

[40] Project RESOLIVE Deliverable 09 : Report on the results from anaerobic digestion stage, (2013).

[41] M. Orive, M. Cebrián, J. Zufía, Techno-economic anaerobic co-digestion feasibility study for two-phase olive oil mill pomace and pig slurry, Renew. Energy. 97 (2016) 532–540. doi:10.1016/j.renene.2016.06.019.

[42] R. Borja, B. Rincón, F. Raposo, J. Alba, A. Martín, A study of anaerobic digestibility of two-phases olive mill solid waste (OMSW) at mesophilic temperature, Process Biochem. 38 (2002) 733–742. doi:10.1016/S0032-9592(02)00202-9.

[43] H. Abu Tayeh, N. Najami, C. Dosoretz, A. Tafesh, H. Azaizeh, Potential of bioethanol production from olive mill solid wastes, Bioresour. Technol. 152 (2014) 24–30. doi:10.1016/j.biortech.2013.10.102.

[44] U. Özveren, Z.S. Özdoğan, Investigation of the slow pyrolysis kinetics of olive oil pomace using thermo-gravimetric analysis coupled with mass spectrometry, Biomass and Bioenergy. 58 (2013) 168–179. doi:10.1016/j.biombioe.2013.08.011.

[45] A. Zabaniotou, D. Rovas, A. Libutti, M. Monteleone, Boosting circular economy and closing the loop in agriculture : Case study of a small-scale pyrolysis – biochar based system integrated in an olive farm in symbiosis with an olive mill, 14 (2015) 22–36. doi:10.1016/j.envdev.2014.12.002.

[46] M.T. Miranda, A. Cabanillas, S. Rojas, I. Montero, A. Ruiz, Combined combustion of various phases of olive wastes in a conventional combustor, Fuel. 86 (2007) 367–372. doi:10.1016/j.fuel.2006.07.026.

[47] D. Vera, F. Jurado, J. Carpio, Study of a downdraft gasifier and externally fired gas turbine for olive industry wastes, Fuel Process. Technol. 92 (2011) 1970–1979. doi:10.1016/j.fuproc.2011.05.017.

[48] S. Arvelakis, H. Gehrmann, M. Beckmann, E.G. Koukios, Effect of leaching on the ash behavior of olive residue during fluidized bed gasification, Biomass and Bioenergy. 22 (2002) 55–69. doi:10.1016/S0961-9534(01)00059-9.

[49] tumejorenergia.com, (2016). http://www.tumejorenergia.com/es/183-calderas-de-hueso-de-aceituna (accessed November 21, 2016).

[50] S.L. cereales Toledo, Biomasatoledo.es, (2016). http://www.biomasatoledo.net/venta-hueso-aceituna.htm (accessed November 21, 2016).

[51] BIOGRAMASA S.C.A, Biogramasa, (n.d.). https://www.biogramasa.es/precio-pellets-en-granada/

(accessed November 21, 2016).

[52] D. Vera, B. De Mena, F. Jurado, G. Schories, Study of a downdraft gasifier and gas engine fueled with olive oil industry wastes, Appl. Therm. Eng. 51 (2013) 119–129. doi:10.1016/j.applthermaleng.2012.09.012.

[53] J.A. Callejo López, T. Parra Heras, T. Manrique Gordillo, Potencial energético de los subproductos de la industria olivarera en Andalucia, (2010) 70. http://juntadeandalucia.es/export/drupaljda/Potencial energ?tico.pdf.

[54] B. De Caprariis, M. Scarsella, A. Petrullo, P. De Filippis, Olive oil residue gasification and syngas integrated clean up system, Fuel. 158 (2015) 705–710. doi:10.1016/j.fuel.2015.06.012.

[55] S. Abbeddou, S. Rihawi, H.D. Hess, L. Iñiguez, A.C. Mayer, M. Kreuzer, Nutritional composition of lentil straw, vetch hay, olive leaves, and saltbush leaves and their digestibility as measured in fat-tailed sheep, Small Rumin. Res. 96 (2011) 126–135. doi:10.1016/j.smallrumres.2010.11.017.

[56] R. Malheiro, N. Rodrigues, G. Manzke, A. Bento, J.A. Pereira, S. Casal, The use of olive leaves and tea extracts as effective antioxidants against the oxidation of soybean oil under microwave heating, Ind. Crops Prod. 44 (2013) 37–43. doi:10.1016/j.indcrop.2012.10.023.

[57] M. Bouaziz, I. Fki, H. Jemai, M. Ayadi, S. Sayadi, Effect of storage on refined and husk olive oils composition: Stabilization by addition of natural antioxidants from Chemlali olive leaves, Food Chem. 108 (2008) 253–262. doi:10.1016/j.foodchem.2007.10.074.

[58] B. Velázquez-Martí, E. Fernández-González, I. López-Cortés, D.M. Salazar-Hernández, Quantification of the residual biomass obtained from pruning of vineyards in Mediterranean area, Biomass and Bioenergy. 35 (2011) 3453–3464. doi:10.1016/j.biombioe.2011.04.009.

[59] Á. Guinda, J.M. Castellano, J.M. Santos-Lozano, T. Delgado-Hervás, P. Gutiérrez-Adánez, M. Rada, Determination of major bioactive compounds from olive leaf, LWT - Food Sci. Technol. 64 (2015) 431–438. doi:10.1016/j.lwt.2015.05.001.

[60] A. García-Maraver, M. Zamorano, A. Ramos-Ridao, L.F. Díaz, Analysis of olive grove residual biomass potential for electric and thermal energy generation in Andalusia (Spain), Renew. Sustain. Energy Rev. 16 (2012) 745–751. doi:10.1016/j.rser.2011.08.040.

[61] R. Spinelli, G. Picchi, Bioresource Technology Industrial harvesting of olive tree pruning residue for energy biomass, 101 (2010) 730–735. doi:10.1016/j.biortech.2009.08.039.

[62] F.J. Lopez, S. Pinzi, J.J. Ruiz, A. Lopez, M.P. Dorado, Economic viability of the use of olive tree pruning as fuel for heating systems in public institutions in South Spain, Fuel. 89 (2010) 1386–1391. doi:10.1016/j.fuel.2009.11.003.

[63] J.M. Rosúa, M. Pasadas, Biomass potential in Andalusia, from grapevines, olives, fruit trees and poplar, for providing heating in homes, Renew. Sustain. Energy Rev. 16 (2012) 4190–4195. doi:10.1016/j.rser.2012.02.035.

[64] M. Barbanera, E. Lascaro, V. Stanzione, A. Esposito, R. Altieri, M. Bufacchi, Characterization of pellets from mixing olive pomace and olive tree pruning, Renew. Energy. 88 (2016) 185–191. doi:10.1016/j.renene.2015.11.037.

[65] M. Lanfranchi, C. Giannetto, A. De Pascale, Economic analysis and energy valorization of by-products of the olive oil process: "valdemone DOP" extra virgin olive oil, Renew. Sustain. Energy Rev. 57 (2016)

1227–1236. doi:10.1016/j.rser.2015.12.196.

[66] EUROSTAT, Europe 2020 indicators - climate change and energy, 2016. http://ec.europa.eu/eurostat/statistics-explained/index.php/Europe_2020_indicators_-_climate_change_and_energy.

[67] R. Saidur, E.A. Abdelaziz, A. Demirbas, M.S. Hossain, S. Mekhilef, A review on biomass as a fuel for boilers, Renew. Sustain. Energy Rev. 15 (2011) 2262–2289. doi:10.1016/j.rser.2011.02.015.

[68] RESOLIVE, Report on screening of current technologies for olive waste reuse and valorisation, 2010.

[69] N. Gao, A. Li, Modeling and simulation of combined pyrolysis and reduction zone for a downdraft biomass gasifier, Energy Convers. Manag. 49 (2008) 3483–3490. doi:10.1016/j.enconman.2008.08.002.

[70] M. van der B. C. Higman, Gasification, Elsevier Ltd, 2008.

[71] K. H.A.M., Handbook of biomass gasification, BTG Publisher, Enschede, The Netherlands, 2005.

[72] F. Centeno, K. Mahkamov, E.E. Silva Lora, R. V. Andrade, Theoretical and experimental investigations of a downdraft biomass gasifier-spark ignition engine power system, Renew. Energy. 37 (2012) 97–108. doi:10.1016/j.renene.2011.06.008.

[73] H. Olgun, S. Ozdogan, G. Yinesor, Results with a bench scale downdraft biomass gasifier for agricultural and forestry residues, Biomass and Bioenergy. 35 (2011) 572–580. doi:10.1016/j.biombioe.2010.10.028.

[74] N.S. Mamphweli, E.L. Meyer, Implementation of the biomass gasification project for community empowerment at Melani village, Eastern Cape, South Africa, Renew. Energy. 34 (2009) 2923–2927. doi:10.1016/j.renene.2009.06.011.

[75] P. Reche-López, Técnicas Metaheurísticas Aplicadas a la Ubicación Óptima de Generación Distribuida Basada en Biomasa (Doctoral Thesis), Universidad de Jaén, 2009.

[76] European Commission, Research & Innovation. Horizon 2020., 2012.

[77] A. Deublein, D. Steinhauser, Biogas from waste and renewable energies, WIley, 2008.

[78] T. Ackermann, G. Andersson, L. Söder, Distributed generation: A definition, Electr. Power Syst. Res. 57 (2001) 195–204. doi:10.1016/S0378-7796(01)00101-8.

[79] J.R. and B.R.O. Howell, Principios de Termmodinámica para Ingeniería, McGRAW-HILL, Austin, 1990.

[80] C. Soares, Microturbines: applications for distributed energy systems, Elsevier Ltd, 2007.

[81] H. Spliethoff, Power Generation from Solid Fuels, Springer, 2010.

[82] Internationa Energy Association, IEA, 2012.

[83] Kyoto Protocol to the United Nations Framework Convention on Climate Change, 2007.

[84] España gastó 770 millones de euros para poder emitir CO2, El Mundo. (2012).

[85] S.L. SENDECO2, SENDECO, (2016). http://www.sendeco2.com/es/ (accessed November 18, 2016).

[86] J. Bao, L. Zhao, A review of working fluid and expander selections for organic Rankine cycle, Renew. Sustain. Energy Rev. 24 (2013) 325–342. doi:10.1016/j.rser.2013.03.040.

[87] F. Vélez, J.J. Segovia, M.C. Martín, G. Antolín, F. Chejne, A. Quijano, Comparative study of working fluids for a Rankine cycle operating at low temperature, Fuel Process. Technol. 103 (2012) 71–77. doi:10.1016/j.fuproc.2011.09.017.

[88] T. Guo, H.X. Wang, S.J. Zhang, Fluids and parameters optimization for a novel cogeneration system driven by low-temperature geothermal sources, Energy. 36 (2011) 2639–2649.

doi:10.1016/j.energy.2011.02.005.

[89] C. Zhang, G. Shu, H. Tian, H. Wei, X. Liang, Comparative study of alternative ORC-based combined power systems to exploit high temperature waste heat, Energy Convers. Manag. 89 (2015) 541–554. doi:10.1016/j.enconman.2014.10.020.

[90] A. Algieri, P. Morrone, Comparative energetic analysis of high-temperature subcritical and transcritical Organic Rankine Cycle (ORC). A biomass application in the Sibari district, Appl. Therm. Eng. 36 (2012) 236–244. doi:10.1016/j.applthermaleng.2011.12.021.

[91] U. Drescher, D. Brüggemann, Fluid selection for the Organic Rankine Cycle (ORC) in biomass power and heat plants, Appl. Therm. Eng. 27 (2007) 223–228. doi:10.1016/j.applthermaleng.2006.04.024.

[92] U. Arena, F. Di Gregorio, G. De Troia, A. Saponaro, A techno-economic evaluation of a small-scale fluidized bed gasifier for solid recovered fuel, Fuel Process. Technol. 131 (2015) 69–77. doi:10.1016/j.fuproc.2014.11.003.

[93] A. Rentizelas, S. Karellas, E. Kakaras, I. Tatsiopoulos, Comparative techno-economic analysis of ORC and gasification for bioenergy applications, Energy Convers. Manag. 50 (2009) 674–681. doi:10.1016/j.enconman.2008.10.008.

[94] J. Kalina, Integrated biomass gasification combined cycle distributed generation plant with reciprocating gas engine and ORC, Appl. Therm. Eng. 31 (2011) 2829–2840. doi:10.1016/j.applthermaleng.2011.05.008.

[95] K.A. Al-attab, Z.A. Zainal, Performance of high-temperature heat exchangers in biomass fuel powered externally fired gas turbine systems, Renew. Energy. 35 (2010) 913–920. doi:10.1016/j.renene.2009.11.038.

[96] K.A. Al-attab, Z.A. Zainal, Turbine startup methods for externally fired micro gas turbine (EFMGT) system using biomass fuels, Appl. Energy. 87 (2010) 1336–1341. doi:10.1016/j.apenergy.2009.08.022.

[97] J.-H. Leu, Biomass Power Generation through Direct Integration of Updraft Gasifier and Stirling Engine Combustion System, Adv. Mech. Eng. 2010 (2010) 1–7. doi:10.1155/2010/256746.

[98] J.-C.M. Lin, Combination of a Biomass Fired Updraft Gasifier and a Stirling Engine for Power Production, J. Energy Resour. Technol. 129 (2007) 66. doi:10.1115/1.2424963.

[99] clean energy ahead TURBODEN, ORC power plants installed, (2016).

[100] S.H. Kang, Design and experimental study of ORC (organic Rankine cycle) and radial turbine using R245fa working fluid, Energy. 41 (2012) 514–524. doi:10.1016/j.energy.2012.02.035.

[101] H.N. Moran, M.J. and Shapiro, Fundamental of engineering thermodynamics, John Wiley & Sons, Inc., USA, 2006.

[102] S. Dasappa, D.N. Subbukrishna, K.C. Suresh, P.J. Paul, G.S. Prabhu, Operational experience on a grid connected 100kWe biomass gasification power plant in Karnataka, India, Energy Sustain. Dev. 15 (2011) 231–239. doi:10.1016/j.esd.2011.03.004.

[103] D. Gewald, K. Siokos, S. Karellas, H. Spliethoff, Waste heat recovery from a landfill gas-fired power plant, Renew. Sustain. Energy Rev. 16 (2012) 1779–1789. doi:10.1016/j.rser.2012.01.036.

[104] I. Pfeifer, J. and Oberberger, Technological evaluation of an agricultural biogas CHP as well as definition of guiding values for the improved design and operation, in: 15th Eur. Biomass Conf. Exhib., Berlin, Germany, 2007.

[105] F. Cano, A., Jurado, La generación eléctrica distribuida con microturbinas de gas, Ed. Koobeht

International, España, 2005.

[106] D. Vera, J. Carabias, F. Jurado, N. Ruiz-Reyes, A Honey Bee Foraging approach for optimal location of a biomass power plant, Appl. Energy. 87 (2010) 2119–2127. doi:10.1016/j.apenergy.2010.01.015.

[107] F. Jurado, Study of molten carbonate fuel cell—microturbine hybrid power cycles, J. Power Sources. 111 (2002) 121–129. doi:http://dx.doi.org/10.1016/S0378-7753(02)00340-3.

[108] M.Y. El-Sharkh, N.S. Sisworahardjo, M. Uzunoglu, O. Onar, M.S. Alam, Dynamic behavior of PEM fuel cell and microturbine power plants, J. Power Sources. 164 (2007) 315–321. doi:10.1016/j.jpowsour.2006.09.100.

[109] C.X. Cáceres, R.E. Cáceres, D. Hein, M.G. Molina, J.M. Pia, Biogas production from grape pomace: Thermodynamic model of the process and dynamic model of the power generation system, Int. J. Hydrogen Energy. 37 (2012) 10111–10117. doi:10.1016/j.ijhydene.2012.01.178.

[110] M. Loeser, M., Redfern, Modelling and simulation of a novel micro-scale combined feedstock biomass generation plant for grid-independent power supply, Int. J. Energy Res. (2009) 303–320.

[111] D. Vera, F. Jurado, K.D. Panopoulos, P. Grammelis, Modelling of biomass gasifier and microturbine for the olive oil industry, Int. J. Energy Res. 36 (2012) 355–367. doi:10.1002/er.1802.

[112] D. Cocco, P. Deiana, G. Cau, Performance evaluation of small size externally fired gas turbine (EFGT) power plants integrated with direct biomass dryers, Energy. 31 (2006) 1459–1471. doi:10.1016/j.energy.2005.05.014.

[113] M. Anheden, Analysis of Gas Turbine Systems for Sustainable Energy Conversion, KTH, Högskoletyckeriet, Stockholm, Sweden, n.d.

[114] M. Kautz, U. Hansen, The externally-fired gas-turbine (EFGT-Cycle) for decentralized use of biomass, Appl. Energy. 84 (2007) 795–805. doi:10.1016/j.apenergy.2007.01.010.

[115] Capstone Turbine Corporation, (n.d.). http://www.capstoneturbine.com/prodsol/solutions/rrbiogas.asp (accessed June 10, 2016).

[116] S. Janjai, J. Laksanaboonsong, T. Seesaard, Potential application of concentrating solar power systems for the generation of electricity in Thailand, Appl. Energy. 88 (2011) 4960–4967. doi:10.1016/j.apenergy.2011.06.044.

[117] M.E. Corria, V.M. Cobas, E. Silva Lora, Perspectives of Stirling engines use for distributed generation in Brazil, Energy Policy. 34 (2006) 3402–3408. doi:10.1016/j.enpol.2004.09.006.

[118] A. Nishiyama, H. Shimojima, A. Ishikawa, Y. Itaya, S. Kambara, H. Moritomi, S. Mori, Fuel and emissions properties of Stirling engine operated with wood powder, Fuel. 86 (2007) 2333–2342. doi:10.1016/j.fuel.2007.01.040.

[119] S.M. Biedermann F., Carlsen H., Obernberger I., Small-Scale CHP plant-based on a 75kWe Hermetic eight cylinder Stirling engine for biomass fuel-development, technology and operating experiences, in: 2nd World Conf. Exhib. Biomass Fore Energy, Ind. Clim. Prot., Rome, Italy, 2004.

[120] A. Poullikkas, Implementation of distributed generation technologies in isolated power systems, Renew. Sustain. Energy Rev. 11 (2007) 30–56. doi:10.1016/j.rser.2006.01.006.

[121] F. Fang, L. Wei, J. Liu, J. Zhang, G. Hou, Complementary configuration and operation of a CCHP-ORC system, Energy. 46 (2012) 211–220. doi:10.1016/j.energy.2012.08.030.

[122] S.K. Kamarudin, W.R.W. Daud, A. Md.Som, M.S. Takriff, A.W. Mohammad, Technical design and

economic evaluation of a PEM fuel cell system, J. Power Sources. 157 (2006) 641–649. doi:10.1016/j.jpowsour.2005.10.053.

[123] A.O. Omosun, A. Bauen, N.P. Brandon, C.S. Adjiman, D. Hart, Modelling system efficiencies and costs of two biomass-fuelled SOFC systems, J. Power Sources. 131 (2004) 96–106. doi:10.1016/j.jpowsour.2004.01.004.

[124] A. Poullikkas, Operating cost and water economy of mixed air steam turbines, Appl. Therm. Eng. 25 (2005) 1949–1960. doi:10.1016/j.applthermaleng.2004.11.016.

[125] X.Q. Kong, R.Z. Wang, X.H. Huang, Energy efficiency and economic feasibility of CCHP driven by stirling engine, Energy Convers. Manag. 45 (2004) 1433–1442. doi:10.1016/j.enconman.2003.09.009.

[126] A. Melgar, J.F. Pérez, H. Laget, A. Horillo, Thermochemical equilibrium modelling of a gasifying process, Energy Convers. Manag. 48 (2007) 59–67. doi:10.1016/j.enconman.2006.05.004.

[127] Z.A. Zainal, R. Ali, C.H. Lean, K.N. Seetharamu, Prediction of performance of a downdraft gasifier using equilibrium modeling for different biomass materials, Energy Convers. Manag. 42 (2001) 1499–1515. doi:10.1016/S0196-8904(00)00078-9.

[128] Dahlman, Excellence in gas purification, (2010).

[129] Delft University of Technology, Introduction of A program for thermodynamic modeling and optimization of energy conversion systems, n.d. http://www.3me.tudelft.nl/fileadmin/Faculteit/3mE/Over_de_faculteit/Afdelingen/Process_and_Energy_PE/Energy_Technology/research/software/cycletempo/downloads/manuals/doc/Introduction.pdf.

[130] P. V. Aravind, T. Woudstra, N. Woudstra, H. Spliethoff, Thermodynamic evaluation of small-scale systems with biomass gasifiers, solid oxide fuel cells with Ni/GDC anodes and gas turbines, J. Power Sources. 190 (2009) 461–475. doi:10.1016/j.jpowsour.2009.01.017.

[131] R. Toonssen, N. Woudstra, A.H.M. Verkooijen, Decentralized generation of electricity from biomass with proton exchange membrane fuel cell, J. Power Sources. 194 (2009) 456–466. doi:10.1016/j.jpowsour.2009.05.044.

[132] C.R. Altafini, P.R. Wander, R.M. Barreto, Prediction of the working parameters of a wood waste gasifier through an equilibrium model, Energy Convers. Manag. 44 (2003) 2763–2777. doi:10.1016/S0196-8904(03)00025-6.

[133] P. Colonna, S. Gabrielli, Industrial trigeneration using ammonia-water absorption refrigeration systems (AAR), Appl. Therm. Eng. 23 (2003) 381–396. doi:10.1016/S1359-4311(02)00212-0.

[134] A. Abuadala, I. Dincer, G.F. Naterer, Exergy analysis of hydrogen production from biomass gasification, Int. J. Hydrogen Energy. 35 (2010) 4981–4990. doi:10.1016/j.ijhydene.2009.08.025.

[135] M.L. de Souza-Santos, Solid Fuels Combustion and Gasification: Modeling, Simulation, and Equipment Operations Second Edition, 2010.

[136] P. Mathieu, R. Dubuisson, Performance analysis of a biomass gasifier, Energy Convers. Manag. 43 (2002) 1291–1299. doi:10.1016/S0196-8904(02)00015-8.

[137] D.U. of Technology, Cycle-tempo software (release 5.0), (2010).

[138] J. Horlock, Advanced gas turbine cycles, Elsevier Science Ltd., 2003.

[139] A. Datta, R. Ganguly, L. Sarkar, Energy and exergy analyses of an externally fired gas turbine (EFGT)

cycle integrated with biomass gasifier for distributed power generation, Energy. 35 (2010) 341–350. doi:10.1016/j.energy.2009.09.031.

[140] A. Datta, R. Ganguly, L. Sarkar, Energy and exergy analyses of an externally fired gas turbine (EFGT) cycle integrated with biomass gasifier for distributed power generation, Energy. 35 (2010) 341–350. doi:10.1016/j.energy.2009.09.031.

[141] R. Karamarkovic, V. Karamarkovic, Energy and exergy analysis of biomass gasification at different temperatures, Energy. 35 (2010) 537–549. doi:10.1016/j.energy.2009.10.022.

[142] P. McKendry, Energy production from biomass (part 3): Gasification technologies, Bioresour. Technol. 83 (2002) 55–63. doi:10.1016/S0960-8524(01)00120-1.

[143] J.D. Martínez, K. Mahkamov, R. V. Andrade, E.E. Silva Lora, Syngas production in downdraft biomass gasifiers and its application using internal combustion engines, Renew. Energy. 38 (2012) 1–9. doi:10.1016/j.renene.2011.07.035.

[144] Ankur Scientific Energy Technologies Pvt. Ltd., (2011). www.ankurscientific.com/ range.htm#wbg.

[145] J.K. Ratnadhariya, S.A. Channiwala, Three zone equilibrium and kinetic free modeling of biomass gasifier - a novel approach, Renew. Energy. 34 (2009) 1050–1058. doi:10.1016/j.renene.2008.08.001.

[146] F. Casella, P. Colonna, Dynamic modeling of IGCC power plants, Appl. Therm. Eng. 35 (2012) 91–111. doi:10.1016/j.applthermaleng.2011.10.011.

[147] I. D. Vera, F. Jurado, K.D. Panopoulos, P. Grammelis, Modelling of biomass gasifier and microturbine for the olive oil industry, Int. J. Energy Res. 36 (2012) 355–367.

[148] S. Cordiner, M. Feola, V. Mulone, F. Romanelli, Analysis of a SOFC energy generation system fuelled with biomass reformate, Appl. Therm. Eng. 27 (2007) 738–747. doi:10.1016/j.applthermaleng.2006.10.015.

[149] K.H. T. Alouli, Analytical modeling of polarizations in a solid oxide fuel cell using biomass syngas product as fuel, Appl. Therm. Eng. (2007) 731–737.

[150] MathWorks, MATLAB ® and SIMULINK® Software, (2010).

[151] EUTech Scientific Engineering GmbH, Thermolib, Toolbox for Thermodynamic Calculations and Thermodynamic Systems Simulations in MATLAB® and Simulink®, 2012. www.mathworks.es/products/connections/product_ detail/product_35808.html.

[152] MathWorks, SimDriveline: Model and Simulate One-dimensional Mechanical Systems, 2010. www.mathworks.es/products/simdrive/.

[153] Cummins Power Generation, (2009). www.planbfirst.com/May 2009%25 20Updates/SpecSheet/Gas 125 spec.pdf.

[154] M.R.T. R. Ebrahimi, D. Ghanbarian, Performance of an Otto engine with volumetric volumetric efficiency, J. Am. Sci. 6 (2010) 27–31.

[155] L. Chen, F. Sun, C. Wu, Optimal performance of an irreversible dual-cycle, Appl. Energy. 79 (2004) 3–14. doi:10.1016/j.apenergy.2003.12.005.

[156] G.H. Abd Alla, Computer simulation of a four stroke spark ignition engine, Energy Convers. Manag. 43 (2002) 1043–1061. doi:10.1016/S0196-8904(01)00092-9.

[157] D. Brown, M. Gassner, T. Fuchino, F. Maréchal, Thermo-economic analysis for the optimal conceptual design of biomass gasification energy conversion systems, Appl. Therm. Eng. 29 (2009) 2137–2152.

doi:10.1016/j.applthermaleng.2007.06.021.

[158] G. Gautam, Parametric study of a commercial-scale biomass downdraft gasifier: experiments and equilibrium modeling., Auburn (Alabama, 2010.

[159] ASIMPTOTE, Cycle-Tempo Software, (2016).

[160] M. Loeser, M.A. Redfern, Modelling and simulation of a novel micro- scale combined feedstock biomass generation plant for grid- independent power supply, Int. J. Energy Res. 34 (2010) 303–320. doi:10.1002/er.1556.

[161] L. Fryda, K.D. Panopoulos, E. Kakaras, Integrated CHP with autothermal biomass gasification and SOFC–MGT, Energy Convers. Manag. 49 (2008) 281–290. doi:10.1016/j.enconman.2007.06.013.

[162] M. J. Prins, K. J. Ptasinski, F. J. J. G. Janssen, Thermodynamics of gas-char reactions: first and second law analysis, Chem. Eng. Sci. 58 (2003) 1003–1011. doi:10.1016/S0009-2509(02)00641-3.

[163] S. Jarungthammachote, A. Dutta, Equilibrium modeling of gasification: Gibbs free energy minimization approach and its application to spouted bed and spout-fluid bed gasifiers, Energy Convers. Manag. 49 (2008) 1345–1356. doi:10.1016/j.enconman.2008.01.006.

[164] G. Cau, V. Tola, A. Pettinau, A steady state model for predicting performance of small-scale up-draft coal gasifiers, Fuel. 152 (2015) 3–12. doi:10.1016/j.fuel.2015.03.047.

[165] M.L. Hobbs, P.T. Radulovic, L.D. Smoot, Prediction of effluent compositions for fixed-bed coal gasifiers, Fuel. 71 (1992) 1177–1194. doi:10.1016/0016-2361(92)90100-3.

[166] H. Yoon, J. Wei, M.M. Denn, A Model For Moving-Bed Coal Gasification Reactors, AlChE J. 24 (n.d.) 1–6.

[167] A. Mountouris, E. Voutsas, D. Tassios, Solid waste plasma gasification: Equilibrium model development and exergy analysis, Energy Convers. Manag. 47 (2006) 1723–1737. doi:10.1016/j.enconman.2005.10.015.

[168] E. research C. of the N. (ECN), Thersites. The ECN tar dew point site, (2016).

[169] A. García-Maraver, L.C. Terron, A. Ramos-Ridao, M. Zamorano, Effects of mineral contamination on the ash content of olive tree residual biomass, Biosyst. Eng. 118 (2014) 167–173. doi:10.1016/j.biosystemseng.2013.12.009.

[170] A. Abuadala, I. Dincer, G.F. Naterer, Exergy analysis of hydrogen production from biomass gasification, Int. J. Hydrogen Energy. 35 (2010) 4981–4990. doi:10.1016/j.ijhydene.2009.08.025.

[171] M. Bahrami, A.A. Hamidi, S. Porkhial, Investigation of the effect of organic working fluids on thermodynamic performance of combined cycle Stirling-ORC, Int. J. Energy Environ. Eng. 4 (2013) 1–9. doi:10.1186/2251-6832-4-12.

[172] H. Ozcan, I. Dincer, Performance evaluation of an SOFC based trigeneration system using various gaseous fuels from biomass gasification, Int. J. Hydrogen Energy. 40 (2015) 7798–7807. doi:10.1016/j.ijhydene.2014.11.109.

[173] Dow Corning Corporation, Heat Transfer Fluids-SYLTHERM (Silicone Fluids), (2016).

[174] W. Chen, K. Annamalai, R.J. Ansley, M. Mirik, Updraft fixed bed gasification of mesquite and juniper wood samples, Energy. 41 (2012) 454–461. doi:10.1016/j.energy.2012.02.052.

[175] H. Liu, J. Hu, H. Wang, C. Wang, J. Li, Experimental studies of biomass gasification with air, J. Nat. Gas Chem. 21 (2012) 374–380. doi:10.1016/S1003-9953(11)60379-4.

[176] D.S. Gunarathne, A. Mueller, S. Fleck, T. Kolb, J.K. Chmielewski, W. Yang, W. Blasiak, Gasification

characteristics of steam exploded biomass in an updraft pilot scale gasifier, Energy. 71 (2014) 496–506. doi:10.1016/j.energy.2014.04.100.

[177] M. Seggiani, S. Vitolo, M. Puccini, A. Bellini, Cogasification of sewage sludge in an updraft gasifier, Fuel. 93 (2012) 486–491. doi:10.1016/j.fuel.2011.08.054.

[178] Y. Huang, M. Anderson, D. McIlveen-Wright, G.A. Lyons, W.C. McRoberts, Y.D. Wang, A.P. Roskilly, N.J. Hewitt, Biochar and renewable energy generation from poultry litter waste: A technical and economic analysis based on computational simulations, Appl. Energy. 61 (2015) 1–8. doi:10.1016/j.apenergy.2015.01.029.